MULTIBEAM BATHYMETRIC SURVEYS IN THE FRASER RIVER DELTA, MANAGING SEVERE ACOUSTIC REFRACTION ISSUES
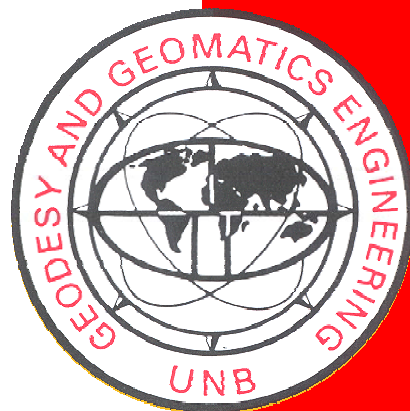
M.Eng. Report

D. S. Cartwright

August 2003

MULTIBEAM BATHYMETRIC SURVEYS IN THE FRASER RIVER DELTA, MANAGING SEVERE ACOUSTIC REFRACTION ISSUES

By

Doug Cartwright

A Report Submitted in Partial Fulfilment of
the Requirements for the Degree of

Master of Engineering

in the Graduate Academic Unit of Geodesy and Geomatics Engineering

Supervisor:	J.E. Hughes Clarke, PhD, Geodesy and Geomatics Engineering
Examining Board:	K. Butler. PhD, Geology
	D.E. Wells, PhD, Geodesy and Geomatics Engineering

This Report is accepted.

_____
Dean of Graduate Studies

THE UNIVERSITY OF NEW BRUNSWICK

September 2003

© Doug S. Cartwright, 2003

i

Acknowledgements

Abstract

The multibeam echosounder is the most efficient and effective tool of the modern hydrographer for the measurement of bathymetry. The ability to ensonify a large swath of the ocean floor with every transmit/receive cycle results in an unprecedented quantity of data being gathered. One of the prerequisites for the required calculations is knowledge of the sound speed, both at the surface and throughout the water column.

When the knowledge of the structure of the water column is incomplete, outdated or unknown, an error in the three dimensional positioning of the bathymetric point will result. The source of these positioning errors are inaccuracies in the raytracing of the acoustic signal through the water mass, and, in the case of electronically steered flat arrays, inaccuracies in the calculations for the electronic steering of oblique beams.

In this report the issues related to sound speed measurement as it relates to oblique incidence echosounding are presented and the currently available solutions are investigated. The survey selected for analysis was completed on the Fraser River Delta. This survey was selected due to the extremely dynamic water column structure, which represents a significant challenge to a multibeam survey. The multibeam system employed consisted of a flat, electronically steered array and a near real-time sound speed measurement solution was used. Using post-processing calculations it was also possible to simulate the use of a curved transducer array and the use of archived sound speed profile solutions.

The survey data was analysed in order to determine the effects of differing acoustic and sound speed measurement techniques on the accuracy of the resulting hydrographic data. This analysis revealed a range of accuracies as well as methods of mitigating errors by the optimum use of currently available equipment. This information will be applied to comprehend and improve the accuracies of hydrographic and oceanographic data derived from multibeam echosounder surveys.

Table of Contents

List of Figures

CHAPTER 1 INTRODUCTION AND OVERVIEW

1.1 Introduction

The Canadian Hydrographic Service (C.H.S.) has the mandate to measure and describe the physical features (water depth, bottom structure, bottom type and composition, tides, water levels, currents and shoreline features) of Canada's navigable waters, with special emphasis on elements that affect safe and efficient navigation. On the west coast of Canada one of the responsibilities of the C.H.S. is the Fraser River Delta. The Delta is a major hub of shipping, is home to the busiest ferry terminal in the world and one of the largest shipping facilities in Canada. A major submarine hydroelectric corridor, which supplies power to Vancouver Island's population, also enters the ocean in the area. There are also concerns for the region's geological stability as the Delta is positioned over an active subduction zone with the trench axis approximately 150 km to the west.

For these reasons the area is of interest to both the Canadian Hydrographic Service and the Geological Survey of Canada. During the summer of 2001 a hydrographic survey was carried out to gather geological and charting data. The use of an oblique echosounder in waters of such variable and unpredictable sounds speeds was considered to be a major challenge. The most effective and efficient use of tools available

is investigated in order to assist future surveys in both the Fraser Delta and similar coastal areas.

1.2 Report Contents

1.2.1 Chapter 2 - Background

Chapter 2 consists of 6 main subsections: the properties of seawater, the properties of sound in seawater, the measurement of sound speed, sound wave propagation, multibeam echosounders and, lastly, the Fraser River Delta. Understanding the properties of seawater is vital when considering it as a medium through which acoustic measurements are made. The relationship of temperature, salinity and pressure,` all have an effect that must be considered when working in this environment.

The use of sound as a measuring tool in the oceans has a long history. Sound is presently the only efficient tool in making measurements to significant depths within the ocean. It is critical to comprehend the nature of the interaction of sound within the water column in order to make useful measurements and to have a concept of accuracies and values.

The multibeam echosounder is an oblique angle echosounder, which can discern multiple beams in a swath along the ocean floor. This tool has recently become one of the

most efficient and accurate tools for the hydrographer. In order to effectively use this tool it is necessary to comprehend its abilities and limitations

The Fraser River Delta is a dynamic changing environment, in terms of its geology, its population, its commerce and its history and most importantly here, its oceanography. These factors require constant monitoring and evaluation of the environment.

1.2.2 Chapter 3. - Analysis of Oceanography and Refraction Issues in the Fraser River Delta Survey

Chapter 3 covers 5 main subsections: an overview of the 2001 survey resources, the survey methodology, the survey area, the observed oceanography, and an evaluation of solutions to the refractions issues encountered. The Canadian Hydrographic Service (C.H.S.) was tasked with surveying the Fraser River Delta in support of research for the Geological Survey of Canada as well as for traditional charting purposes. This chapter will summarize the survey methodologies used as well as an overview of the survey statistics and results.

The use of a real time water column profiling system enabled the recording of spatially dense sound speed profiles. It was hoped that this information could be used to infer oceanographic properties that would be useful in terms of survey planning as well as oceanographic research.

The effectiveness of the various methods of measuring and applying the refraction solutions based on measured sound speed profiles is explored. All possible scenarios are examined including conducting a survey without the real time profiling system that was available to the hydrographic party for this survey along with more traditional methods.

1.2.3 Chapter 4. - Applications to C.H.S. Hydrographic Operations

Chapter 4 covers two main subsections. The first section reviews the results as they apply specifically to the use of the sound speed measurement system in use by the Pacific region of the Canadian Hydrographic Service, covering its effectiveness, for both hydrography and oceanography

The second section covers the applications to the two different types of multibeam in use by the C.H.S. There is currently a flat transducer, electronically steered system and a curved, physically steered system in use by the Service and they have their strengths and weaknesses for different types of applications

Finally a summation of the overall effect of the findings of the report on CHS survey methods and planning.

CHAPTER 2 BACKGROUND

2.1 Properties of Seawater

2.1.1 Introduction

The varied characteristics of the oceans are in large part due to the properties of the water it contains. Water consists of one oxygen ion with a positive charge and two hydrogen ions with negative charges with a bonding angle of 105 degrees. The asymmetry of these charged elements of the molecule result in a polar nature that leads to waters ability to act as a universal solvent, dissolving more substances than any other fluid. In the fields of oceanography and hydrography, the properties of seawater of primary concern are salinity, temperature and density.

2.1.2 Temperature

Temperature is perhaps the easiest measured parameter in the oceans and, as such, it is one of the earliest parameters recorded and studied. From the point of view of sound in the ocean, it has been shown that temperature, in combination with depth, is the

primary determinant of sound speed through the water column. This is true for the open ocean under normal conditions, however under coastal conditions where systems have yet to stabilize, salinity plays a large and sometimes more significant role. Temperature of seawater is displayed in units of Celsius (° C) Temperatures range from 0 to 30 degrees Celsius throughout most of the world's oceans, with higher extremes present in localized areas such as the Persian Gulf and inland seas. Typically, a change in temperature of one degree would correspond to an approximate change in sound speed of 4 m/s [Medwin 1998].

2.1.3 Salinity

The amount of dissolved material in seawater is termed salinity. The precise definition is "the total amount of solid materials in grams contained in one kilogram of seawater when all the carbonate has been converted to oxide, the bromine and iodine replaced by chlorine and all organic matter completely oxidized" [Pickard 1968]. Seawater is a complex solution containing a large number of compounds, primarily in their ionic forms. The 5 most abundant ions are chloride (55%), sodium (30.6%) sulphate (7.7%) magnesium (3.7 %) and potassium (1.1 %). The units of salinity are usually termed as grams of dissolved salts per kilogram of seawater and written as $^o/_{oo}$ or ppt (parts per thousand). The average salinity of the ocean is approximately 35 grams per kilogram, which is then written as 35 $^o/_{oo}$ or 35 ppt. Salinity ranges from 0 to 40

parts per thousand throughout most of the world's oceans, with higher extremes present in the Persian Gulf and inland seas. Typically, a change in salinity of one part per thousand would correspond to an approximate change in sound speed of 1 m/s [Medwin 1998].

2.1.4 Density

For Hydrodynamic studies, the most important parameter may be considered to be the density of seawater. This is important to the oceanographer as its variations within the water mass determines the baroclinic balance or the direction water bodies will tend to move to achieve equilibrium. For underwater acoustics, the primary concern is the amount of pressure, which is a function of depth, along with atmospheric pressure and latitude. The density is then a function of pressure, temperature and salinity.

2.2 Properties of Sound in Seawater

2.2.1 Physical Dependencies

The speed of sound is determined by the relationship of fluid compressibility and density [Pickard 1968].

$$V = \sqrt{(E / \rho)}$$

(2.1)

Where: V = Sound Speed (m/s)
E = adiabatic bulk modulus of water (N/m^2)
ρ = density of water (kg/m^3)

These factors are all dependant on the temperature, salinity and pressure of the seawater. Water is considered to be relatively incompressible, however its compressibility under extreme pressures is a consideration in deep, offshore waters.

There are numerous equations for the determination of sound speed from salinity, temperature and pressure. These equations are developed by very accurate measurements of sound speed combined with associated measurements of temperature, pressure and salinity. The resulting measurements are then fitted to an equation using regression analysis. These measurements and their associated equations have been refined over the years by researchers such as Wilson [1960], Chen and Millero [1977], Del Grosso [1972] Mackenzie [1981] and Fujii [1993]. The equations have different ranges of temperature, salinity and pressure for which they are considered valid. While the accuracy of the equations has clearly increased, the relative accuracies of currently

8

accepted equations are not clearly defined and have been the subject of much debate, mainly centring on different experimental techniques used to derive the equations [Dushaw 1993].

The most easily utilized equation is the Mackenzie Equation, which is a nine term equation originally developed for the ability to make calculations with a handheld programmable calculator. The equation is valid, based on the oceanographic measurements from which it is derived, from -2 to 30 °C, salinity of 30 to 40 ppt and depth 0 to 8000 m [Mackenzie 1981]. This equation requires temperature, salinity and depth. The use of depth rather than pressure introduces a small error that is accounted for in other, more accurate equations.

Two equations that are most accepted by the scientific community are the Chen-Millero and the Del Grosso's Equation. The Chen and Millero equation has the wider range of validity, based on the oceanographic measurements from which it is derived, of 0 to 40 °C, salinity 0 to 40 ppt and pressure of 0 to 1000 bar [Millero 1994] . Both equations use pressure rather than depth for increased accuracy. If pressure is not directly measured, there are formulas to convert to pressure as a factor of depth and latitude, however some errors are introduced as average temperatures and salinities are assumed. Currently, the Chen and Millero equation has been accepted by UNESCO (United Nations Educational, Scientific and Cultural Organization) as their standard, however, both equations are commonly used [N.P.R. 2001].

2.2.2 Sound Speed Variability

The sound speed profile will vary due to many diverse factors. In the open ocean the main factors will be time of day, season and latitude. In the offshore the primary determinants are temperature and depth. The salinity is considered stable and predictable with only a small variation on the surface due to evaporation and precipitation.

The temperature profile of the open ocean can be arbitrarily divided into a surface layer and a deep layer, with a boundary at approximately 100 metres. The deep layer has a relatively constant thermocline, or decreasing temperature gradient, that remains in place throughout the year. The surface layer is subject to changes in the temperature profile with depth because of the influence of solar heating, wind influence and wave action. Typically during winter months, with the associated stormy weather, the entire surface layer is well mixed resulting in a surface layer of relatively constant temperature transitioning directly into the permanent deep thermocline. Conversely in the summer months there is only a small mixed layer at the surface followed by a shallow thermocline, created through solar heating, that transitions more smoothly into the deep thermocline.

In a coastal situation such as the Fraser River delta, the water column consists entirely of the surface layer previously discussed. In coastal areas, and particularly in fluvial zones, the salinity becomes much more variable in addition to temperature. This is primarily due to the influence from inland waterways with the associated freshwater runoff and suspended sediment. In addition, the influence of the tides interacting with the shoreline and the ocean floor, in combination with wind forces, results in mixing,

alongshore currents, and upwelling of water bodies (Figure 1). As in the open ocean evaporation and precipitation play a role in the variability of the surface salinity while solar heating will vary the surface temperature on a daily scale. However in the case of coastal waters these factors represent a much larger percentage of the entire water
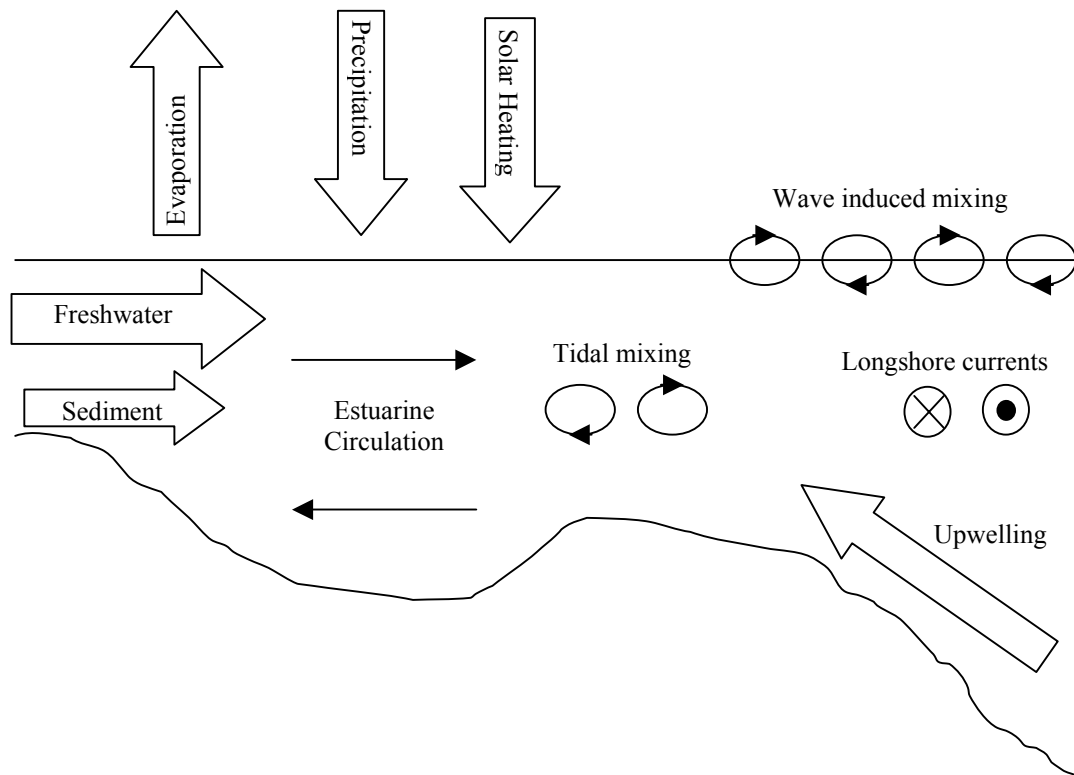
column.

Figure 1. External factors influencing sound speed in coastal waters (after Hughes-Clarke 1994)

Temperature has long been considered the dominant cause of change in sound speed throughout the world's oceans, with salinity as a secondary source. Figure 2 illustrates the effect of a small change in either of these factors throughout the ranges normally found through the world oceans.
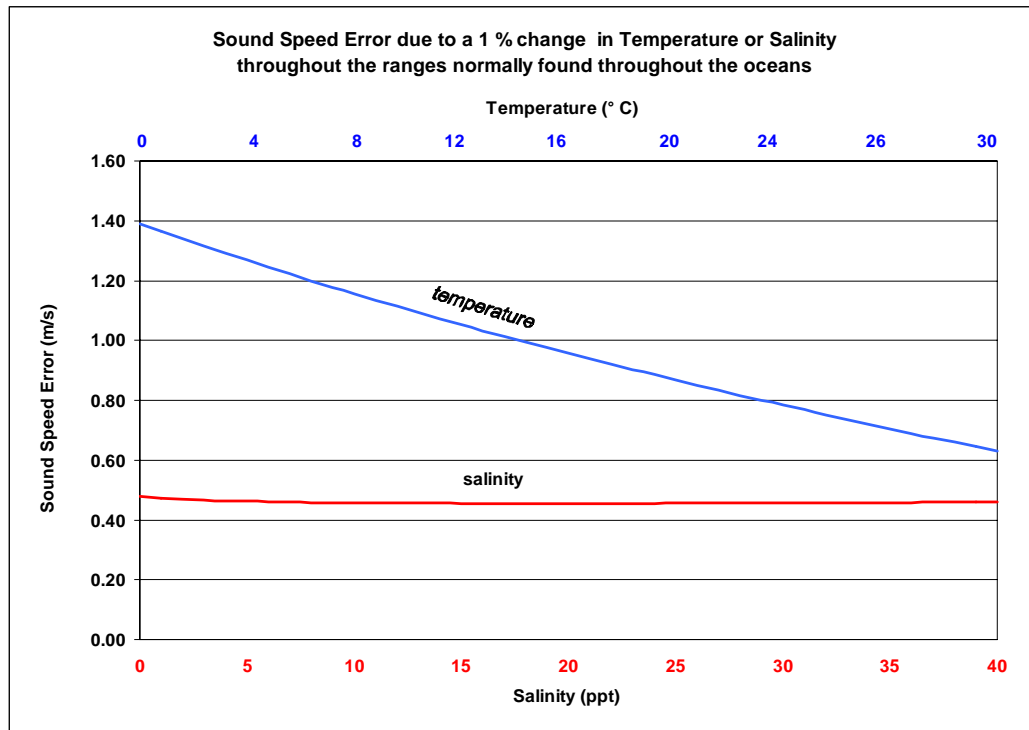
Figure 2. Sound speed errors in the world's oceans due to change in salinity or temperature

A contrasting situation is found under many coastal situations. With the influence of fresh water, the salinity variations quickly become the dominant source of change in sound speed. Figure 3 illustrates how, in the specific case of the Fraser River Delta in 2001, salinity variations were in fact the dominant factor in sound speed change. This was exacerbated by the fact the temperature and salinity changes that were encountered were often abrupt changes, as the transition was made from saltwater to freshwater.
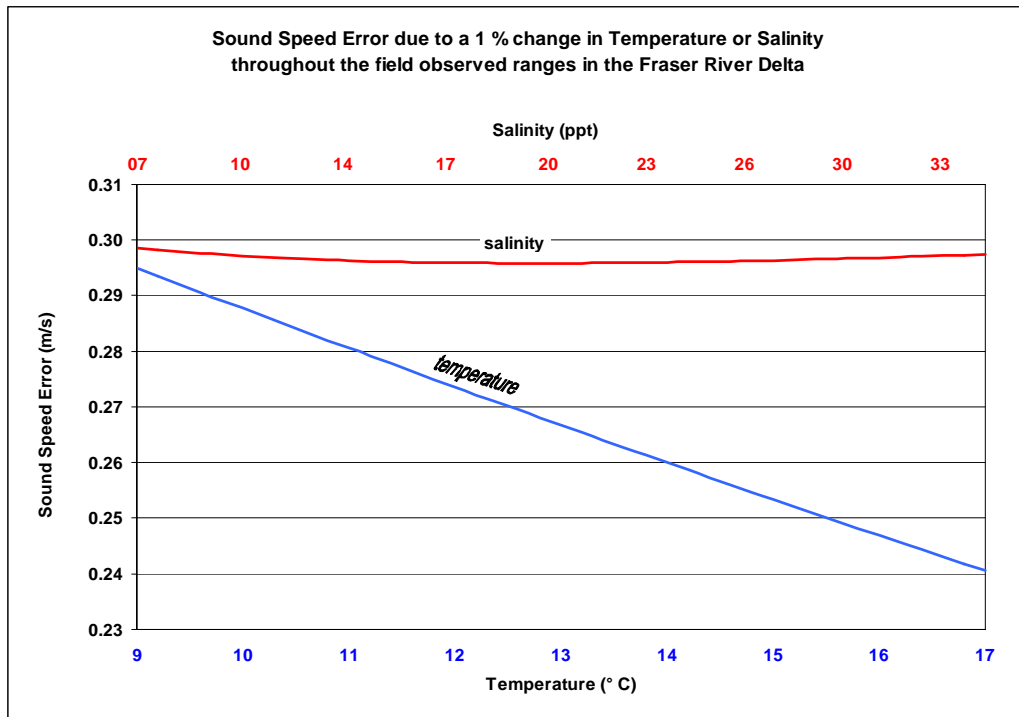
Figure 3. Sound speed errors on the Fraser River Delta due to a change in salinity or temperature.

2.3 Sound Wave Propagation in Echosounding

2.3.1 Introduction

The fundamental principle of echosounding is that an acoustic pulse is transmitted into the water column and the time required for the echo to return is measured. If we oversimplify the situation by assuming a water column of a constant sound speed we can multiply this time value by the speed of sound in the water column determining the length of the acoustic travel path. The source of this sound speed is

13

generally a discrete measurement or a measurement over less than a decimetre on an instrument lowered through the depth of the water column concerned.

2.3.2 Vertical Incidence

When a sound wave is transmitted through the water column in a vertical (downward) direction it is necessary to account for variable sound speed layers as it travels towards the ocean floor.

Traditionally, in single beam echosounding, the method used is to compute a single harmonic sound speed to be applied to all soundings in a localized survey area wherein the depths and sound speed profiles are expected to be relatively homogenous. This value is based on a measured sound speed profile where the depths "z" and associated sound speeds "c" are known quantities. Using the depths and sound speeds from the profile, a harmonic sound speed is calculated by dividing the water column into layers "$[z_i, z_{i+1}]$" of assumed homogeneous sound speed "C_i" and summing the travel time through each layer by multiplying the distance by the layers sound speed of the layer through each layer until the complete depth is measured. This value is then divided into the total depth to obtain a single harmonic sound speed value "C_H".

$$C_H = \frac{z - z_0}{\sum_{i=1}^{N} \int_{z_i}^{z_{i+1}} \frac{dz}{C_i(z)}}$$

(2.2)

Where: z = total depth
z_0 = initial depth
N = number of layers
[z_i,z_{i+1}] = layer travelled at sound speed C_i(z)

The sound speed used will have a slight error when applied to travel times due to the depth being more or less than the value calculated, however these errors are small and are accepted within the scope of a single beam echosounder survey.

However a more accurate method is to calculate depth for every ping directly using the travel time and a layered velocity model. This is the method used for ray tracing for oblique acoustic rays. This method can be used with an assumed acoustic ray tangential to the transducer which is equivalent to using a harmonic sound speed without using an assumed depth. This method entails iterating through the layers, calculating time spent within each layer until half the measured travel time is reached. This requires a calculation for every depth, increasing real time computation requirements, and in vertical incidence soundings is not usually required.

2.3.3 Oblique Incidence Echosounding.

In the case of determining depth using oblique incidence we have to correct for two variables. The first is the distance travelled through the water column based on the travel time multiplied by the sound speeds in each layer. Secondly we have to account for deviation of the actual travel path, as any ray that travels obliquely through a water column that consists of layers of varying sounds speeds will be "bent" or refracted along its path.

Refraction is quantified in Snell's law (see Figure 4), which states that the ratio of the sine of the angle of incidence of the ray through a layer over the sound speed in the layer remains constant as the ray transits through to a layer of different sound speed. For example, if the acoustic ray transits into a layer of increased sound speed then the sine of the angle of incidence must also increase.
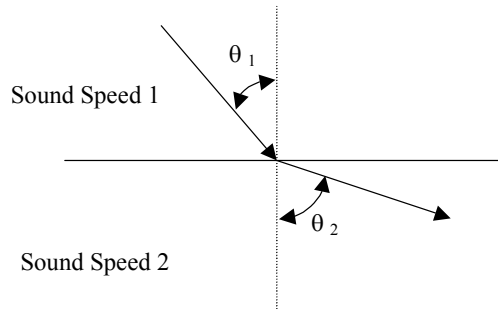
$$\frac{\sin \theta_1}{\text{Sound Speed 1}} = \frac{\sin \theta_2}{\text{Sound Speed 2}} = \text{Snells constant, p} \qquad (2.3)$$

Figure 4. Graphical representation of Snell's law

16

In order to determine a depth value, one needs to determine the horizontal and vertical components of the ray path through the water column. The required input parameters are the starting depth, departure angle, with respect to local level, the two way travel time and the sound speed profile.

In order to take advantage of Snell's law, it is necessary to determine the Snell's constant p. This is most easily calculated using the initial sound speed to angle ratio at the transducer face. This is calculated based on the departure angle of the beam as it is transmitted into the water and the speed of sound at the transducer. This parameter will be maintained as the ray travels throughout the entire water column. The calculated ratio is also termed the "ray parameter" which is equivalent to the Snell's constant.

$$ p = \frac{\sin \theta_o}{C_0} $$

(2.4)

where: p = ray parameter (Snell's constant)
θ_o = departure angle
C_o = sound speed at transducer

After the initial ray parameter is defined, it is essentially a matter of trigonometry to trace the horizontal and vertical components of the ray path until it reaches the seafloor. Using the ray parameter, if the sound speed at a particular depth is known, then the ray angle at that depth can be calculated even without the rest of the sound speed profile being known.

There are two approaches to making these calculations that will be considered. The first is to subdivide the water column into layers and assuming a constant sound speed within each layer and the second is to assume within each layer a constant sound speed gradient.

2.3.3.1 Layers with Constant Sound Speed

The simplest method to calculate these values is to subdivide the water column into layers of constant sound speed. Then using Snell's law we can sequentially sum the horizontal components and the time traveled until we reach one half of the recorded two-way travel time.

$$t = \sum_{i=1}^{N} \frac{\Delta_i}{C_i \sqrt{1-(C_i p)^2}} \qquad x = \sum_{i=1}^{N} \frac{C_i p \Delta_i}{\sqrt{1-(C_i p)^2}}$$

Where: t = time travelled
              x = horizontal distance travelled
              N = number of layers
              p = ray parameter
              C_i = sound speed in layer
              Δ_i =layer thickness

(2.5)

While sequentially summing the horizontal distance and the time through the layers of the water column, the horizontal distances and layer thicknesses are summed. At the point that the time is equal to one half of the recorded two way travel time, the

solution is reached. Summation of the layer thicknesses Δ_i provides a depth solution relative to the transducer. The point at which the time is equal to one half of the recorded two way travel time will generally not occur on the end of one of the predetermined layers and therefore the last layer must be calculated using interpolation.

The number of layers used in the summations determines the accuracy of this solution. Due to the fact that this calculation subdivides the ray path into sections of staircase type steps, the smaller the steps that are used, the closer the calculated ray path will approximate a true, smooth ray path.

2.3.3.2 Layers with Constant Sound Speed Gradient

A second method is to calculate the time and horizontal distance based on layers of constant sound speed gradient. This method can be considered equivalent to fitting a smooth curve to the ray path rather than the step function that is a result of calculating using layers of constant sound speed.

With each layer having a constant sound speed gradient, the ray path within that layer will have a constant radius of curvature as illustrated in Figure 5.
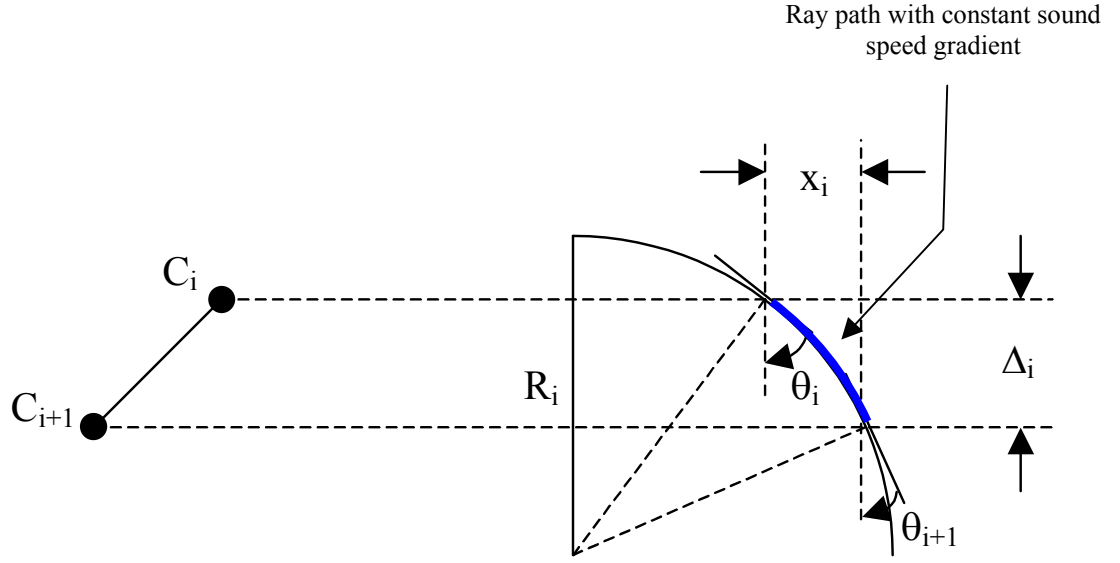
where: R_i = radius of curvature at layer i
C_i = sound speed at start of layer
C_{i+1} = sound speed at end of layer
Δ_i = layer thickness
x_i = horizontal distance
θ_i = ray angle at start of layer
θ_{i+1} = ray angle at end of layer

Figure 5. Ray path with constant sound speed gradient (after de Moustier 1998)

This constant radius of curvature can be calculated using equation 2.6 [de Moustier 1998].

$$R_i = -\frac{1}{pg_i}$$

$$g_i = \frac{C_{i+1} - C_i}{\Delta_i}$$

(2.6)

where: R_i = radius of curvature at layer
p = ray parameter
g_i = sound speed gradient of layer
C_i = sound speed at start of layer
C_{i+1} = sound speed at end of layer
Δ_i = layer thickness

The horizontal distance covered in each layer can then be calculated based on the radius and the ray parameter as detailed in equation 2.7 [de Moustier 1998].

$$x_i = R_i(\cos\theta_{i+1} - \cos\theta_i) \quad = \quad \frac{\cos\theta_i - \cos\theta_{i+1}}{pg_i}$$

where: x_i = horizontal distance
θ_i = ray angle at start of layer
θ_{i+1} = ray angle at end of layer
p = ray parameter
g_i = gradient in layer

(2.7)

And the time can be calculated using the harmonic sound speed as in equation 2.8 [de Moustier 1998].

$$t_i = \frac{R_i(\theta_i - \theta_{i+1})}{C_{H_i}} \quad = \quad \frac{\theta_{i+1} - \theta_i}{pg_i{}^2\Delta_i} Ln\left[\frac{C_{i+1}}{C_i}\right]$$

where: t_i = time in layer
θ_i = ray angle at start of layer
θ_{i+1} = ray angle at end of layer
p = ray parameter
g_i = gradient in layer
C_i = sound speed at start of layer
C_{i+1} = sound speed at end of layer
C_{Hi} = harmonic sound speed to end of layer
Δ_i = layer thickness

(2.8)

However, in practice, the known parameters that we have in order to calculate the time and horizontal and vertical distances are the two-way travel time, the ray parameter, the sound speeds at the start and end of each layer and the thickness of each

layer. Using the following formulas [de Moustier 1998] it is possible to calculate the time and the horizontal distance for each layer.

$$t_i = \frac{a\sin[p(C_i + g_i\Delta_i)] - a\sin[pC_i]}{pg_i^2\Delta_i} Ln\left[1 + \frac{g_i\Delta_i}{C_i}\right]$$

$$x_i = \frac{\sqrt{1-(pC_i)^2} - \sqrt{1-(p(C_i + g_i\Delta_i))^2}}{pg_i}$$

(2.9)

Where: t_i = time in layer
x_i = horizontal distance
p = ray parameter
g_i = gradient in layer
C_i = sound speed at start of layer
C_{i+1} = sound speed at end of layer
Δ_i = layer thickness

While iterating through the sound speed gradient layers in the water column, the horizontal distances and the layer thicknesses are summed until one half of the two-way travel time has been reached. The sums of these two values provides a complete, transducer relative, position for the sounding. The point at which the time is equal to one half of the recorded two way travel time will obviously not commonly occur exactly on the end of one of the predetermined layers. It is therefore necessary to iteratively subdivide for this last layer to converge on a solution with the total two way travel time. [O.M.G. 1998].

2.4 Sound Speed Measurement

2.4.1 Introduction

The accurate determination of the speed of sound in water has been a goal since 1826 when Colladon, Sturm and Wood made the first recorded measurements on Lake Geneva, Switzerland. This was accomplished by striking a bell underwater at one station while simultaneously setting off a visible flash of gunpowder. At another station 10 miles distant, an observer measured the interval between the visible flash and the arrival of the underwater sound. Using this method, the sound speed was determined to be 1435 metres per second with a temperature of 8°C [Colladon 1827]., which was probably relatively accurate for the location and time

In modern sound speed measurement, there are two primary methodologies used. The first is the indirect method where the sound speed is calculated from measured parameters, such as temperature salinity and depth. The second, more recent method is to directly measure the speed of the sound through the medium using an acoustic transducer

2.4.2 Indirect Methods

Most indirect methods rely on the relationships of sound speed with temperature, salinity and depth. The assumption is made that these relationships are constant throughout the oceans. While this has been shown by the overwhelming majority of data to be true, there have been small disparities observed, due particularly to an observed variability in the ratios of the ions discussed in section 2.1.3 [Pickard 1968].

2.4.2.1 Temperature

In the open oceans the salinity is a fairly well known value that is often predicted. Due to this property the simplest method to determine sound speed is to assume a standard salinity profile with depth and measure the temperature and depth profiles. The sound speed can then be inferring from the one predicted (salinity) and two measured (temperature and depth) profiles. This has been done in the deep ocean for many years using the bathythermograph (see Figure 6), which is usually an expendable sensor with a thermistor that measures temperature and has a known constant rate of descent in order to determine depth.
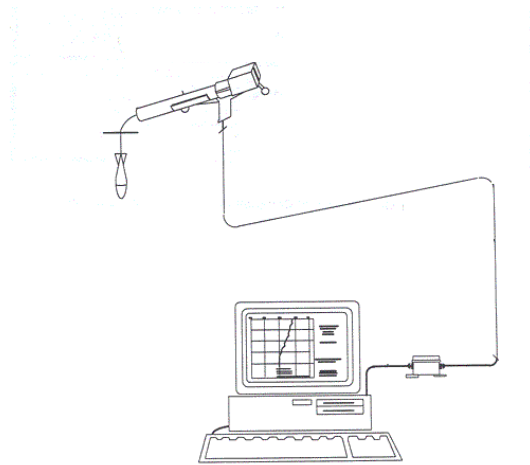
Figure 6. Expendable bathythermograph system

While the method using an assumed salinity is useful for the open ocean, its use is limited in coastal waters where water bodies have not stabilized and salinity and temperature are much more variable. The assumption of an assumed salinity restricts the possible accuracies.

2.4.2.2 Salinity

Temperature is relatively straightforward to measure, while salinity is considered to be much more of a challenge. The original method, and still the standard to which others are referred, is the Knudsen silver nitrate titration measurement. This method actually determines the amount of chlorine ion, and from this, the total salinity is calculated using the known ratio of chorine ions to total dissolved ions. This resultant

value is known as the *absolute salinity* denoted by "S$_A$". The accuracy of this method is considered to be +/- 0.02 ppt, which translates to 0.5 m/s in sound speed [Pickard 1983].

2.4.2.3 Conductivity

The titration method is obviously not suited to in-situ measurements and is time-consuming to perform. More commonly salinity is measured using the relationship of salinity to the electrical conductivity of water. The electrical conductivity of water is also very dependant on temperature and therefore accurate temperature measurements must be made in conjunction with conductivity measurements. This method has given rise to a class of instruments called C.T.D.s (Conductivity, Temperature and Depth) as shown in Figure 7.

Figure 7. Conductivity Temperature and Pressure Sensor (Applied Microsystems Ltd.)

These instruments vastly improved the accuracy and ease with which in situ measurements can be made. The value obtained from this method is known as the *practical salinity* denoted by "S". The accuracy of current instruments is claimed to be in the range of +/-0.01 ppt in salinity or 0.25 m/s in sound speed.

This method makes the assumption that the relationships between conductivity and salinity, and between salinity and density are constant throughout all the oceans. Although this is usually a reasonable assumption, studies have shown that there are global variations in these ratios, especially with respect to salinity [Pickard 1968].

2.4.3 Direct Methods

The direct measurement of sound speed requires an acoustic measurement technique. For the purposes of echosounding, where the sound speed is the variable of primary concern, it is perhaps most desirable to measure the speed of sound directly.

2.4.3.1 Interferometry

Interferometry is currently considered to be the most accurate direct method for the measurement of sound speed [Fujii 1993]. Interferometry has been used in different configurations by scientists such as Del Grosso, Mader and Carnvale [Carnvale 1983] to make baseline measurements of the speed of sound in pure and salt water for the development of speed of sound equations. This method has been accomplished in several different manners, however the principle is to measure the phase nulls of overlapping acoustic wave trains to measure the wavelength of an acoustic signal through a water sample over a known distance at a specific frequency.

Carnvale described a simple example of this method in his early work [Carnvale 1968]. In this method an acoustic signal at a known frequency is transmitted through a water sample over a very accurately measured distance. A portion of the sample is reflected back through the sample as shown in Figure 8 to produce a second signal with precisely two times the direct signal path length.
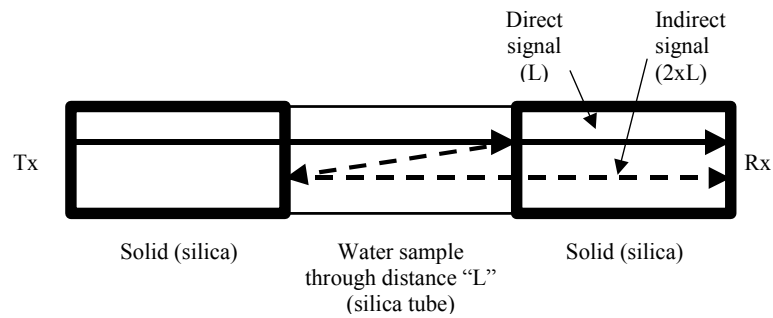
Figure 8 Principle of ultrasonic interferometer construction.

The frequency is then adjusted until a null is observed from the overlap of the direct and the reflected wavetrain. A null will only be created when there are an integral number of waves being transmitted through the sample. By performing this exercise through a range of frequencies the integer number of wavelengths can be resolved resulting in an accurate wavelength measurement.

Using the relationship of $c = f_n \lambda$ where c is the speed of sound, f_n is the frequency at which a null appeared and λ is the wavelength at that null frequency, the sound speed is very accurately calculated. Modifications have since been made to the technique including variable ranges and corrections for internal reflections [Del Grosso

1972]. The resulting modern measurements are considered to be accurate to 0.015 m/s [Fujii 1993].

2.4.3.2 Sing-around

The first technique is termed the "sing-around" method. This method transmits short pulses of sound over an established, stable distance. When the reflection of the sound pulse is received, it triggers another sound pulse to be transmitted. What is then measured is the number of pulses transmitted or the pulse frequency, which will vary directly with sound speed. There are two classes of instrumentation in this field, the first being laboratory instrumentation and the second being field sensors that are practical and cost effective to use in a hydrographic survey. In the case of lab equipment, it is possible to obtain accuracies of up to 0.045 m/s[Fujii1993], while in the case of field equipment accuracies have to date been limited to approximately 0.25 m/s [Eaton 1996].

2.4.3.3 Time of Flight

A more recent method is termed a true "time of flight" method. This method is based on a conceptually much simpler procedure of measuring the time for a single pulse to travel an established distance. This method has some significant advantages that

enable more accurate results in field applications. The use of the sing around method previously discussed is prone to errors due to multiple echoes and transducer ringing. With the time of flight method there is only one pulse in the water at a time, eliminating the multiple echo errors. The use of modern transducer construction has also limited the ringing problems. The use of a single pulse also means that the response time of the sensor is much higher than previous systems. Modern time of flight sensor response times are in the order of 0.15 ms as compared to 85 ms for C.T.D.s and 1 ms for the sing-around method. This faster response time removes the requirement to slowly lower the sensor through the water column. These sensors have a resolution of 0.015m/s and an accuracy of 0.05 m/s. The accuracies attainable by these sensors is suggested to be even higher, however there is currently a limitation on the calibration of the systems due to the accuracies of the original measurements used to create the speed of sound in water equations that are necessary for instrument calibration [Eaton 1996].

2.4.4 Calibration of field deployable, direct method instruments

Instrumentation used for direct sound speed measurement must be calibrated for different pressures, temperatures and salinities.

Currently instrumentation is calibrated by referring to one of the equations discussed in section 2.2.1. While these equations are considered very accurate, there are two sources of uncertainties. The first is the accuracy of the original measurements and

the second is the fit of the measured parameters; sound speed, temperature, salinity and pressure to the equation.

Of the two currently accepted equations, the Chen-Millero and the Del Grosso's, the Del Grosso equation is considered by some to be more accurate, but it has a narrower range of parameters for which it is valid. While both equations are considered to be the most accurate solutions available, there is a discrepancy between the two equations that results in a small amount of ambiguity when determining sound speed from temperature, pressure and salinity. While the discrepancy is relatively small, with modern sound speed sensors capable of 0.05m/s resolution, it is becoming a significant concern when attempting to perform sensor calibrations (see Figure 9).
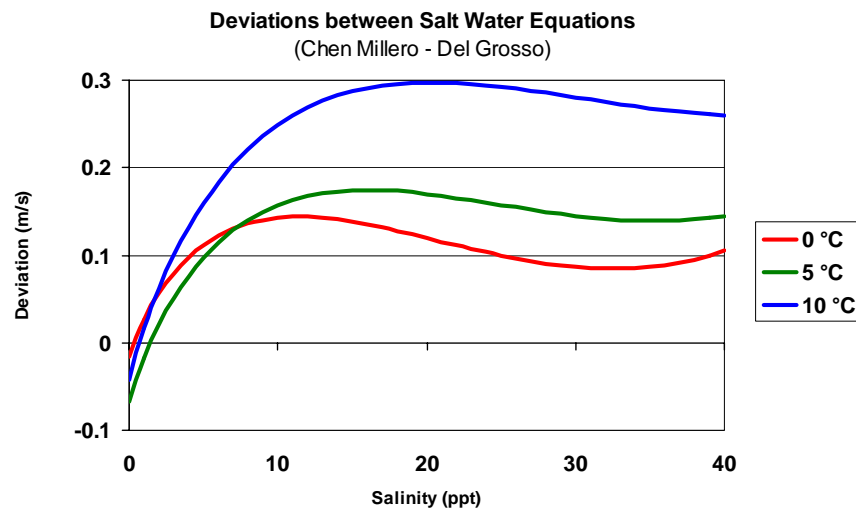
Figure 9. Differences between sound speed equation solutions at temperatures of 0, 5 and 10 degrees Celsius at a pressure equivalent to 5m depth, at a latitude of 49º north.

Presently there is no universal agreement on the equation that should be utilized in calibration and this is becoming the limiting factor to field sound speed sensors as the

precision is approaching that of the original measurements used for seawater sound speed equation development

2.5 Multibeam Echosounders

2.5.1 Introduction

The advent of the multibeam echosounder has given the hydrographer an extremely capable, high-density mapping tool. While the traditional tool of the hydrographer, the single beam echo sounder, can be accurate in the vertical component, the majority of the seafloor is not ensonified and a large part of the ocean floor must be derived by interpolation between these sparsely measured values.

Multibeam sonars consist of a transducer, a receiver, a processing unit and a controller unit and logger. The transducer transmits a beam that is narrow in the along track direction and wide in the across direction. After this beam is reflected or backscattered off the ocean floor, it is sensed by the receive array of the transducer which is separated into multiple discrete beams. The resulting returns are processed for bottom detection by the processing unit. The bottom detection is then associated with ancillary data from the positioning and orientation system and stored as a depth positioned in three dimensions and time.

2.5.2 Transducer Array

Multibeam transducers are made of a material with piezoelectric properties. Piezoelectrics have the capability to convert electrical energy into mechanical energy and vice versa. This gives the transducer the capability to transmit an acoustic pulse into the water when it is activated by an electrical current. The same transducer is then able to produce an electrical charge when it is mechanically compressed by an echo of the originally transmitted pulse [Urick 1983].

The transducer is constructed in such a way as to form the beam into a particular shape (beam forming). In the theoretical case of an ideal point source, the beam will be in the form of a sphere with the acoustic pulse travelling out equally in all directions. The first returning echo would then be from the reflection point closest to the source.

However, through careful design, a transducer can be constructed in such a way as to restrict the sensitivity of the transducer into a particular angular sector and direction. By using a string of theoretical ideal point sources we can produce another theoretical transducer called the line array. The effect of combining multiple point sources in a line is that, through constructive and destructive interference, a beam sensitivity that is wide in a plane that is drawn orthogonaly to the line of the point sources, and narrow in a plane drawn along the line of point sources is formed.

While a point source is only a theoretical concept, a series of transducer elements can be combined into a rectangular array, with a resulting beam pattern that approximates the theoretical line of point sources as shown below.
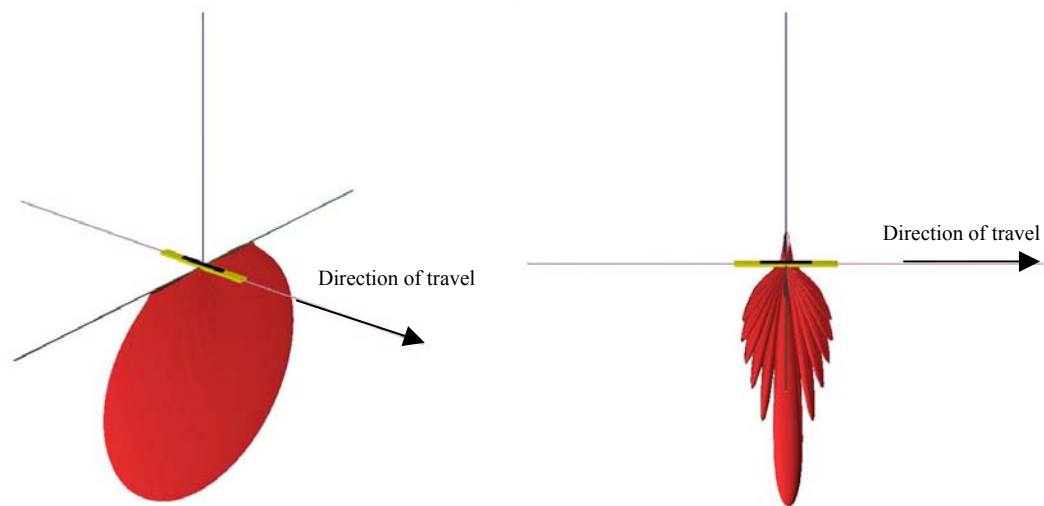
Transmit beam view from starboard quarter   Transmit beam viewed from side

Figure 10. Rectangular array beam configuration (images from synSwath by Hughes Clarke)

By combining transducer elements in various configurations, an array of transducers can be designed to be ideal for the use of directional multibeam echosounders. The combination of transducers to develop a narrow resulting beam is commonly referred to as beam forming (the same term is also used when referring to the forming of a single beam by transducer shape). The two main configurations for multibeam echosounders that will be discussed are the flat array and the arcuate array.

2.5.3.1 Introduction

The use of a combination of transducers to produce a narrow beam by intersecting a portion of a transmit beam with a portion of the receive beam is referred to as combination beam forming. Depending on the transducer array configuration this is accomplished in different manners.

2.5.3.2 Flat transducer Array Beam Intersections

The Mill's Cross is an example of a flat array that uses two rectangular arrays that are placed orthogonal to one another. The transmit portion is the component that is narrow in across track direction and long in the along track. This has the effect of a transmit beam that is narrow in the along track and wide in the across track. The receive array is narrow in the along track and long in across track. Therefore the receive array is "listening" only inside this narrow across track beam; the signal that it will receive from the transmit beam will be the very small intersection of the two beams. If the transducer were to be utilised in the simple configuration, with the entire transmit array simultaneously transmitting and the entire receiver array simultaneously receiving (Figure 11), a narrow resultant beam would be formed directly beneath the transducers (Figure 12).

Transmit array

Direction of travel

Transmit Beam

Receive array

Direction of travel
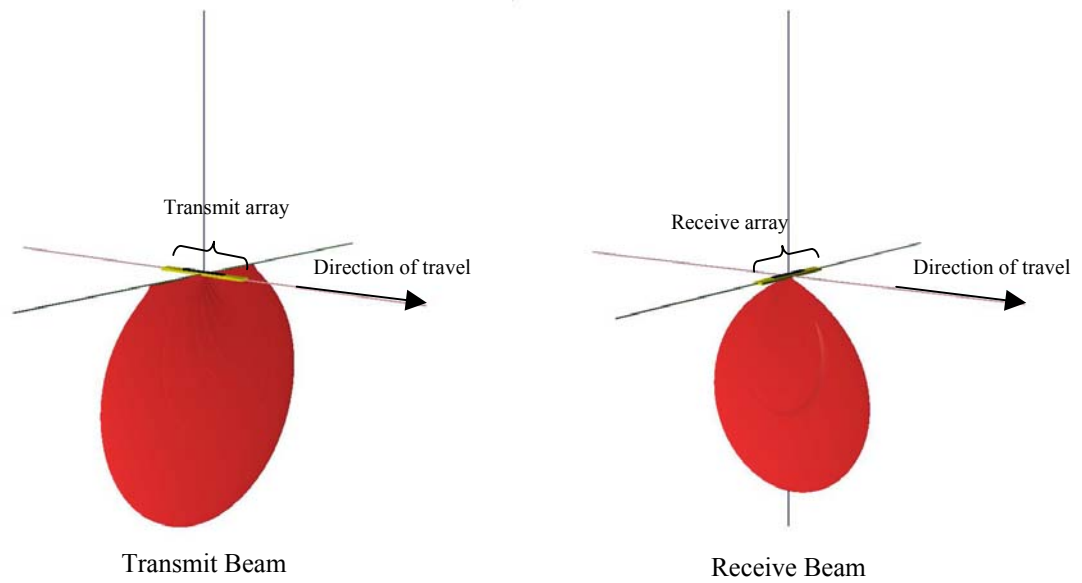
Receive Beam

Figure 11. Transmit and Receive arrays for Mill's Cross

Transmit array

Receive array

Direction of travel

Resultant
beams
intersection
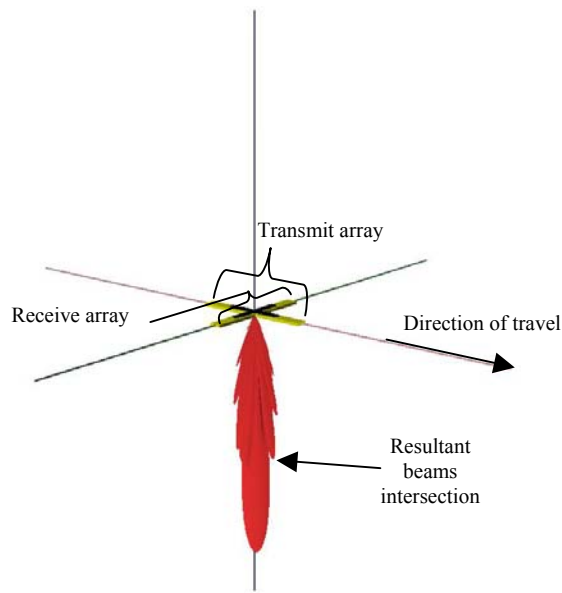
Figure 12. Combined beam form resulting from the intersection of transmit and receive

While this configuration is commonly referred to as the Mill's Cross, it can also be arranged such that the two arrays form a "T" shape instead of an "X", as is the case in the Simrad EM3000, however all the same principles apply.

2.5.3.3 Arcuate Array Transducer Beam Intersections

An example of an arcuate array is used in the Simrad EM1002 [Kongsberg 1998] and is often referred to as a "barrel" array. This arcuate array uses multiple line array staves that are aligned along track of the ship and arranged in an upward curving arc. Each stave is composed of a number of elements as illustrated in Figure 13.
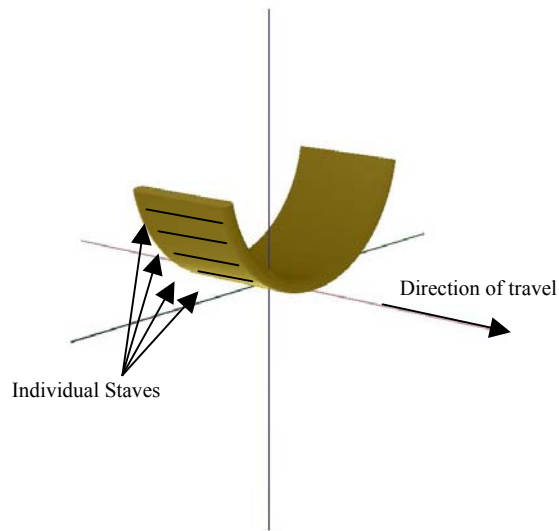
Figure 13. Barrel or arcuate transducer array

In the transmit, some or all of the staves transmit to make wide across track beam. One advantage of this type of transmission is that, while a single element is capable of forming the narrow acoustic beam, the combination of multiple elements

enables more power to be transmitted within the same narrow (in the alongtrack) beam. A second advantage is that, in contrast to the Mill's Cross configuration, the transmitting staves in the Arcuate array are relatively long in the alongtrack direction, resulting in a narrow alongtrack beam.

In order to make a narrow beam on the receive; a number of staves are selected such that their addition makes an array with enough across track length to make a narrow across track beam. When this is combined with the narrow alongtrack beam, the product is relatively narrow in both the along and across track directions.

In order to account for the slight curvature of the arrangements of the staves, slight time delays are added to the outer staves. The larger the number of staves used (the longer the effective receive array length) the narrower the receive beam. If one was only concerned with the beam that is directly tangent to the base of the arcuate array, it is conceivable to receive on all elements (with time delays to account for the curvature) that would result in a very narrow beam in the across-track. An example of this type of transducer is the Simrad EM1002.

2.5.4 Beam Array Processing

2.5.4.1 Introduction

As previously noted, it is possible to produce a single narrow beam directly below a transducer with the two array types discussed. However, the full potential of a multibeam system is only realized when multiple beams over a range of angles are produced. Beam steering is the process that is employed that enables a beam to be received from a desired angle which is oblique to the transducer array. The methods of beam steering vary, depending on the transducer configuration.

The two principle methods of beam steering are physical and electronic. Physical steering employs either an array being mechanically moved to point in the desired direction or, as in the case of the Odom Echoscan in Figure 14, an echosounder may be composed of multiple transducers, each individual transducer pointing in the desired direction.
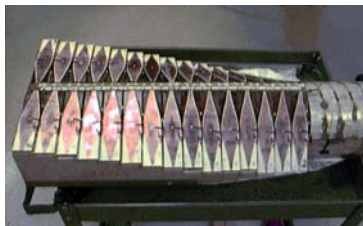
Figure 14. Internal photograph of Odom Echoscan revealing 30 individual transducers, 15 per side, each pointing in the desired direction

Electronic steering is accomplished by digitising the signal and computing beams at the desired angles and beam widths, constrained only by the physical transducers, the electronics and the algorithms used.

The possible beam steering methods used in the flat array and the arcuate array will be discussed in detail.

2.5.4.2 Beam Array Processing, Flat Array

2.5.4.2.1 Mechanical

Conceptually, the simplest method to receive beam steer a flat array transducer would be to physically rotate the receive line array to receive the signal at the desired angle as illustrated in Figure 15. In order to from an array of beams, however, it would be required to mechanically move the entire transducer through the range of angles desired. While this method could theoretically be employed It would be mechanically complex, costly and provide a slow repeat rate

Direction of travel

Transmit beam

40 deg

Direction of travel

Receive beam physically rotated 40 degrees

40 deg

Direction of travel

40 deg
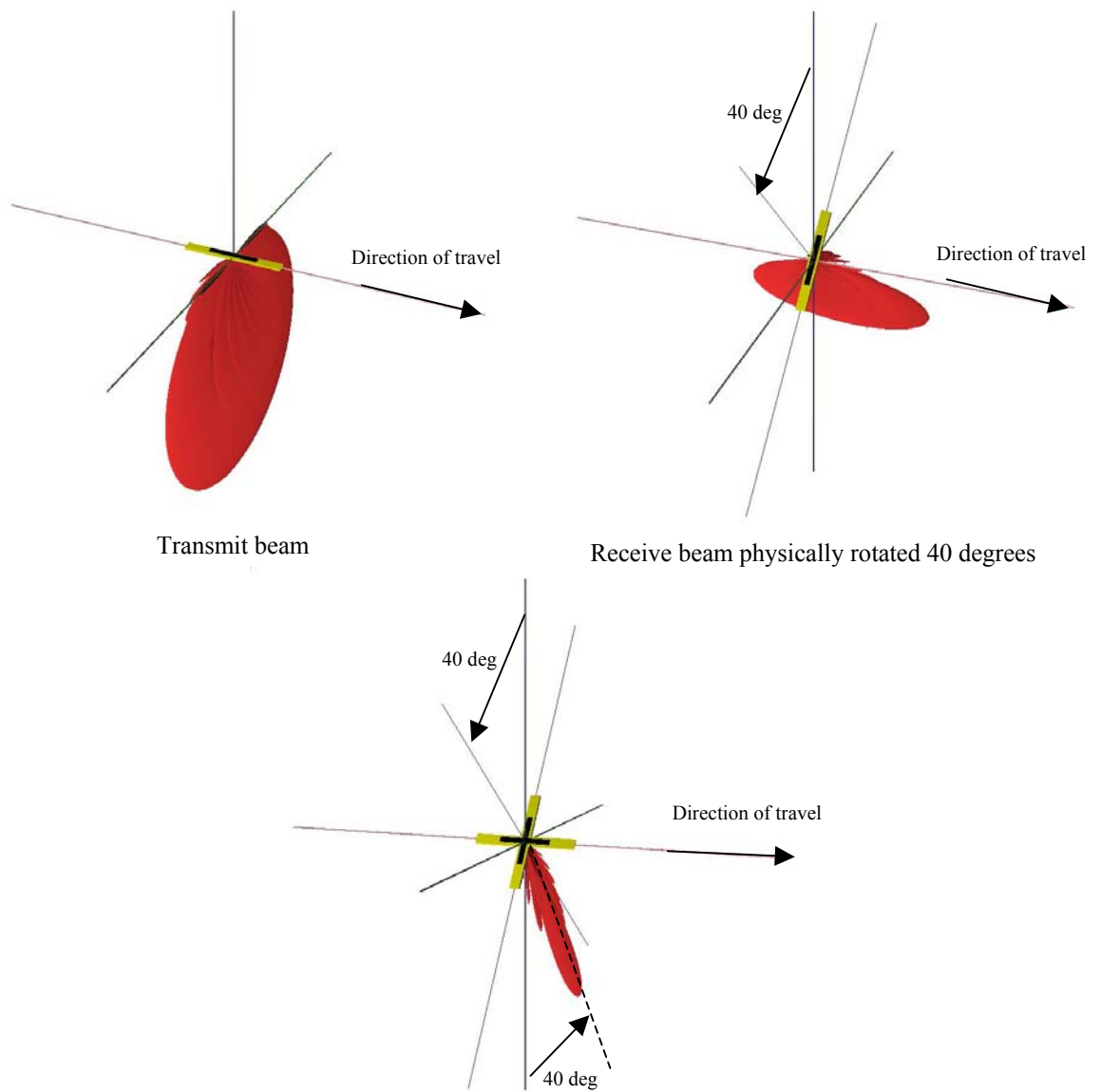
Figure 15. Intersection of physically steered transmit/receive beam

2.5.4.2.2 Electronic Beam Steering

In contrast to physically steering, electronically steering the beams of a flat array enables the formation of a complete array of beams with every transmit receive cycle of the transducer. These electronic methods "virtually" steer the receive beam and in some cases the transmit beam. For a flat array transducer the two primary methods are time or phase delay and Fast Fourier Transform method.

Electronic beam steering methods take advantage of the fact that transducers are not one single element but are composed of many individual elements that can be controlled and monitored individually. These calculations depend on the sound speed at the transmitter, the frequency used and the spacing between individual elements. It should be noted that any error in the sound speed would result in beam pointing errors. This is a critical consideration when surveying in areas where sound speed values are unpredictable and variable such as coastal estuarine areas as is exemplified by the area under consideration in this paper.

2.5.4.2.2.1 Time and Phase Delay

The time delay method introduces graduated time delays at each individual element to virtually "steer" the array as shown in Figure 16. In practice, in a digital system, all of the received waveforms are digitised and placed in a buffer where it is possible to simultaneously calculate all of the required angles to result in many narrow receive beams. Time delay array processing is extremely flexible in its ability to form any number of beams at any angle, limited only by the achievable sampling period of the incoming waveforms and the available computer memory.
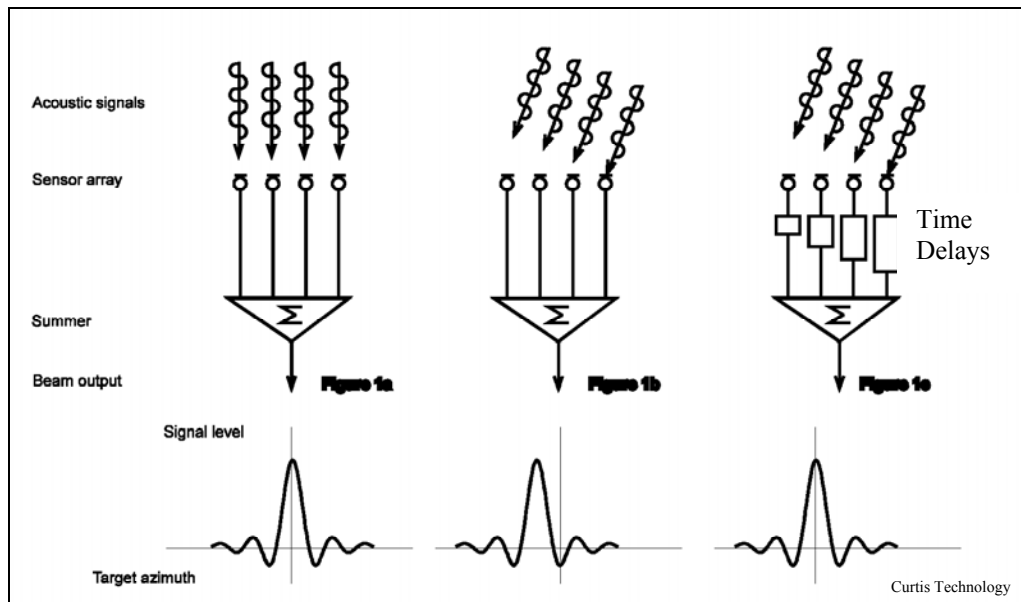
Figure 16. The use of time delays to create a virtual array to detect oblique angle return [Curtis technology 2002]

Formula 2.10 defines the relationship of the acoustic and physical parameters that need to be considered in determining the time delays to be applied. These relationships also illustrate the complexity and challenge in building a modern multibeam transducer and the accuracy of the calculations that the system must perform. For example, a theoretical 300 KHz system with one-half wavelength element spacing (a typical value) would require accurate transducer element spacings of 2.5 millimetres and time steps around 3.5 μsec to obtain a steering resolution of 0.5 degree.

$$\text{time delay at } n^{\text{th}} \text{ element } = \frac{n \times \text{d}}{f \times \lambda} \times \sin \theta \qquad (2.10)$$

Where θ = angle steered
λ = wavelength
d = element spacing
k = element number
f = frequency

Phase delay method is similar in concept to time delay, however rather than time delays; phase shifts are added to each element before they are summed. After adding the phase shifts, the desired steered beam will result in all of the elements receiving the wave fronts at the same time, or in phase. While this is a similar method to time delay, the steering directions are not limited by the sampling frequency, however the number of beams that can be produced is limited by the number of individually monitored staves [Hampson 1997].

2.5.4.2.2.2 Fast Fourier Transform

The final method commonly used with a flat transducer array is Fourier Transform (FFT) beam steering. This method records the instantaneous set of signal magnitudes across the transducer elements. This recorded signal is transformed into a power spectrum distribution using a Fast Fourier Transform. The power spectrum is equivalent to the angular distribution of energy at an instant in time and it is therefore possible to discriminate echo strengths and angles.[O.M.G. 1998]

A Fourier Transform is a mathematical method of breaking up a signal into its set of sine and cosine components. A Fast Fourier Transform is simply an optimization of the discrete Fourier Transform that allows many of the values to be pre-computed and eliminates redundant calculations. This method dramatically speeds up the computation process such that it was possible for early multibeam systems, with their limited computational power, to complete the calculations for beam forming in real time [Williams 1968].

In order to use the FFT algorithm there are certain constraints placed on the calculations. The number of elements, N, must in theory be a power of 2 and the elements must be equally spaced. This does not require that there are physically this many elements however, as the use of null elements as filler at either end of the array will satisfy the requirement. The angular spacing that results is given in formula 2.11 [de Moustier 1998].

$$\theta_k = \sin^{-1}\left(\frac{\lambda}{d} \bullet \frac{n}{N}\right)$$

(2.11)

Where   θ = angle steered
        λ = wavelength
        d = element spacing
        n = element number
        N = number of elements

The negative aspect of this method is that the calculations performed for this FFT binning result in angular beam spacing with each beam being equivalent to a single FFT bin. This results in beam spacing that increases away from nadir reducing the angular resolution as evidenced in the Simrad EM3000 echosounder.

2.5.4.2.2.3 Summary of Electronic Steering

There are two properties of electronic steering that are unique to the method. The electronic steering of beams results in a virtual array that is shorter in length than the true array. As the beamwidth is dependant on array length, this will cause the beamwidth to grow in inverse proportion to the cosine of the steered angle.

Most importantly, in the context of raytracing, electronic steering has the property that any error in the sound speed at the transducer will result in an associated error in the departure angles used for the first step in the raytracing solution. However, as we will be observed later in this paper, under certain condition it is possible for this

error to be offset by further steps in the raytracing calculation based on the same erroneous sound speed value.

2.5.4.3 Beam Array Processing, Arcuate Array

In the case of the arcuate, or barrel array, the beam steering is done by taking advantage of the physical shape of the transducer combined with an appropriate selection of transducer elements.
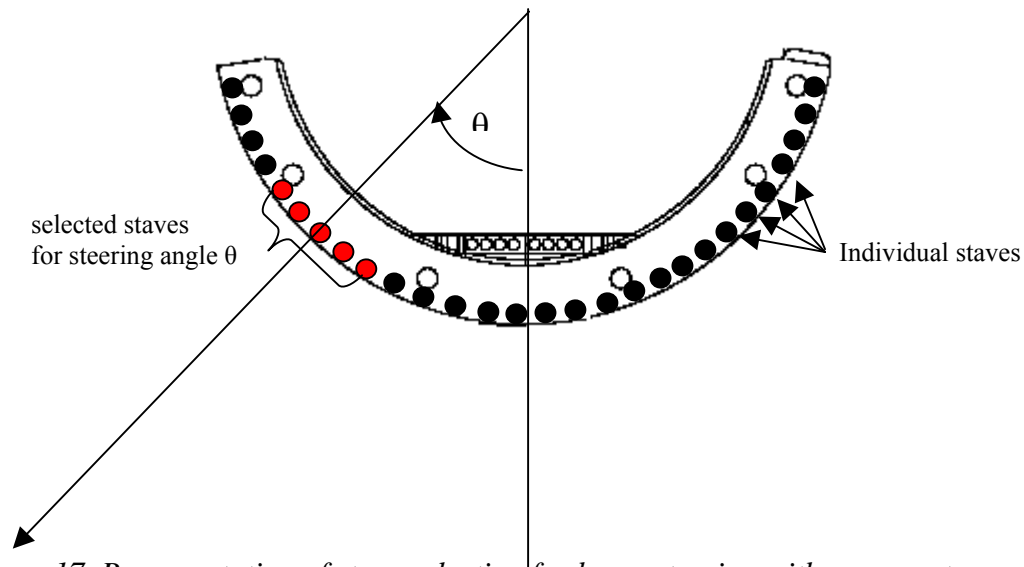
Figure 17. Representation of stave selection for beam steering with an arcuate transducer array (image Simrad Kongsberg EM1002)

By selecting a number of staves along a section of the arcuate array a receive beam can be selected based on their location on the array. As shown in Figure 17, the steered beam will be orthogonal to the tangent of the curve created from the addition of the selected elements. The use of physically pointed sections of the arc also results in

beam widths that are consistent throughout the across track angular range of the transducer. This provides a resolution advantage over the electronically beam steered systems with their increasing beam widths due to their use of electronic steering.

In order to compensate for the amount of curvature in the selected section of the array, minor time delays to the outer staves in the selected arc is required. It should be noted that many systems, in order to increase the angular coverage available to a transducer, employ electronic beam steering in the upper portions of the arc as shown in Figure 18. This has the desired effect of increasing the number of outer beams, but coincident with this are the errors in beam steering and the widening of beam widths associated with electronic beam steering. These effects, however, are mitigated by the fact that the amount of electronic beam steering is small resulting in minimal beam steering errors and beam width widening.

Beam angle determined by physical shape of transducer

Virtual array created using time delays

Increased beam angle determined by physical shape of transducer combined with time delays that increase towards the upper staves
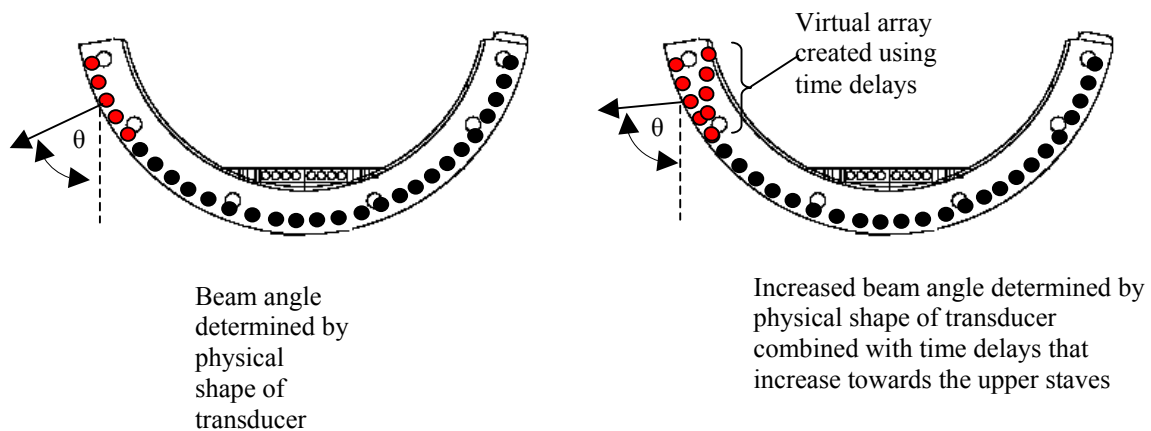
Figure 18. Schematic representation of the use of electronic beam steering in the upper portions of an arcuate array in order to increase angular coverage.

Due to the fact that the beam direction is primarily a result of the physical shape of the transducer, the beam angle is generally not affected by knowledge of the sound speed at the transducer. While any errors in the measured sound speeds will result in raytracing errors through the water column, the initial departure angle will always be correct, with the exception of any steered beams in the upper portion of the arc. This departure angle property is critical in understanding the behaviour of arcuate array systems in areas with variable and unpredictable surface sound speeds.

2.5.4.3.1 Summary of Beam Array Processing, Arcuate Array

The steering of Arcuate array transducers has unique qualities. The amount of computation is drastically reduced compared to electronically steered arrays, due to the use of physical pointing with only minimal calculations required for time delays to account for the curvature and steering in the upper portions of the array, meaning that the departure angle will always be correct, unless steering is employed. This has the detrimental effect of providing an incorrect ray parameter (section 2.3) if the correct surface sound speed is not known. The ability to use multiple staves allows an increased amount of power to be input into the water column. Finally the beam width does not increase as a function of beam angle as is the case in all flat array transducers.

2.6 Fraser River Delta

2.6.1 Introduction

The Fraser River Delta is located on the southern coast of mainland British Columbia. The delta is adjacent to Vancouver, Canada's 3rd largest city.
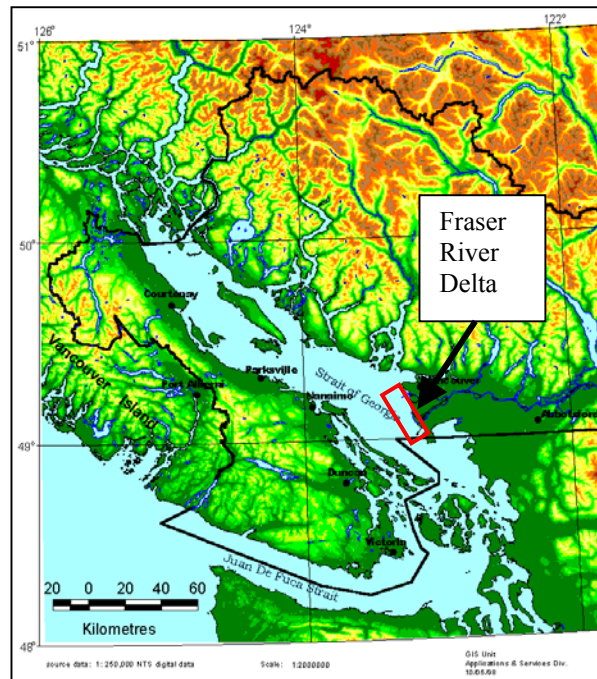
Figure 19. Location of Fraser River Delta within Southern British Columbia and Strait of Georgia (source: Environment Canada, 1:250 000 NTS digital data)

The Fraser River is one of Canada's major rivers with a watershed that covers approximately one quarter of the province of British Columbia (Figure 19). The delta has a 37 km long front with 4 major channels (Figure 20). The South Arm being the

most significant, with seventy five percent of the flow, followed by the North Arm with fifteen percent and then the Middle Arm and Canoe Pass each with five percent [Thomson 1981]. The Fraser is a major source of fresh water and sediment to the estuary. The tides of the estuary are mixed, predominantly semidiurnal with a mean range of 3.1 metres and a spring tide range of 4.8 m. These conditions combine to form a dynamic oceanographic environment.
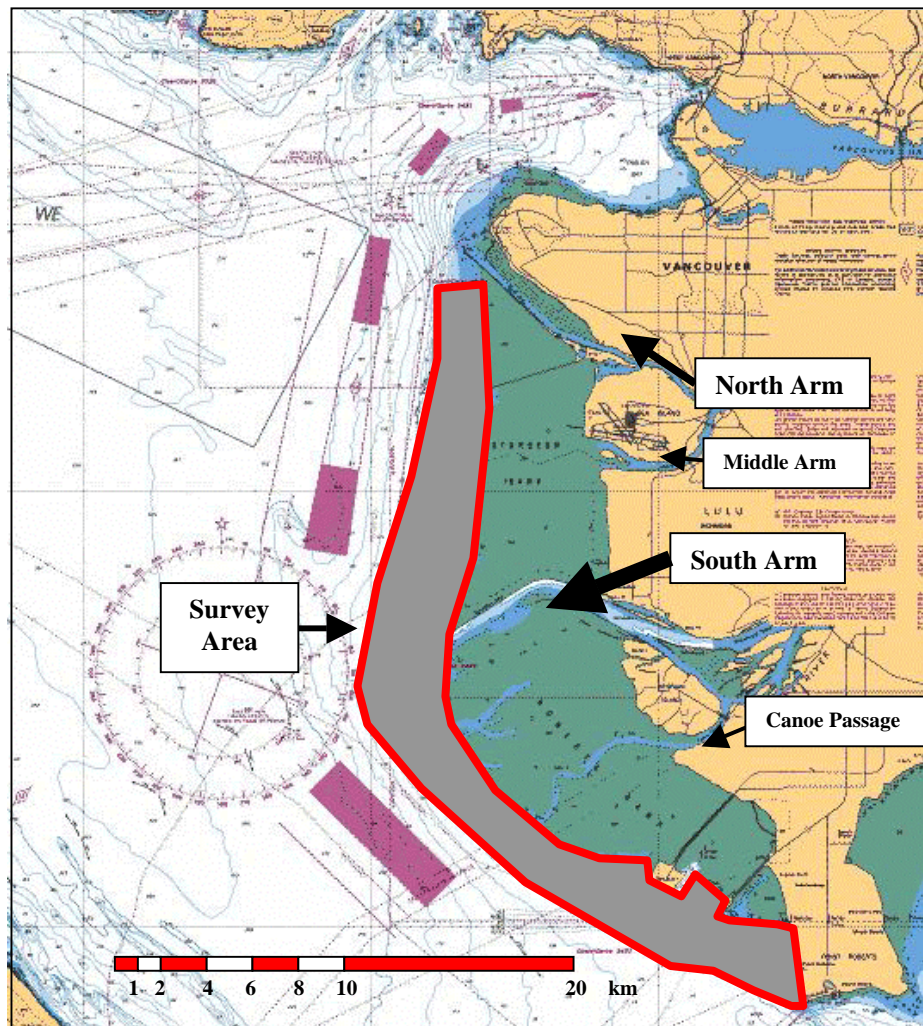
Figure 20. Fraser River Delta identifying Fraser River channels (extract of CHS chart # 3463)

2.6.2 Geology

"In terms of the local geologic setting of the Fraser River delta, it is located in a structural depression of Late Cretaceous and Tertiary clastic sediments near the west margin of the North American plate. This depression forms what is now the Strait of Georgia. Overlying these basement rocks and underlying delta sediments are Quaternary deposits resulting from various stages of Pleistocene glaciation." [Mosher et al 2001]

The Fraser River Delta has been forming for approximately 10 000 years. After the glaciers retreated the land rebounded, causing relative sea level to fall. 8000 years ago the water level fell to more than 12 m below modern levels. However the level was back to near present levels approximately 5000 years ago. The river at one time flowed in a southerly direction into Boundary Bay, but more than 5000 years ago, it switched to its present course of west into Georgia Strait. For the last 5000 years the delta has been prograding westward into the strait. During this time there were major changes in the main water channels until the early 1900s when the channel was contained by the present system of dykes and dredging [Mosher et al 2001].

Tidal flats now extend about 9 km from the diked edge of the delta to the sub tidal slope. The sub-aerial and submarine extent of the delta is over 1000 km² in area. The slope break, marking the transition from the delta plain to the fore slope, lies at about 10 m water depth. The western delta slope is inclined 1-23° (average ~2-3°) towards the marine basin of the Strait of Georgia and terminates at about 300 m water depth, 5-10 km seaward of the edge of the tidal flats [Mosher et al 2001].

The Fraser has an average estimated flow of 3000 cubic metres per second and a sediment transport of 17.3 million tons annually both centred mainly off the mouth of

the South Arm Thomson 1981]. Most of the Fraser River drainage area is alpine or plateau country, with elevations above 1000 m. Due to this fact the most important hydrological event is the snowmelt or "freshet" that occurs every spring. The sediment concentration tends to precede the peak of freshet flow as the source of easily erodable sediment is exhausted as shown below.
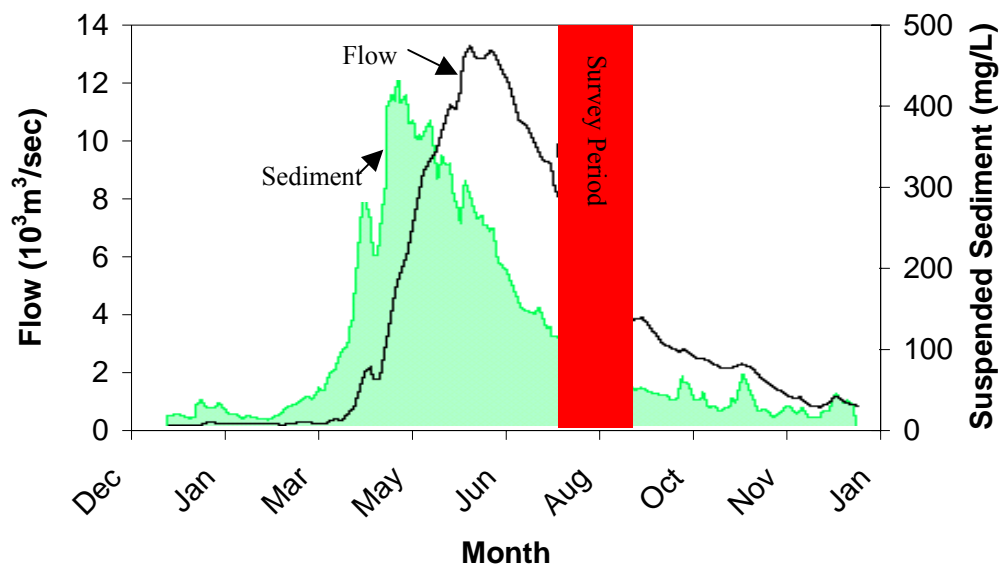
Figure 21. Example hydrograph and Suspended Sediment graph (Water Survey of Canada 1972)

The presence of suspended sediment will have an influence on the sound speed measurements in an area, however the effect is minor and quickly becomes negligible once the fresh and seawater have mixed.
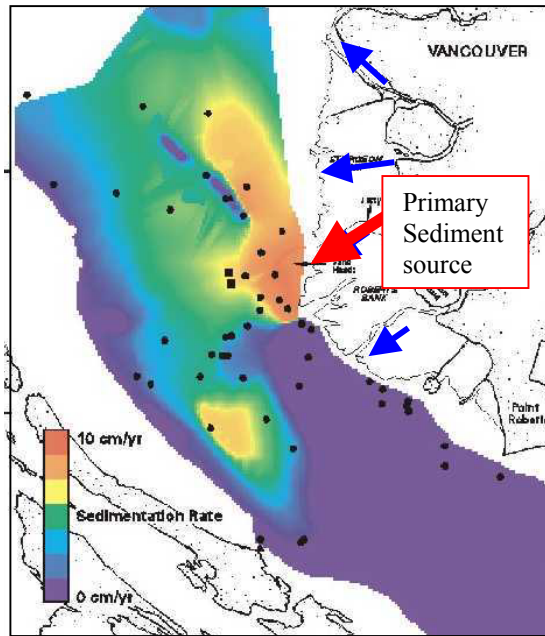
Figure 22. Sedimentation rate for the Fraser Delta slope and prodelta, based on radiation fallout stratigraphy (Hart et al., 1998)

The sediment deposition on the delta is asymmetrical, due to the interference of the dykes and other artificial barriers (Figure 22). There is a residual northward tidal current that accounts for the concentration to the north of the primary source [Mosher et al 2001].

The sediment is composed of approximately 65% muds and clays with 35% sand as observed by Barrie et al [2000]

2.6.3 Oceanography

The Oceanography in the Sturgeon Bank area is dominated by the influx of the Fraser River. The South Arm is the predominant source with 75% of the flow with the

North Arm contributing 15%. The flow of the river is primarily constrained by artificial factors. There are currently dikes on the both the North and South Arms. Due to these artificial constraints, the area can no longer be considered to be following normal deltaic processes. Dikes are generally built in order to channel the river and control its floodplain for the purpose of protecting against flooding and extreme tides. However, the side effect is that sediment transport from the river to the natural floodplain is interrupted, resulting in increased deposition in the river and near its mouth. Due to this effect, rather than a normal prograding deltaic front there is a small amount of net erosion caused by sediment starvation. It is also speculated that there are effects from other artificial features in the area including a lighting pier for the airport and a sewer outfall. The principle effect of these features is to further distort the natural current patterns in the area resulting in asymmetrical sediment movement and deposition.

In terms of the effect on a hydrographic survey, the two principal oceanographic factors of concern in this area are the temperature and the salinity effects from the river. Before interaction with seawater there is already a significant variability in the temperature of the fresh water on both a day-to-day scale and a seasonal scale. This is shown in figure 27 for a station that is monitored 140 km upstream from the delta, which, while not representative of the temperatures found in the delta, it does gives an indication as to the trend introduced from the river. The salinity of the river is variable on a seasonal scale, however, is not considered to be significant within the timeframe of the hydrographic survey.

Fraser River Temperature
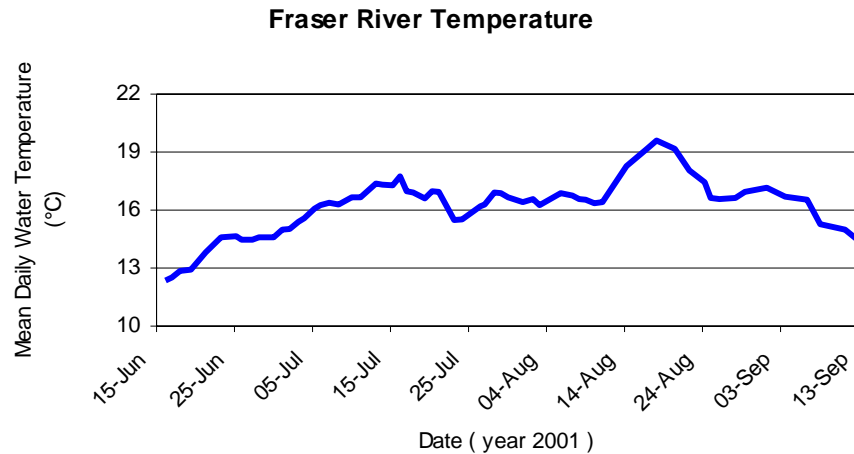
Figure 23. Fraser River temperature summer 2001 at Hope, British Columbia (Fraser River Environmental Watch Report- Department of Fisheries and Oceans)

The primary concern for the hydrographer is the manner and rate at which the fresh water and the salt water mix in the delta area as both temperature and salinity have drastic effects on the speed of sound in water. There are many forces to be considered in this process as discussed in section 2.2.2, however the primary forces that are variable on a time scale that effects a hydrographic survey are the influx of fresh water from the river, the tidal forces and resulting currents and the mechanisms by which both forces interact with artificial and natural topographic features.

It has been shown that there is an overall northern residual current throughout the area, however this is also complicated by numerous eddies and currents caused by natural and artificial topography.

2.6.4 Human Intervention

The Fraser River Delta area is home to one half of the population of British Columbia and its population grew eight percent between 1996 and 2001 [Government of B.C. 2003]. Along with the urban population is a major shipping industry with over 3 million tonnes of international cargo shipped through the Fraser River port in 2001. The Delta is also home to a large coal terminal and the ferry terminal is considered one of the busiest in the world. The combination of the industrial traffic and the need to control the River within the urban environment requires that the river be consistently constrained within its present channels and dredged to ensure safe navigation and easy access for heavy shipping [Thomson 1991].

Since the early 1900s the North and South arms of the Fraser River have been contained by dykes and routinely dredged to maintain their depth. As well, barriers have been placed that restrict the free movement of water including a sewer outfall and airport lighting pier. Dredging has resulted in the majority of moved sand that would normally be deposited in the delta being moved out to dumping areas in Georgia strait and to construction projects alongside the river upstream. The dykes and dredging have resulted in channels that are no longer able to significantly change their course. The course of the main channels has not significantly deviated since the early 1900s, with the exception of Canoe Passage, which has little navigation value and contains a minor part of the total river flow. The effect of the dykes and other barriers has also been the production of eddies and currents. This results in an asymmetrical deposition of sediment as well as the creation of steeper than normal delta front slopes. There is some

concern that this may result in unstable slopes that have the possibility of slumping with possible damaging effects due to earth movement and wave action (especially in the event of the anticipated great 200 year earthquake) [Mosher et al 2001].

The survey on the Fraser River Delta was in part designed to investigate the sedimentation and the stability of the area. With maximum sedimentation rates of 10cm per year significant changes should be easily detectable in surveys as close as 5 years apart.

CHAPTER 3 ANALYSIS OF REFRACTION ISSUES IN

FRASER RIVER MULTIBEAM SURVEY

3.1 Survey Resources

3.1.1 Overview of CHS Resources

The Pacific Region of the Canadian Hydrographic Service currently has two multibeam systems, the Simrad EM1002 and the Simrad EM3000. The EM1002 uses a arcuate array transducer, capable of depths of up to 1000 metres and is outfitted with a real time surface sound speed sensor. This system is currently mounted on the Canadian Coast Guard ship "Vector", a 40-metre vessel capable of extended offshore work. The Simrad EM3000 uses a Mill's Cross flat array transducer, without a surface sound speed sensor and is capable of depths of up to 150 metres. This system is currently mounted on the Canadian Coast Guard survey launch "Revisor", a 12-metre launch capable of working inshore and calm near shore waters.

The region has two systems for measuring sound speed profiles. The first is a traditional winch deployed sound speed sensor, which requires the vessel to stop for profile measurement. The second is the Moving Vessel Profiler 30 discussed in this

report, which can be mounted on either vessel, but only has a depth capability of 30 metres when used while the vessel is underway.

3.1.2 Survey Platform

The survey vessel applicable to the work reported here is the "Revisor", a 12-metre fibreglass survey launch that was originally designed and built for surveys in support of updating hydrographic charts. The vessel has since been adapted to multibeam surveys. All systems, including echosounder, sound speed measurement and data processing, are aboard the vessel making it a self-contained multibeam survey platform. The vessel size and manoeuvrability enable it to be used within busy shipping lanes and into minimum depths of three metres.

3.1.3 Depth Measurement

The depth sensor is a Simrad EM3000 single transducer multibeam echosounder. This is a 300 kHz, 127-beam system, with an effective 120° of swath width. The transducer is a flat Mill's T cross, flush-mounted on the keel in a near-level configuration, pitched bow upward 3 degrees for improved water contact. The system has

beam widths of 1.5 degrees at nadir which increases in their across track dimension as the beams are steered away from nadir to approximately 3 degrees at a pointing angle of 60 degrees. The system is capable of measuring depths in excess of 100 metres, depending on the bottom backscatter strength and water column attenuation [Kongsberg Simrad 2001].

3.1.4 Sound Speed Measurement

Sound speed was measured with a Moving Vessel Profiler 30 (MVP 30). This is an "underway ocean-profiling system" built by Brooke Ocean Technology Limited. The term "underway" is used to signify that water sound speed profiles can be collected without the need for the vessel to stop or reduce speed. As a reference, these profiles can be collected approximately every 3 minutes to a depth of 30 metres with the survey vessel travelling at 8-10 knots. [Brooke Ocean Technology Ltd. 2003].

The system is comprised of four subsystems; the winch, the overboarding sheave, the free fall fish (Figure 23) and the electronic controllers. The sound speed sensor on the free-fall fish is an acoustic true time of flight sensor as discussed in section 2.4.3.2. The sensor has a 0.05 m/s accuracy, a response time of 0.15ms and an update rate of 25 Hz. The depth is measured with a semiconductor strain gauge pressure sensor with an accuracy of 0.05 % [Applied Microsystems Ltd. 2003].
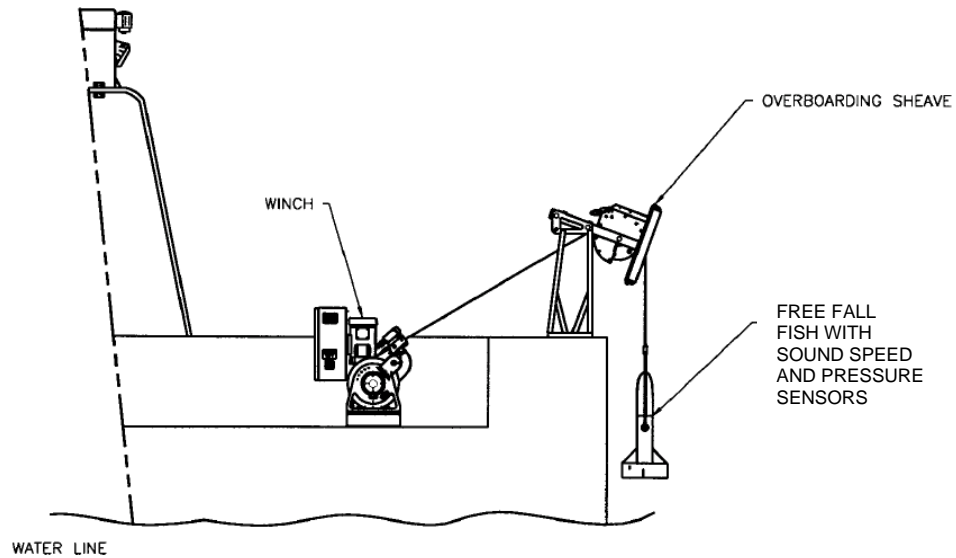
Figure 1. Components of MVP 30 sound speed profiling system situated on stern of survey vessel (image courtesy Brooke Ocean Technology)

The principle of the system is to release the fish, with the mounted sensors, off the stern of the vessel with enough weight to enable the fish to essentially free-fall to a desired depth at operational speeds. When the pressure sensor on the fish detects that the desired depth has been reached, a brake is automatically applied by the winch, arresting the free-fall. The fish is then retrieved to near the stern of the vessel by the winch. soon as the fish is close to the stern of the vessel, the cycle can commence again, without the need to bring the fish on to the vessel deck. At all times during operations the depth and sound speed is being transmitted through the cable to the controlling software where it can be logged.

A water depth measured by an independent system, in this case a single beam echosounder, at the time of fish release determines the depth allowed in the free-fall. Due to the fact that the fish descends in a near vertical direction, this depth measured at sensor release can be used as a guide to stop the descent at a safe distance above the ocean floor. The depth is also continuously monitored while the fish freefalls and compared to fish depth in order to stop the descent if the depth is less than at the fish release.

Due to the design of the fish and associated bracket, its trajectory after the descent is arrested is initially very close to vertically upward (see Figure 24). This combination of a near vertical free-fall and a near vertical initial ascent results in significant reduction in the risk of losing the sensor by grounding or snagging on rising topography.
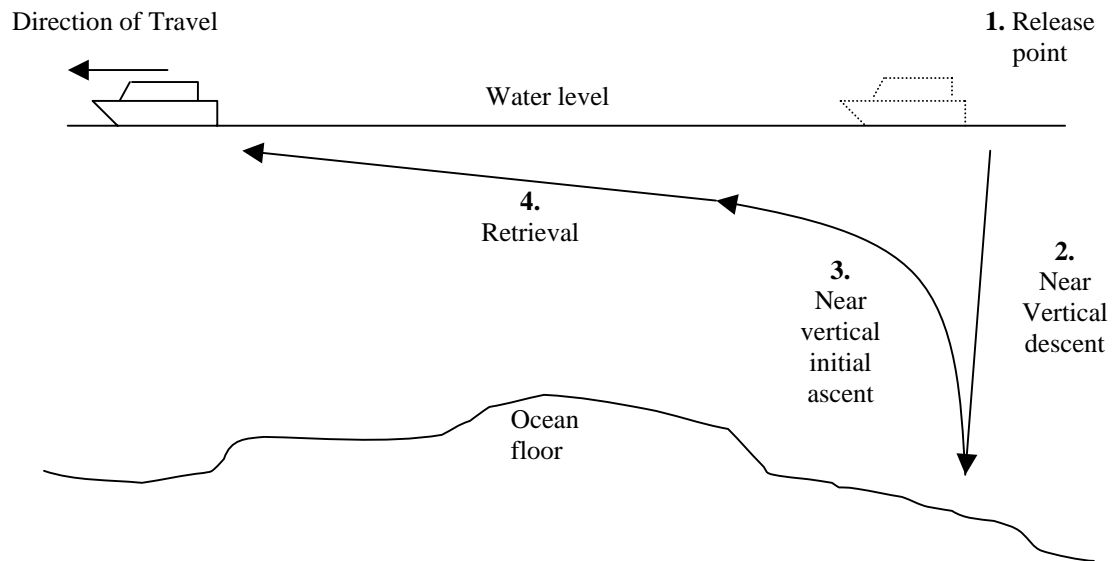
Figure 25 Sound speed measurement sequence profile

3.1.5 Positioning and Orientation

Navigation and attitude information is provided by a "POS/MV" G.P.S.-aided inertial system built by Applanix Corporation. This system uses a combination of two global positioning system receivers and a strap-down inertial sensor. The combination of these sensors enables the output of complete position and attitude solutions at rates of up to 100 Hz. Horizontal position accuracy is +/- 5 m using a wide area differential GPS link [Geographic Data BC, 2003]. Attitude measurement has a claimed accuracy of 0.04 (95%) degrees in roll, pitch, and heading. Heave measurement accuracy is the greater of 10 cm (95%) or 10 percent of heave amplitude. within motion periods of less than 20 seconds [Applanix Corporation2002].

The offset distances and bearings between the transducer, the inertial sensor and the two G.P.S. antennae, as well as associated time delays are checked using a "patch test" procedure that uses reciprocal survey lines and varying vessel speeds to highlight any erroneous offsets.

3.2 Survey Methodology

3.2.1 Echo Sounding Methods

The multibeam survey was carried out using standard Canadian Hydrographic Service practice. This practice requires that lines be run in order to obtain 200% coverage (Figure 25) at maximum speeds of 12 knots. Lines are run freehand in order to "paint" the area by following the previous line's outer beams. Using an EM3000, with its swath aperture of 120°, this results in an effective line spacing of 1.7 times the water depth. Check-lines run perpendicular to the main survey lines in order to assist in the validation of the sounding and tidal data.
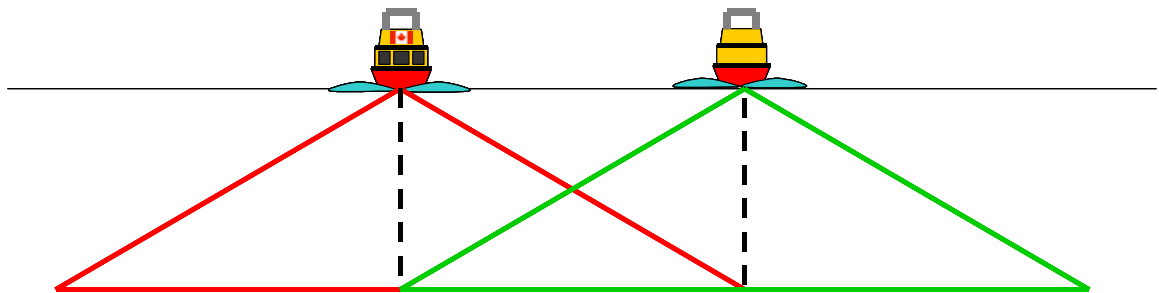
Figure 26. Overlap of the multibeam swath of two consecutive lines showing the centre of the current survey line being run at the outside edge of the previous survey line.

3.2.2 Sound Speed Measurement Methods

The 2001 Fraser River survey was the first official survey with the MVP 30 for the Pacific Region of the C.H.S. and, accordingly, procedures were developed and improved throughout the survey. The frequency of casts was set at every two thousand meters along-track (approximately every 10 minutes) or when the observed surface sound velocity changed by greater than 3 metres per second, whichever occurred first. The surface sound speed was observed by monitoring the readout from the fish being towed behind the vessel between casts, simulating a hull mounted surface sound speed sensor. The actual technique used to drop and retrieve the sensor consisted of two separate procedures depending on the desired depth of the cast.

For casts shoaler than 30 m, the tow fish was released and allowed to stream out the stern of the vessel with no reduction in vessel forward speed. The system is capable of reaching this depth while cruising at 12 knots, which is a maximum for this vessel. As soon as the sensor reached the target depth, the profile is automatically sent, via serial line, to the Simrad multibeam controller software. At this point, it is then manually checked and edited if necessary. It was then necessary to briefly stop logging in order to introduce a new profile.

For depths of over thirty metres it was decided to slow down the vessel just prior to starting the cast, enabling the fish to descend farther, owing to the fact of not using cable for forward movement. With the vessel in minimum forward motion (1-2 knots)

this technique typically enabled depths of up to 90m to be reached. As soon as the profile had been loaded the vessel resumed full speed and the survey continued.

The fact that the vessel was still in motion while data logging was stopped, in order to enter the sound speed profile, meant that there were small gaps in the sounding coverage. For a typical sound speed profile cycle, this would result in a maximum of 20 metres along track of missed soundings. This was seen as a compromise between survey efficiency and data quality. Due to the methodology of 100 percent overlap, it was rare that an area was completely missed by the system, however redundancy was obviously lost.

The system is fully capable of automatically cycling through casts non-stop, with the primary time-limiting factor being the time required to retrieve the fish. In order to most effectively utilize this system it would be ideal to cycle the MVP at its maximum rate and obtain higher resolution coverage of water layer structure in an area. However, as noted, there were two reasons this was not feasible. The first reason is that it is presently necessary to stop logging in order to input a new profile. Continuous casts would then result in a much larger number of along track sounding gaps with a high likelihood of areas of the seafloor being completely missed on adjacent lines. The second reason is that it is sometimes desirable to sample deeper profiles, requiring the vessel to slow down, making continuous casts impractical. Sonar system software updates would solve the first problem while the second problem is simply a factor of this specific model of profiling system and its capabilities. For surveys that routinely survey deeper waters, profiling systems that are capable of underway profiles to deeper depths are available.

3.3 Survey Area

A subset of the Fraser River Delta survey was selected in order to empirically determine how well the use of the MVP30 solved the problem of refraction errors. The portion of the survey selected was the Sturgeon Bank area, which is bound on the north and south by the two major arms of the Fraser River as shown in Figure 26. The area is approximately 15 square kilometres with depths ranging from 2 to 140 metres. The subsection of the survey consists of 15 nearly parallel lines split into 66 separate segments to enable the updating of sound speed profiles. A total of 60 separate casts were used for the entire area over a period of three days in the month of July.
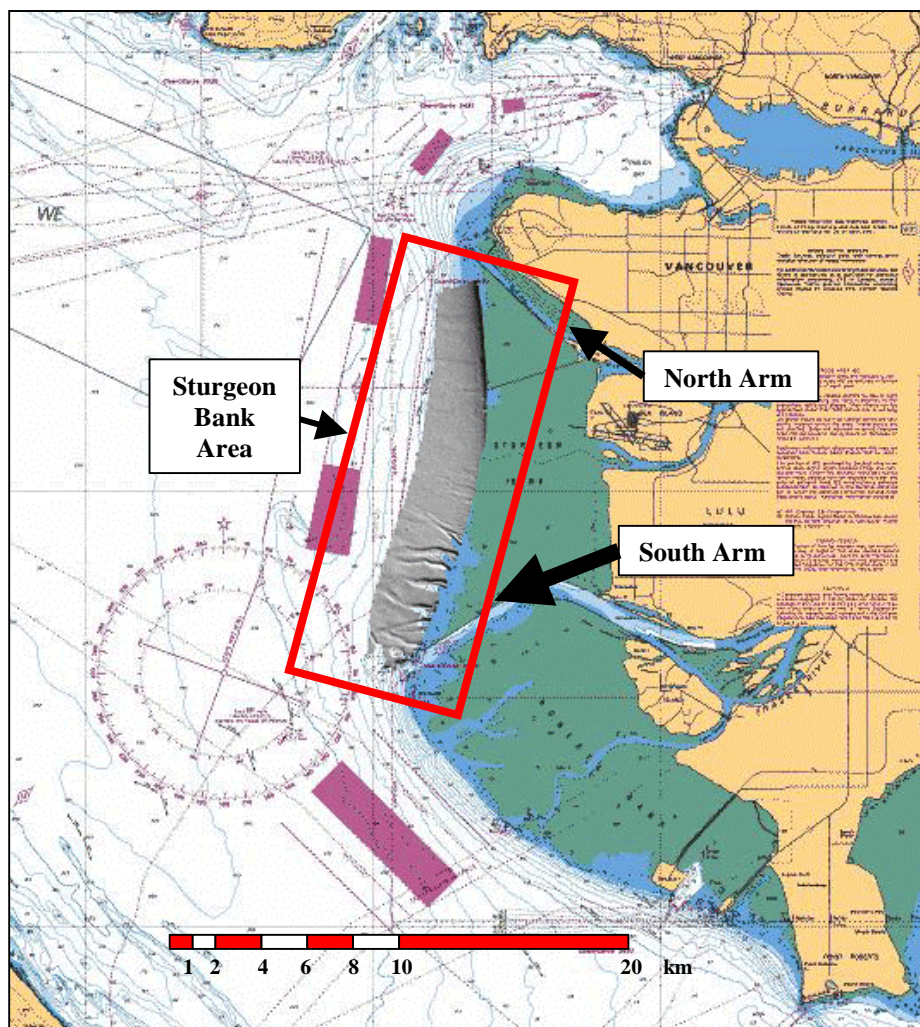
Figure 27. Fraser River Delta survey area showing sun-illuminated EM3000 survey coverage of Sturgeon Bank Section of Survey (background is extract of CHS chart # 3463)

The influx of the two major arms of the Fraser River, which together account for the bulk of freshwater flow and transported sediment, creates a dynamic oceanographic environment. The stratification of the water column under these conditions, which varies spatially and with tide, is particularly critical when echo sounding with an oblique incidence echo sounder due to the associated refraction errors.

3.4 Observed Oceanography

3.4.1 Introduction

While the purpose of this survey is specifically for the determination of the morphology of the ocean floor, as well as charting for safety to navigation, the ability to gather useful oceanographic data while at sea is becoming an ever more important goal within the C.H.S. As well as providing data for other agencies and scientific groups, the data is expected to be instrumental in aiding the hydrographer in making informed decisions on survey planning and accuracy expectations.

To this end all recorded sound speed data from the complete Fraser River survey was entered into GRASS (Geographic Resources Analysis Support System), a geographic information system [GRASS Development Team 2003]. It was hoped that the ability to spatially view the data would enable interrelationships between sound speed data and other factors including tides, time of day, and topography to become apparent.

Although daily sound speed measurements during the survey did not have associated temperature readings, at one point during the survey, the launch was anchored at a central location and a sound speed sensor equipped with a temperature sensor was used to hourly record data through a tidal cycle. This data was also analyzed in order to determine what benefits could be derived from the use of a temperature sensor as well as to attempt to correlate salinities and temperatures with tidal phases.

3.4.2 Sound Speed

Sound speed is the most critical value in terms of echosounding, it was hoped that it would be possible to map the distribution of sound speed values with reference to tides and time of day. It was also hoped that it could be used as an indicator of other oceanographic parameters. Unfortunately the sound speed value alone cannot uniquely provide a solution for water temperature or salinity. Ideally the use of a temperature sensor alongside a sound speed sensor would constrain the solution. However, for the case of measurements with the MVP30 on this survey, sound speed alone was measured.

3.4.2.1 Sound speed relationship to tides

In order to determine the relationship of sound speed measurements to the phase of tide, sound speed measurements were identified as belonging to a particular "phase type" of the tide. The Fraser River Delta has a mixed, mainly semi diurnal tide which means that there are two high-waters and two low-waters each lunar day with a significant inequality in their heights. The tide was divided into six "phase types" based on the relative amplitudes and type. These types were identified as: start of greater flood,

end of greater flood, lesser ebb, lesser flood, start of greater ebb and end of greater ebb. These groupings are illustrated in an example tidal signature in Figure 28. It was hoped that a relationship would be observed between the tidal phases and sound speed in order to develop simple rules as to when would be ideal times to survey this type of area to encounter the least variable sound speed conditions.
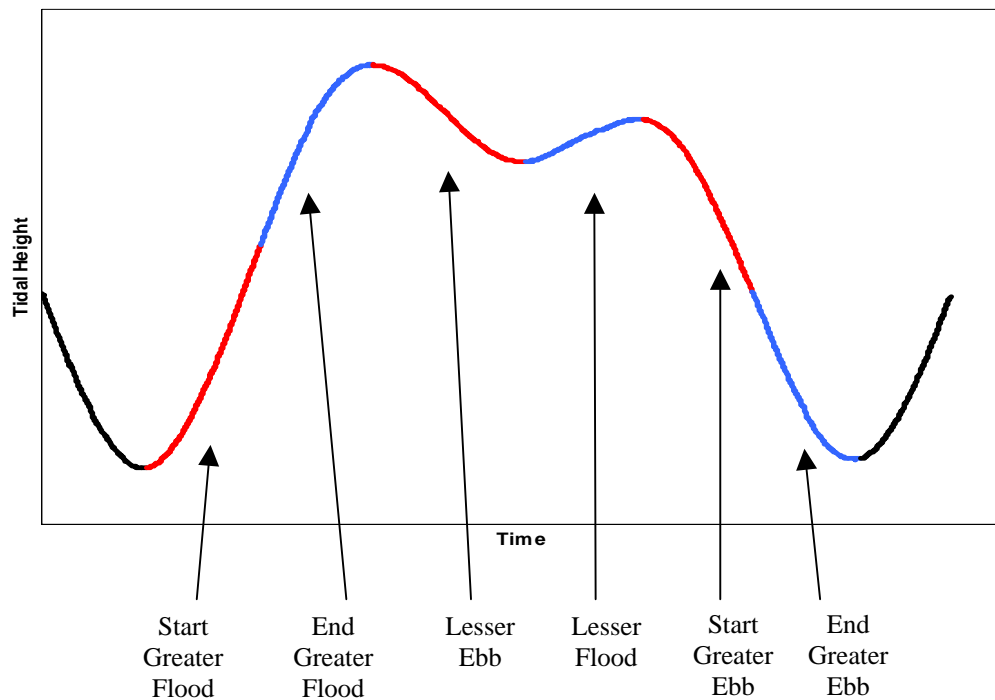
Figure 28. Tidal "phase types" used in analysis

The tidal groupings are plotted in Appendix II. Unfortunately, when the tidal phase groupings are compared, there is no clear relationship between the tides and the sound speed groupings. While a clear correlation between sound speed and the phase of tide would have provided a simple and useful guideline for the timing of multibeam surveying, it is clearly not possible to make any such conclusion.

This is due to a complex set of interrelated factors beyond simply the tidal phase. These include; tidal and fluvial currents, natural and artificial geography, seafloor topography, and wind. In an area with an inflow of fresh water, wind becomes a critical consideration which can only be predicted in the short term. With these two bodies of water at different densities, a wind of over 10 knots will have the effect of controlling the direction of the layer of fresh water on the surface, even to the point of completely reversing its direction with respect to the salt water layer beneath. While all of these factors can, and have been modelled, this is beyond the scope of this paper and beyond the measurement and prediction abilities of a typical hydrographic survey [de Lange Boom 2003].

3.4.2.2 Sound speed relationship to time of day

In a manner similar to the tidal information, the sounds speed readings were slotted into 2 hour sections starting at 8:00 until 20:00 Pacific Daylight Savings time (P.D.T.) Local time was utilized in order to get a sense of solar heating effects. The primary effect expected to be visible was a solar heating raising the surface and near surface water temperatures during the day.

Unfortunately, there was not a strong indication of this solar heating effect throughout the day. Initially it was hypothesized that the mixing mechanism in the area was so strong that the mixing effects overcame the solar heating before any significant

sound speed changes could be seen. However while considering additional data discussed in section 3.4.3, it is clear that this is not the case, but rather that the ambiguity of the sound speed value in isolation makes it impossible to derive any strong conclusions from this information.

3.4.3 Sound Speed, Temperature and Derived Salinity Related to Tide and Time of Day

During the survey the speed of sound and temperature readings were recorded at a single location through a tidal cycle in order to ascertain a more complete picture of the temporal oceanographic profile. From these readings it is possible to derive the salinity using any one of the speed of sound equations. Typically the salinity is derived using the relationship with conductivity as discussed in section 2.4.2.3, however calculating the salinity from sound speed and temperature is an equally valid derivation, however the accuracy of this solution is not clear. In the future this needs to be investigated to determine the value of this derived salinity value.
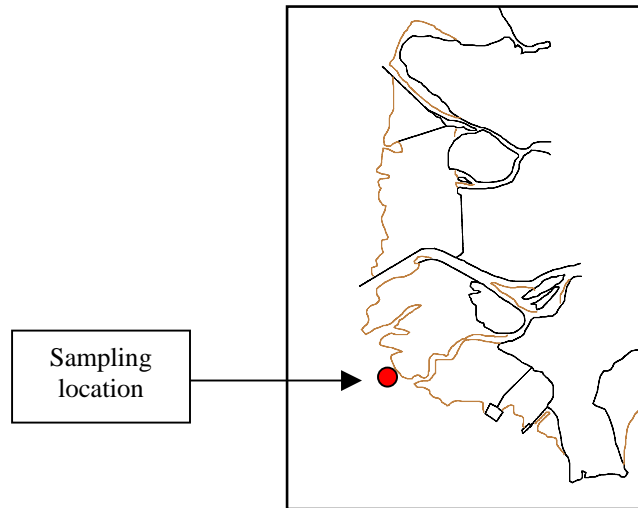
Figure 29. Location of sound speed and temperature readings

The sampling location is situated between the South Arm and Canoe Passage and was occupied from 9:00 am July 5 to 5:00 am July 6, 2001. While it would be invalid to assume that one location could represent the entire system throughout the delta, it was hoped that a snapshot would give an indication of the usefulness of sound speeds collected alongside temperature values.

Figure 30. Illustrates the relationship of the temperature and salinity values with the tidal phase and the time of day.
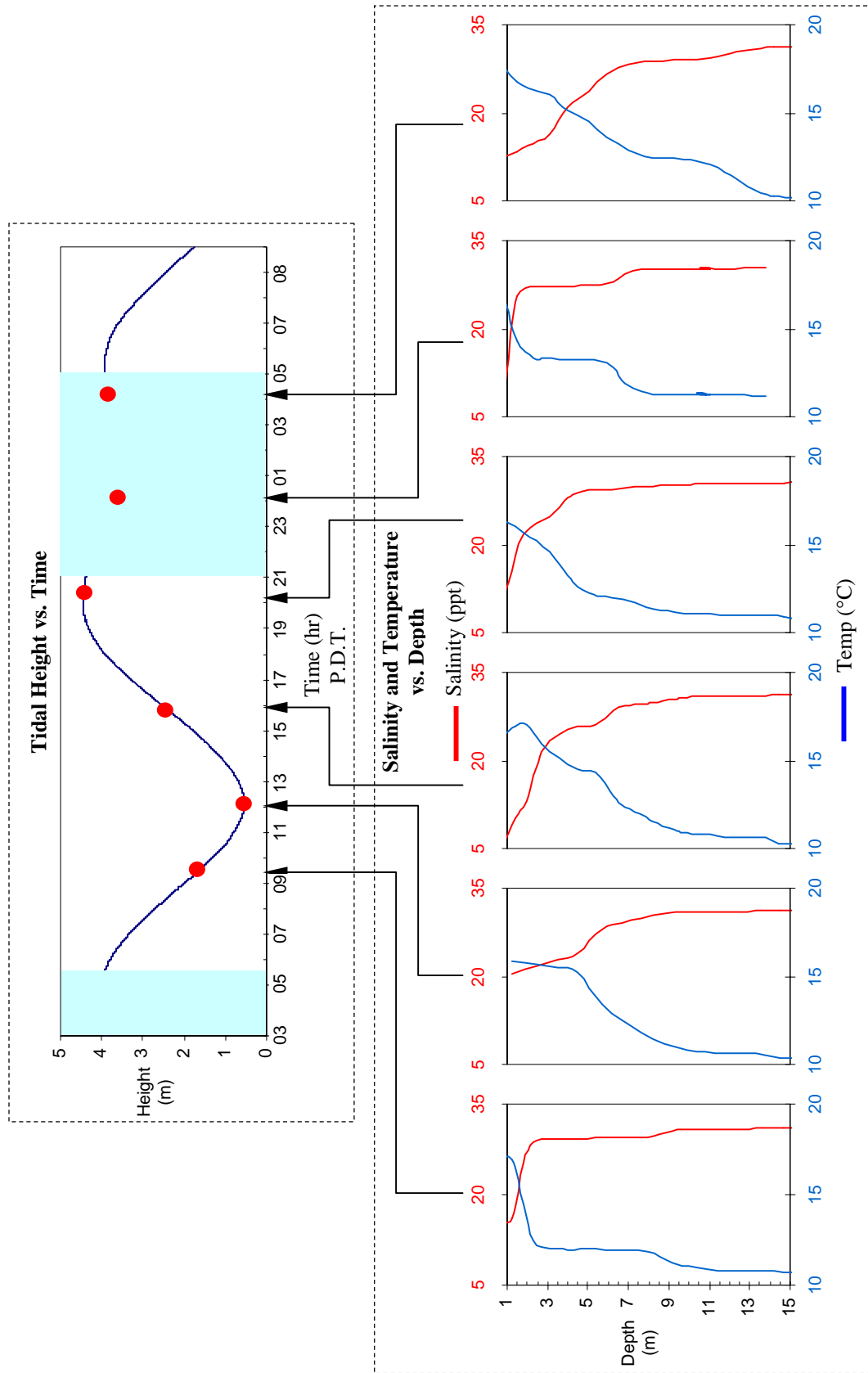
Figure 30 Example relationship of temperature and salinity with time of day and phase of tide

The results of the casts are again unclear in terms of interrelationships between temperature, salinity, tidal phase and time of day. The effect of the incoming fresh water can be seen throughout all casts in the upper water column. It is also possible to see a general build-up of the salinity with the rise of tide, but this is clearly combined with complex mixing patterns. The variability seen makes it impossible to derive clear relationships between all of the factors.

It is informative, however, to see the ambiguity resolved with the use of a temperature sensor, which enables us to see exactly what is causing the changes in sound speed. It should be noted that there would be a small effect due to the suspended sediment that is present in varying amounts at different times of the year. Without the direct measurement of sediments it is not possible to remove its influence when determining salinity from temperature and sound speed. However this effect can be considered minimal and in the range of 0.5 m/s at the maximum sediment load of 400mg/L and would have likely been less than 0.2 m/s at the time of this survey when positioned directly in the flow of the river.

In order to more completely visualize the relationship of temperature salinity and sound speed these values are plotted in Figure 31
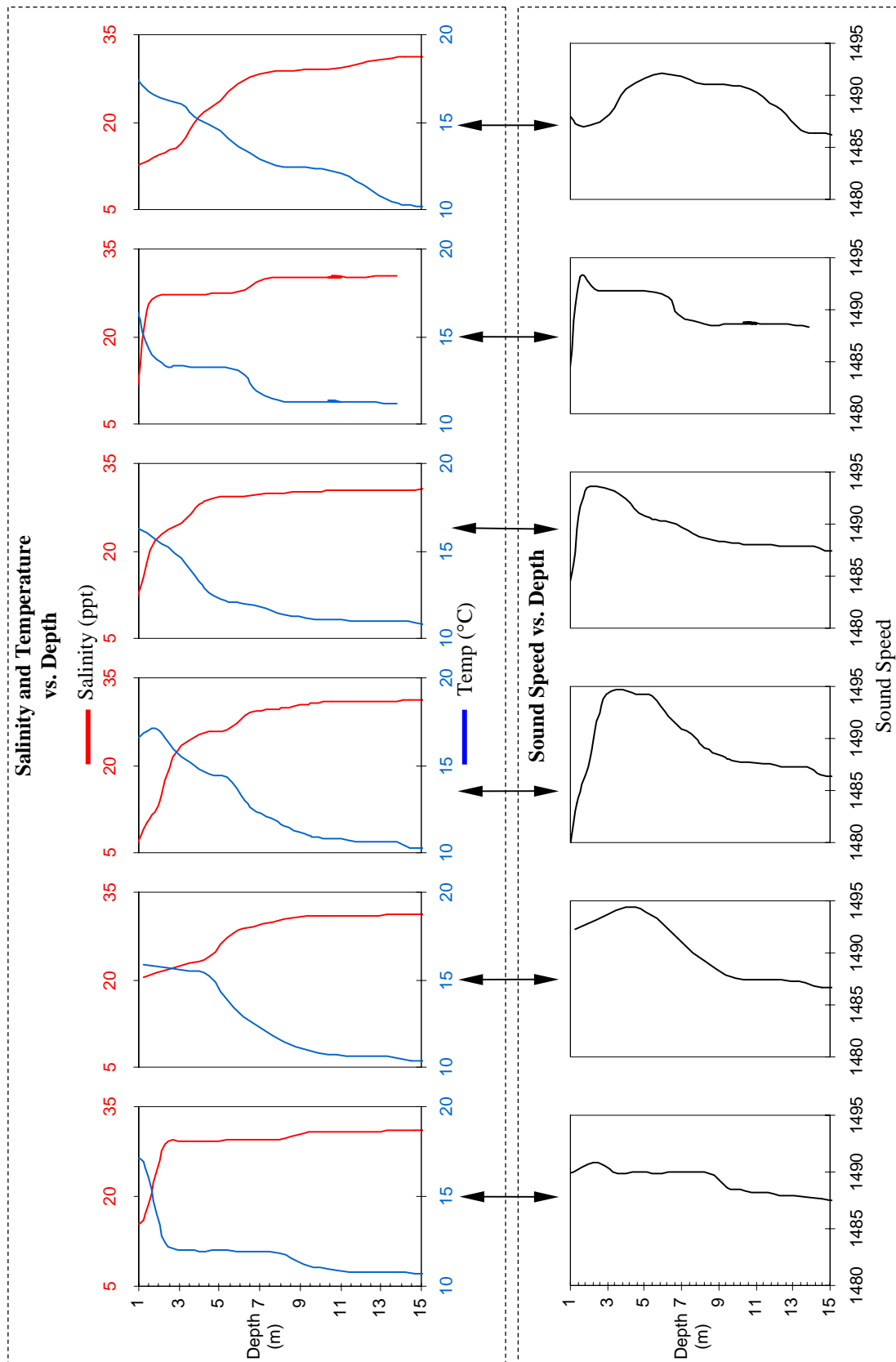
Figure 31 Example relationship of temperature, salinity and sound speed

It is clear from these illustrations the use of a temperature sensor enables us to almost completely resolve the ambiguity and uniquely identify the source of sound speed changes .An excellent example of this is the sound speed cast taken at 9:15 am shown in Figure 32 below.
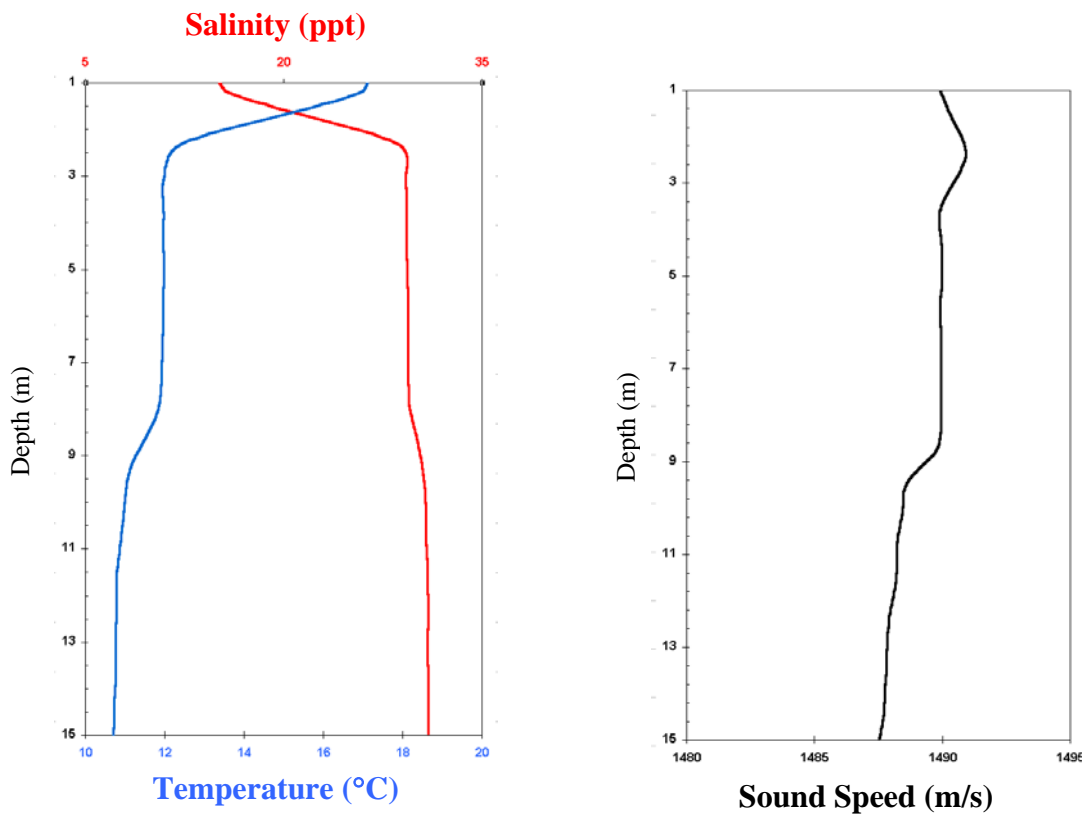
Figure 32. Relationship of temperature, salinity and sound speed at 9:30 P.D.T. July 5 2001

When comparing the temperature, salinity and sound speed at this time, it can be confidently said that the observed high temperature and low salinity seen at the surface is caused by the fresh water plume that is only partially mixed in with the surface layer. What is also evident is that the higher temperature of the fresh water is offset by the

lower salinity, which results in a sound speed profile that shows little evidence of the anomaly. While this can be considered a coincidence that would not occur frequently, it clearly illustrates the ambiguity in sound speed measurements in isolation and the benefit of a temperature sensor.

It is therefore clear that, while sound speed profiles give a clear indication of relative sound speeds of the different water layers, in a complex mixing system such as the Fraser River Delta it is impossible to identify specific oceanographic parameters or bodies of water using this value alone. While this is not a problem in offshore systems where density is correlated very clearly with temperature, in the dynamic mixing environment of the Fraser River Delta, the correlation between sound speed, salinity and temperature cannot be confidently drawn.

If a temperature sensor had been included on the MVP fish along with sound speed and depth sensors, there would have been a high-resolution picture of salinity and temperatures throughout the survey area. It is suggested that with such information it might be possible to model currents and mixing throughout the area by uniquely identifying water bodies by the oceanographic parameters of temperature and salinity (derived).

3.4.4 Effect of Oceanography on Hydrographic Survey Planning

An objective when planning a survey in an area such as the Fraser Delta is to minimize the variability of the sound speeds within individual survey areas. This is due to the fact that there is always a finite number of sound speed casts that can be performed and an associated limited resolution to the observed structure of the water column. If the survey is traversing areas of drastically changing sound speeds, these changes will be smoothed out by the spatial sampling resolution of the sound speed measurements resulting from the intervals between measurements.

It has become clear that the mixing processes in a deltaic environment are complex and cannot be easily correlated to tidal phases or time of day. There is, however, a correlation of sound speed to geographical area. Throughout the tidal phases, time of day and depths there are areas that tend to have groupings of similar sound speed values. Figure 33 illustrates all of the surface values for the entire survey.
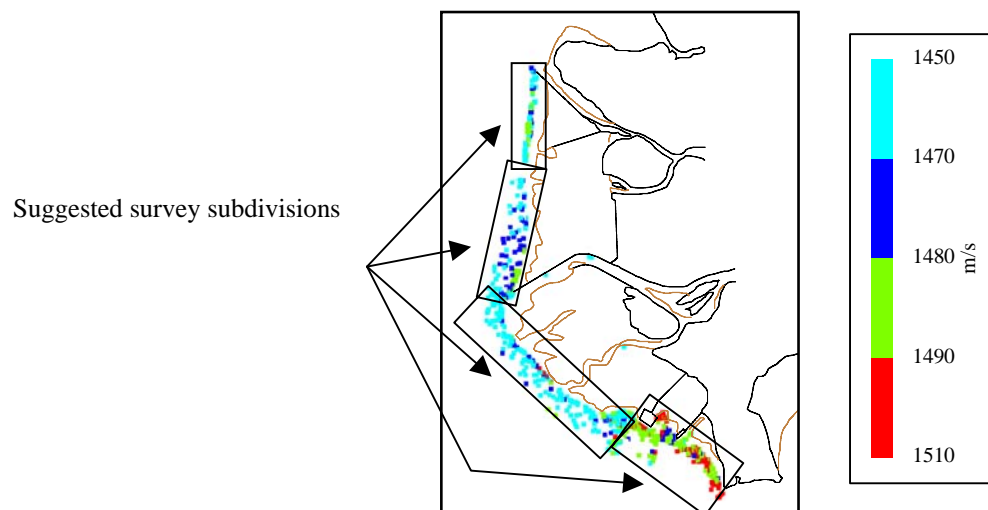
Figure 33. Surface sound speeds grouped according to geographical area

While there are still significant changes over time and tidal phases within the suggested subdivisions, it is the most effective method of minimizing sound speed variability. These cells of similar sound speeds are consistent through to depths of 30m but with a marked decrease in variability with depth as shown in images in Appendices I and II.

Coincidentally, these observed cells correspond very closely to the method in which the area was subdivided for the actual survey. It can therefore be concluded that in the absence of additional information, survey areas should be planned by carefully taking into account the topography and bathymetry that affects the flow and mixing of the influx of fresh water. This method coincides intuitively with dividing a survey area up according to the presence of dikes and other features that obviously exert a strong influence on the water column structure.

3.5 Evaluation of Refraction Solutions

3.5.1 Introduction

The 2001 survey of the Fraser River Delta was the first survey for the Pacific Region of the C.H.S. to use a near real time sound speed profiling system. The use of a system that measures the structure of the water column in high resolution, both spatially

and temporally, is expected to significantly reduce errors due to refraction. The use of such a system also presents the opportunity to evaluate the method of determining the structure using a minimum number of archived profiles, as few as one sound speed profile per day. While this is not an ideal situation, it can still be considered a common practice with many of the multibeam surveys today.

The first goal of the evaluation is to estimate the effectiveness of the near real time profiling system. The second goal is to use the extra information that we have to simulate the use of archived profiles. As well, due to the fact that we have updated profiles for the whole time period, it is possible to use only the surface sound speeds from the updated profiles in combination with the archived profiles to simulate the method of using archived profiles with a surface sound speed sensor.

Finally while determining the effect of using archived profiles with and without surface sound speed, it is possible to use software to calculate the different effects of using an electronically steered array and an arcuate array under conditions of variable sound speeds.

For comparison purposes the ray tracing for all the lines were recomputed for three different application methods. The first method was to interpolate the sound speed values between profiles. This was done using the two profiles from before and after each line. For each individual ping a new profile was calculated by weighting the two profiles depending on relative time.

The second was to ray trace using the updated profile logged with the survey line and applied by the sonar manufacturer's software during the survey. These are the calculations that were performed by the processing system of the multibeam echosounder

in the field. These calculations were recomputed with the raytrace software to confirm the ray tracing method and to ensure results similar to the manufacturer's values.

The third was to ray trace with a single profile selected for the entire survey in order to determine the effect of not updating the profiles as often as was enabled by the MVP. These calculations were performed for an electronically beam steered array and, as well, the software was used to simulate the effect of an arcuate array that does not use electronic beam steering as its primary beam selection method. In addition the effect of using a sound speed sensor to update the transducer sound speed was simulated.

Ray tracing was calculated using the method of layers with constant sound speed gradient as was covered in section 2.3.3.2. The results of the evaluation will be presented followed by the details of the raytracing and the analysis of the mechanisms involved.

3.5.2 Evaluation Methods

In order to have a method of evaluating the accuracies of the entire depth data set, a "pseudo" reference surface was calculated [Hughes Clarke & Godin 1993]. This was done by taking advantage of the large amount of overlap and resulting redundancy that is enabled by C.H.S. survey methods. The lines that had been processed with interpolated sound speed profiles were used for this surface. All of these sounding lines were processed with "weigh_grid", a weighted gridding program that gives a higher weight to the beams at nadir and less weight to the beams as they are steered out. The result is a

computed surface that is dominated by the effect of the nadir beams where the effect of refraction, although not necessarily propagation, was least.
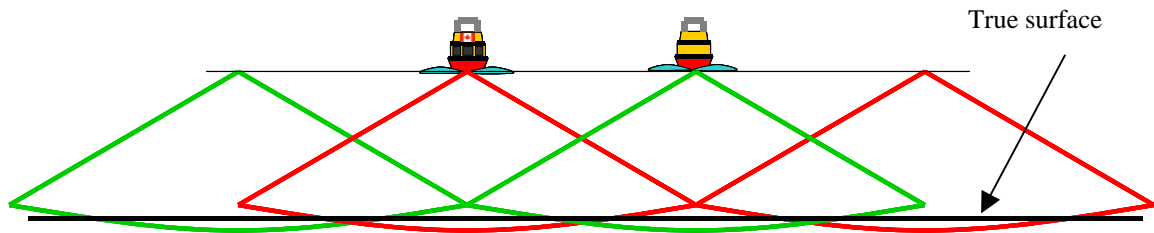
Figure 34 Representation of Survey line coverage with refraction errors over true surface
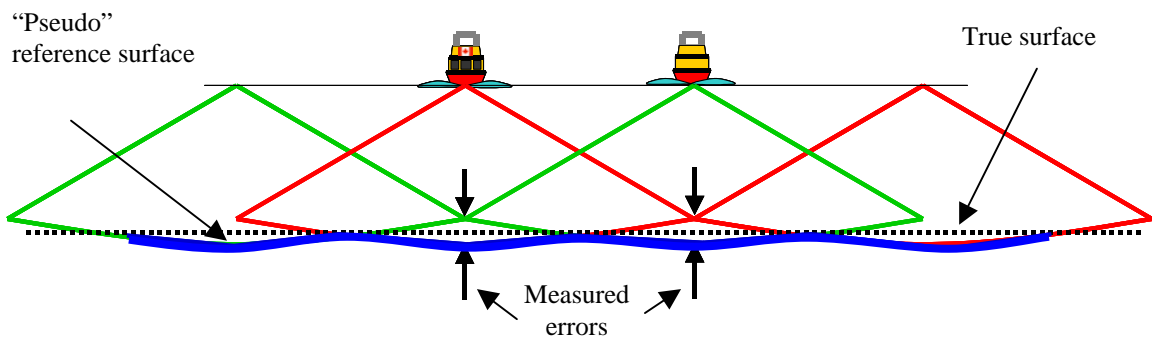
Figure 35. Representation of "pseudo" reference surface (indicated by blue line) fitted to profiles with weighted central beams

The second step was to compare individual lines with the pseudo reference surface in order to approximate the effect of refraction errors. As can be seen from Figure 35, the method results in the outer beams of the lines being compared to the reference surface, which is weighted towards the nadir beam values. The effect is that we are comparing the most refracted outer beams in each one of the selected survey lines with the least refracted nadir beams.

85

This method of using a pseudo reference surface is however, an approximation. As noted by Capell [1999], for a horizontally oriented, electronically steered line array, the refraction errors actually cross zero at approximately 45 degrees port and starboard. This effect was clearly seen with this data. However it is considered that the large number of sound profile casts results in a reference surface that closely approximates the true surface, and provides a useful check, particularly when considering alternative, inherently less accurate methods of sound speed application.

3.5.3 International Hydrographic Organization Standards

The International Hydrographic Organization (I.H.O.) has published a set of survey accuracy standards in a document entitled "S44 IHO Standard for Hydrographic Surveys, Edition 4". In this document surveys are subdivided into four "orders" depending on survey requirements. In order of decreasing accuracy requirements, the categories are: special order, order1, order 2 and order 3.

Depth uncertainties are calculated based on a scalar and a depth dependant value for each order. Figure 36 illustrates the depth uncertainties versus depth for all of the designated orders.
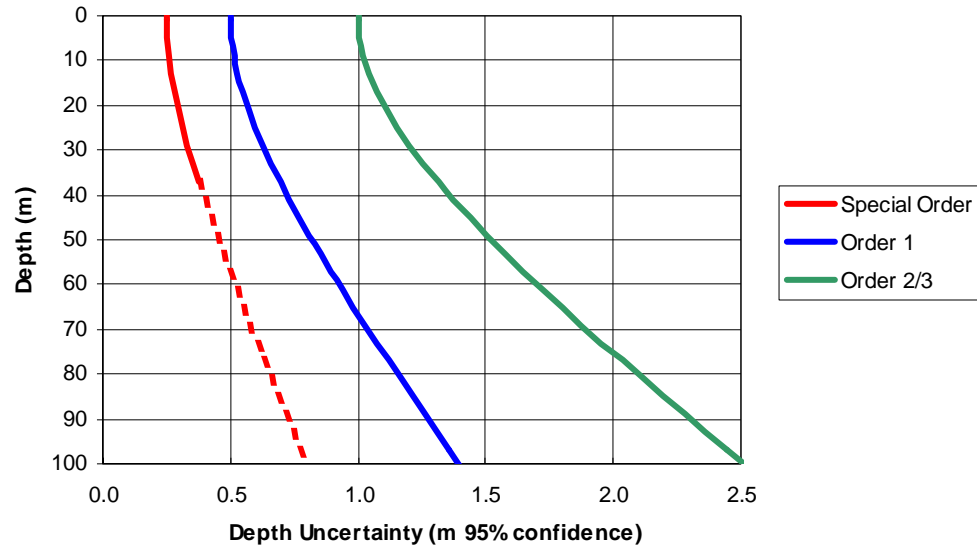
$$Special\ Order\ \ +/-\sqrt{0.25^2 + (0.0075*depth)^2}$$

$$Order\ 1\ \ +/-\sqrt{0.5^2 + (0.013*depth)^2}$$

$$Order\ 2\ \ +/-\sqrt{1.0^2 + (0.023*depth)^2}$$

Figure 36. I.H.O. allowable depth uncertainties, S44, Edition 4 [1998]

The majority of multibeam surveys conducted by the C.H.S. fall within the scope of Order 1 specifications. Order 1 is defined by the I.H.O as "harbours, harbour approach channels, recommended tracks, inland navigation channels and coastal areas of high commercial density".

While the errors obtained from comparison of survey lines with an interpolated surface cannot be considered absolute, for the purpose of evaluation in this paper, 0.5 % uncertainty in depth measurement will be considered a maximum acceptable error.

3.5.4. Raytracing Calculations

The calculations for raytracing involved two basics steps. The first step is to determine the departure beam angle and the second is to determine the ray path through the water column. The source data for these calculations was obtained from the Simrad depth telegrams in the logged binary multibeam file as listed in Figure 37.

Data Description	Format	Valid range
Number of bytes in datagram	4U	–
Start identifier = STX (Always 02h)	1U	–
Type of datagram = D(epth data) (Always 44h)	1U	–
EM model number (Example: EM 3000 = 3000)	2U	–
Date = year*10000 + month*100 + day (Example: Feb 26, 1995 = 19950226)	4U	–
Time since midnight in milliseconds (Example: 08:12:51.234 = 29570234)	4U	0 to 86399999
Ping counter (sequential counter)	2U	0 to 65535
System serial number	2U	100 –
Heading of vessel in 0.01°	2U	0 to 35999
Sound speed at transducer in dm/s	2U	14000 to 16000
Transmit transducer depth re water level at time of ping in cm	2U	0 to 65536
Maximum number of beams possible	1U	48 –
Number of valid beams = N	1U	1 to 254
z resolution in cm	1U	1 to 254
x and y resolution in cm	1U	1 to 254
Sampling rate (f) in Hz **or** Depth difference between sonar heads in the EM 3000D	2U 2S	300 to 30000 −32768 to 32766
Repeat cycle – N entries of :	16*N	–
– Depth (z) from transmit transducer (unsigned for EM 120 and EM 300)	2S or 2U	−32768 to +32766 or 1 to 65534
– Acrosstrack distance (y)	2S	−32768 to 32766
– Alongtrack distance (x)	2S	−32768 to 32766
– Beam depression angle in 0.01°	2S	−11000 to 11000
– Beam azimuth angle in 0.01°	2U	0 to 56999
– Range (one–way travel time)	2U	0 to 65534
– Quality factor	1U	0 to 254
– Length of detection window (samples) (Example: −20 dB = 216)	1U	1 to 254
– Reflectivity (BS) in 0.5 dB resolution/4	1S	−128 to +126
– Beam number	1U	1 to 254
End of repeat cycle		
Transducer depth offset multiplier	1S	−1 to +17
End identifier = ETX (Always 03h)	1U	–
Check sum of data between STX and ETX	2U	–

Figure 37. Simrad Depth telegram showing beam depression angle and one way travel time utilised in calculations.

89

The departure angle given by the Simrad telegram was based on the updated profiles being measured by the real time sound speed sensor. In order to calculate depression angles for sound speed applications other than this real time method, it was necessary to adjust the beam depression angle for the archived sound speed that would have been applied had the updated value not been known. This was an artificial calculation used to simulate the situation of using a single archived sound speed profile for a prolonged amount of time. This was calculated using equivalency of the ratio of the correct angle with the correct sound speed and the ratio of the incorrect angle with incorrect (archived) sound speed shown in formula 3.1)

$$\left(\frac{\theta_{correct}}{Sound\ Speed_{correct}} \right) = \left(\frac{\theta_{incorrect}}{Sound\ Speed_{incorrect}} \right) \qquad (3.1)$$

While this greatly simplified calculations, it does not allow for the effect of roll on the receive beam. Roll error is, however, considered to be minimal in the survey depths and sea states encountered. The evaluation method that will be discussed also takes the mean of depth values over 100 pings, effectively mitigating these errors through averaging.

The raytracing through the water column was calculated using layers of constant gradient as outlined in section 2.3.3.2. The process is to iteratively calculate the time and horizontal distance traveled through each layer of known sound speed gradient until one half of the two-way travel time has elapsed. In practice, it is necessary to develop a

method to interpolate for the last layer, as the layers will not conveniently coincide with the required travel time. The calculations were iterated through until the total time exceeded one half of the two way travel time. At this point the solution was returned to the layer prior to exceeding the time value and the gradient at this layer was used to iterate in small increments until the required time value was met. At this point the summed layer thicknesses, the summed times and the summed horizontal distance are used to determine an across track direction and depth. This value is then combined with the beam azimuth to determine a transducer relative position. The calculated values where then written back to the binary file were it could then be used in Ocean Mapping Group tools such and for processing and DTM analysis [Hughes Clarke 2003].

The source of the sound speed profiles used for raytracing can be classified into three methods. The first is to use the most recently measured sound speed profile to raytrace all depths until the next measurement is made whereupon the new profile will be used for following calculations. This will be termed "real time raytracing". The second method is to interpolate between the sound speed profiles and apply the interpolated values in post processing, which will be termed "interpolated" ray tracing. Finally the use of a single profile, usually taken at the start of the day's survey operations, is termed "archived sound speed profile ray tracing". These differing methods are illustrated in Figure 38.
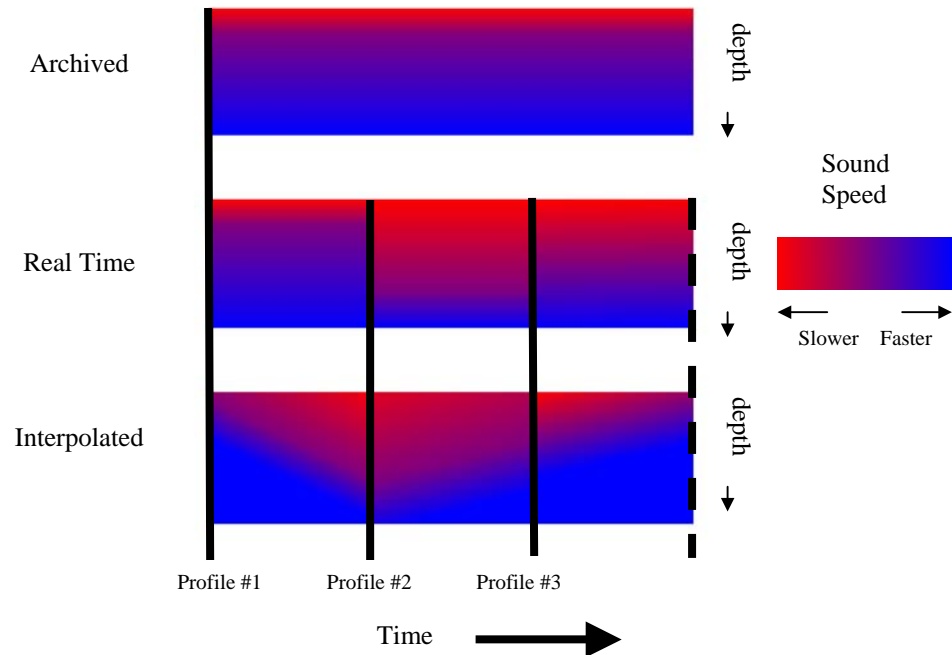
Figure 38.Representation of the application methods of typical sound speed profiles for raytracing calculations.

3.5.4.1 Real time Ray tracing

The application of sound speed profiles for data that follows them in time is the method that is used in real time while sounding. These calculations are previously done by the multibeam processing software, but recalculation is useful for confirming results. These calculations will provide a confirmation of the validity of the ray tracing program and algorithm.

3.5.4.2 Interpolated Ray Tracing

The primary purpose of raytracing with interpolated profiles is to produce the best possible reference solution to compare other sound speed applications methods. This interpolation was calculated using the two profiles from before and after each line segment. For each individual ping, a new profile and departure angles were calculated by weighting the two profiles depending on relative time. This can only be done in post processing when all of the profiles are known.

3.5.4.3 Archived Sound Speed Profile Ray tracing

If a multibeam survey does not have access to a near real time profiling system, archived profiles would have to be used. It is useful to calculate what results would have been obtained, had this been the case, as we have a much more accurate picture of the water column from the multiple profiles with which to compare the results.

In order to provide an overview of errors from using archived profiles, three profiles were selected by a cursory examination to obtain significant change from an original updated profile. Figure 39 shows the three sound speed profiles selected for comparison. After completing ray trace calculations with each profile, it was determined that the largest errors occurred using the profile taken at 12:48:17. In order to look at a near worst-case scenario, this profile was used in all further calculations when simulating the use of an archived profile.
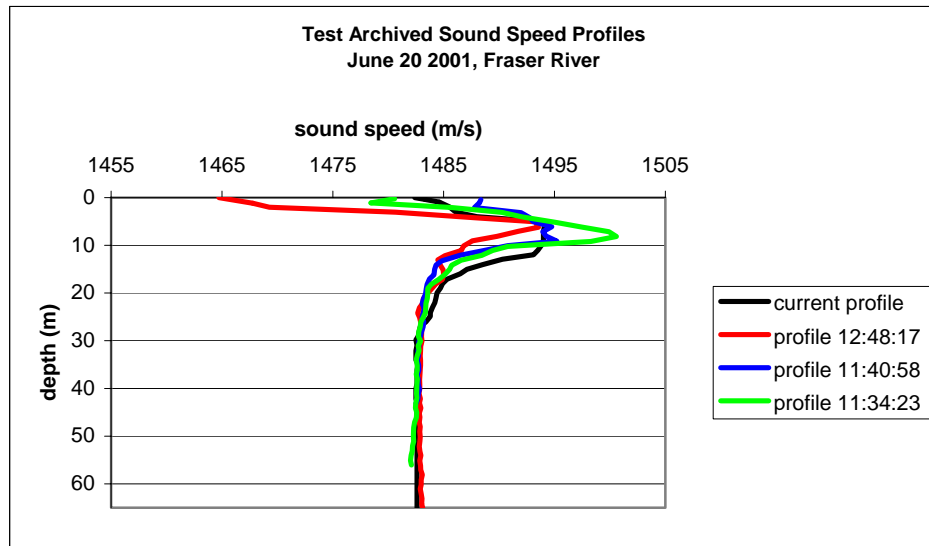
Figure 39. Sound speed profiles used for testing ray tracing methods

When ray tracing with the archived profiles, three methods where used to examine the effects of applying speed of sound at the transducer. In the first case, the effect of the speed of sound at the transducer was removed by recomputing the departure angle. This would be equivalent to using an archived profile and continuing to survey with no knowledge of the changing water column, including the surface sound speed. This would be the case with using archived profiles with an electronically steered array.

In the second case, the departure angle was corrected for the surface sound speed and the archived profile was used even though a mismatch existed between the surface sound speed and the archived profile. This would be equivalent to using archived profiles with an arcuate array without an updated surface sound speed.

In the third method, the departure angle was corrected for the surface sound speed and a small "snapback" layer at the start of the water column was changed to the same value as the sound speed at the transducer face while using the archived profile for the

remainder of the water column. This would be equivalent to using archived profiles with an arcuate array and an updated surface sound speed as previously illustrated in Figure 38.

3.5.4.4 Summary of Ray Tracing Calculations

The goal of the calculating raytracing solutions is to simulate the various multibeam transducer types and their associated sound speed sensor solutions. Figure 40 is a synopsis of the calculations and the resultant equivalent multibeam systems.
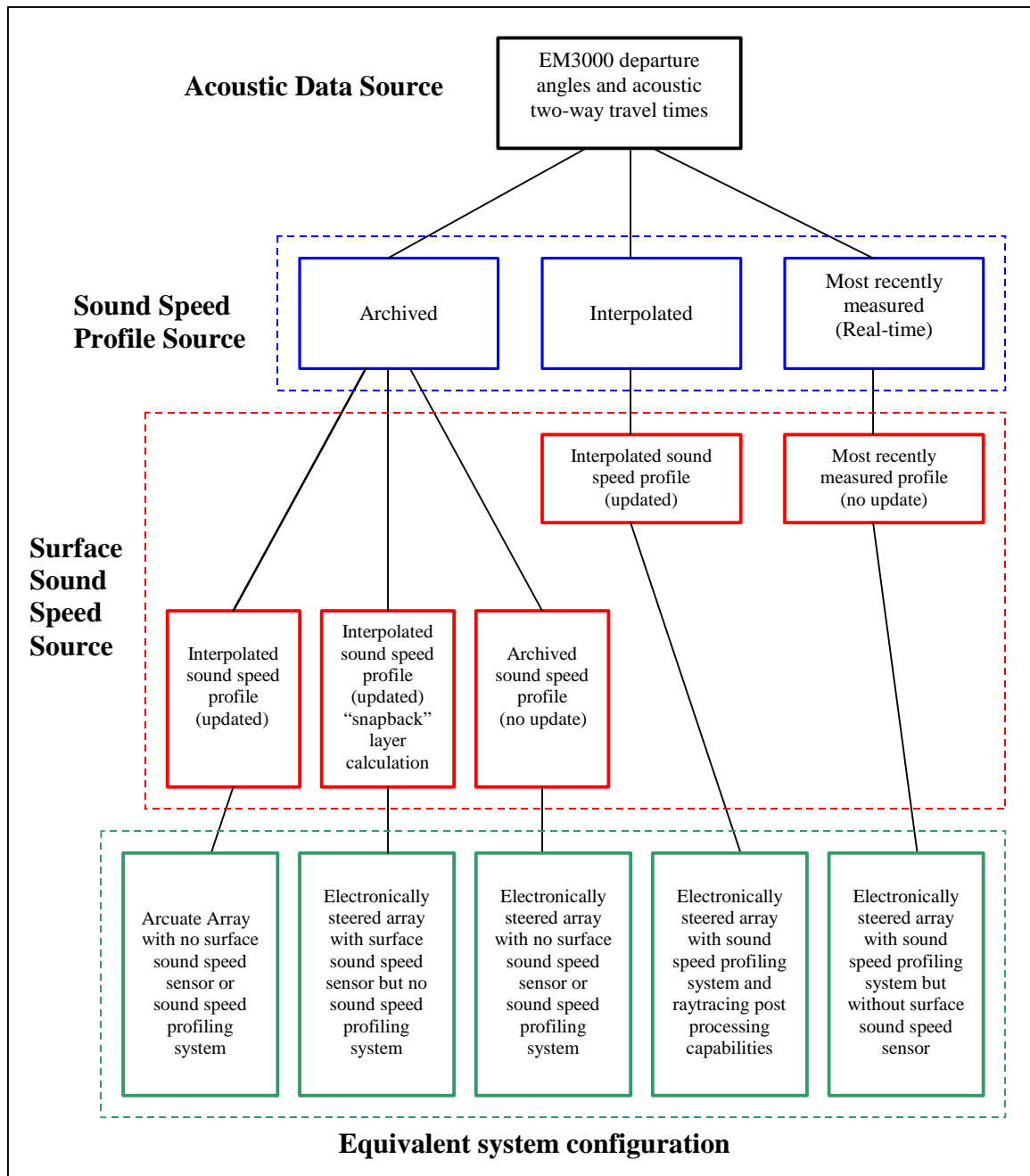
Figure 40.Flow chart of raytracing calculations and the resulting equivalent system configurations

3.5.4 Evaluation Results

3.5.4.1 Introduction

In order to graphically represent the overall errors obtained from the various raytracing methods used, each survey line file was compared to the reference surface. The survey line is defined by the files created by the sonar manufacturer every time data logging was stopped in order to insert a new sound speed profile. The method then used was to take the last 100 pings from each file and, using Ocean Mapping Group software, to calculate an average percentage depth difference from the pseudo reference surface, binned by beam angle. The end of the file was used in order to look at soundings that were furthest in time from the last sound speed profile update. This was done at every beam angle from –60 to +60 degrees. The use of 100 pings helps to eliminate individual noisy soundings, while retaining the overall trend of depth errors.

3.5.4.2 Ray tracing methods resulting in acceptable errors

The next figure illustrates the percentage depth errors from ray tracing methods that result in acceptable error values. Case A is the method of using an archived profile without updating the sound speed at the transducer (electronically steered). Case B is the method of applying each cast to the sounding data in real time as the casts are received.

Case C is the post processing method of interpolating between sound speed profiles so that each ping uses a profile that is a weighted combination of the profile at the start and end of each line.
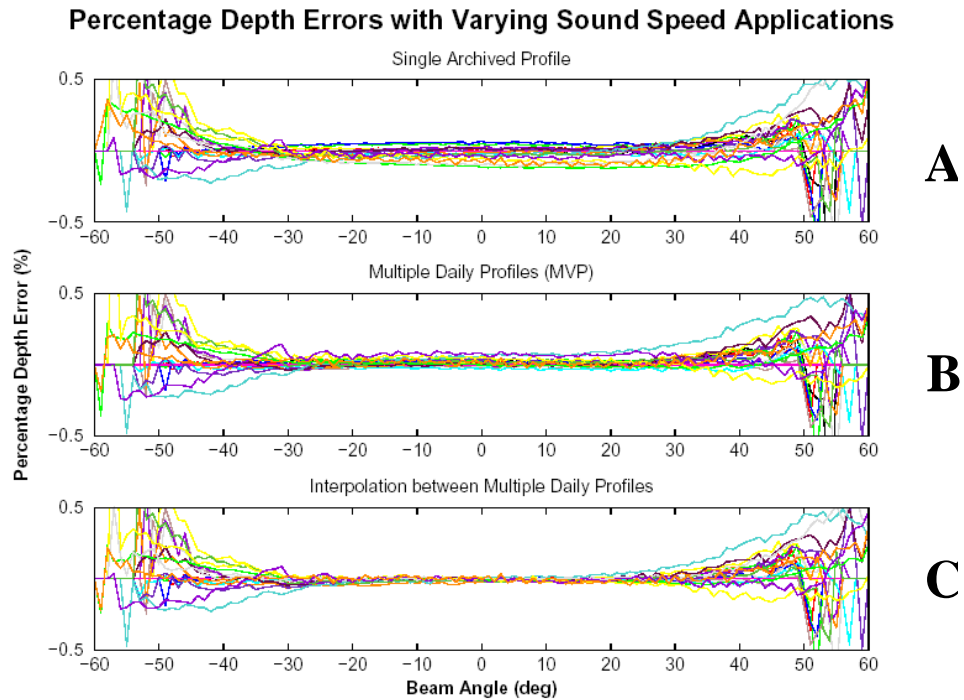
Figure 41. Percentage depth errors comparison using archived and updated profiles. A represents pings obtained when using a single archived sound speed profile, B represents using the updated profiles provided by the MVP and C represents using the MVP profiles with weighted interpolation

As can be seen from Figure 41A, the overall errors, especially in the outer beams, are not significantly higher when using an archived profile with uncorrected sound speed at the transducer over multiple updated casts. However one can see in Figure 41A that at nadir the data does have increased errors. This is due to the fact that the calculations were done with an archived profile with grossly incorrect sound speeds near the surface. The incorrect sound speed values partially cancels out the refraction errors, however the

harmonic sound speed (which controls propagation) will be incorrect. This would be the equivalent effect that would be observed when using a single beam echosounder with incorrect sound speeds. Although this error is much smaller in magnitude than the refraction errors, it still needs to be seriously considered in the overall error estimations.

The second conclusion that can be gained from Figure 41 B and C is that the difference between using all the daily profiles and the interpolated values between each profile provides only a small improvement in accuracy. This would indicate that the method of using the MVP30 (at approximately 10 minute intervals) took a reasonably complete picture of the water column structure in the area. This conclusion is in agreement with the findings of Hughes Clarke et al [2000] for Georges Bank survey operations. However, by interpolating between profiles it would eliminate the "step" effect that occurs due to the sudden switch from one profile to the next. Such steps would tend to obscure spatial patterns that occur over a large area but which might have a small vertical magnitude. In the case of this survey, there was a pause between start and end of line and so this effect could not easily be seen. However, it is recommended that logging software be modified to accept profiles in real time. This increase in accuracy and the smooth transition from one profile to the next would be useful in being able monitor these large-scale changes as well as compensating for instances where there is a lower frequency of sound speed profile casts.

In order to clarify these effects further, the 100 final pings that were ray traced using archived and multiple profiles were directly compared to lines that were ray traced using interpolated sound speed profiles. This has the effect of displaying only errors related to ray tracing while eliminating other errors seen previously that could be due to

positional, tide, or long term heave errors. From Figure 42 it is clear that the refraction errors are within reasonable error expectations, and again the effect of the incorrect harmonic sound speed can be seen, especially at nadir. The point at which the errors cross zero corresponds to approximately 45 degrees as predicted by Capell, [1999]. In the majority of multibeam survey projects, the harmonic sound speed is an insignificant error. However in the case of conditions like that on the Fraser River delta, where there is a large sound speed anomaly at the surface, it is possible for this to become the dominant error which actually offsets and partially cancels the refraction error in the outer beams.
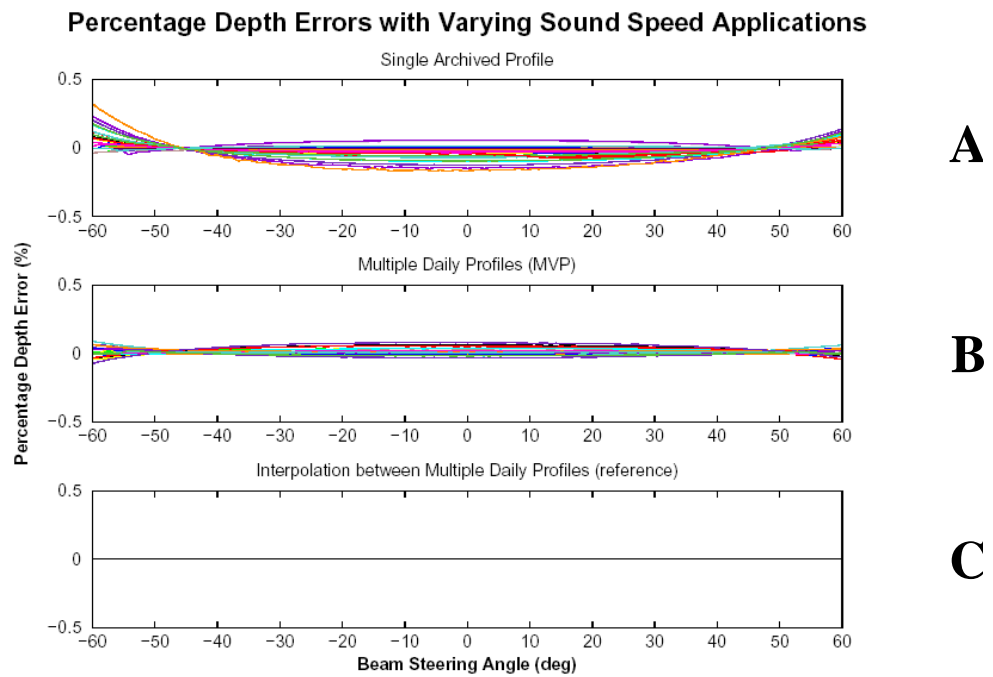
Figure 42. Idealized percentage depth errors comparison using archived and updated profiles. These errors are calculated for refraction and sound speed errors only. A represents pings obtained when using a single archived sound speed profile, B represents using the updated profiles provided by the MVP and C represents using the reference lines with weighted interpolation between MVP profiles (therefore will have null value when compared to itself).

What is also clear from comparing Figures 41 and 42 is that there remain some significant errors that are clearly not directly related to refraction. The specific source of these errors is uncertain, however they appear to be similar throughout differing raytracing approaches. These errors can be attributed to a combination of long period heave, roll biases and the position uncertainty on steep slopes of the bank and its channels. Although the errors appear to grow as one moves to the outer beams, much as would be expected with refraction errors, this is in fact due to the weighting applied in the pseudo reference surface, which is based on the same nadir beams, the errors are common to the reference surface and the data.

3.5.4.3 Ray tracing method resulting in unacceptable Errors

Figure 43 depicts the errors resulting from using an archived profile and adjusting the speed of sound at the transducer even though a mismatch is seen between the surface sound speed and the sound speed profile.

Percentage Depth Error vs Beam Angle

Archived Profile with Updated Sound Speed at Transducer
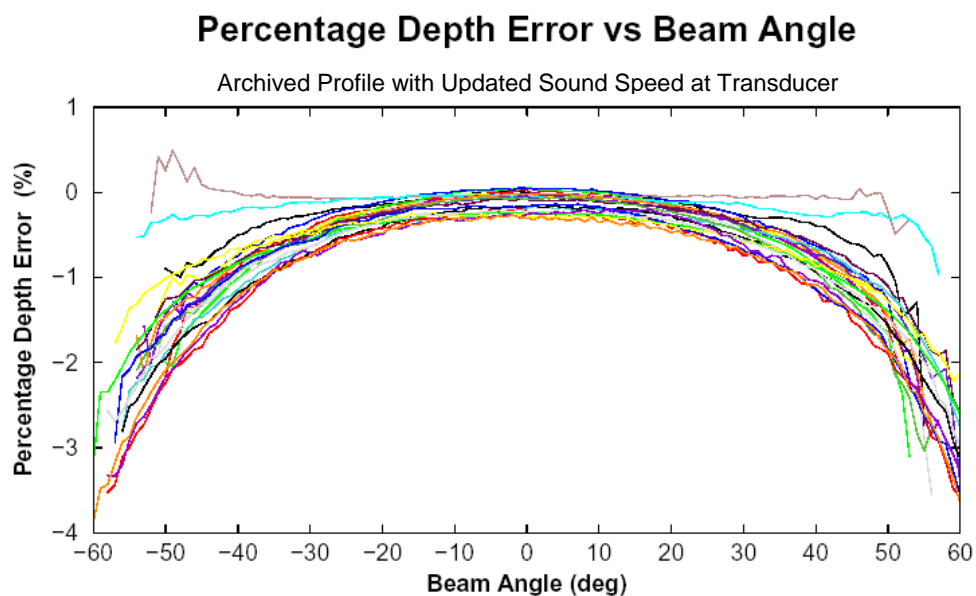
Figure 43. Percentage depth error using archived profile and updated sound speed at transducer

This in effect means that the departure angle has been corrected while the true profile is diverging from the archived profile. It is clear that the change in the water column after the archived cast was taken, very quickly diverged to the point that any soundings obtained in this way far exceeded accuracy standards.

This calculation simulates the case of an arcuate array that uses an archived profile. This would not occur with an electronically steered array, as the incorrect sound speed would result in the cancellation of errors as previously illustrated in Figure 41.

3.5.5 Analysis of Results

3.5.5.1 Real time raytracing

These calculations were intended to repeat the calculations made by the manufacturer in the original echosounding process. The ray tracing calculations made with the updated profiles resulted in depths that were within +/- 1 cm of the values obtained by the manufacturer. These differences can be attributed to round off errors, as the digital logging resolution of the system is 1 cm. This confirms the validity of the raytracing solutions.

3.5.5.2 Interpolated raytracing

The results obtained for the interpolated sound speeds correlated very well with the reference surface. This is to be expected, as the reference surface was compiled from the lines developed form interpolated profiles. However, as discussed in section 3.5.2, the total surface was complied using a weighted gridding algorithm which uses the large amount of overlap from line to line to obtain a surface that uses the least refracted inner beams over the outer beams resulting in a surface that is considered more accurate than any one line in isolation.

3.5.5.3 Archived sound speed profile ray tracing

The use of an archived profile resulted in some results that were within I.H.O. specification and other results that were outside of the specification. This depended on whether the surface sound speed was updated. The use of an updated sound speed in isolation results in significant errors.

3.5.5.3.1 Archived profile with no update to surface sound speed

When raytracing with the archived profile and no update to the surface sound speed the departure angle is incorrect due to the change in the sound speed. However this is offset by the error in the first step of the ray trace calculation. Following this the solutions of the updated and the archived converge towards a parallel path as the sound speed profiles merge towards the same value as shown in Figure 44.
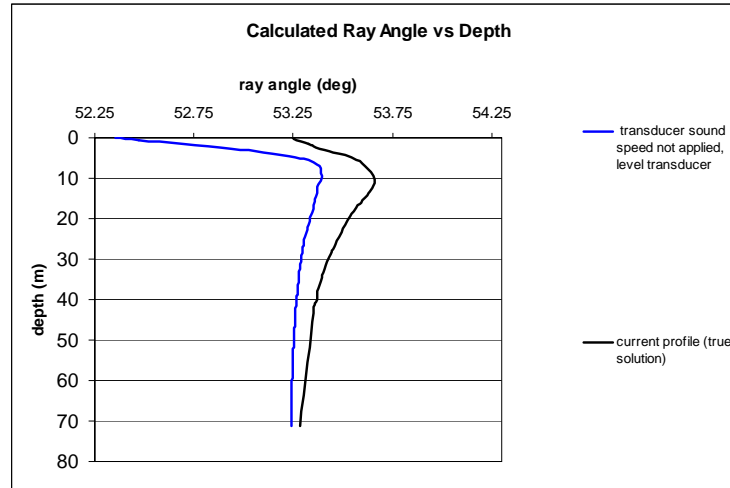
Figure 44. Ray angle vs. depth for raytracing with archived profile and no surface sound speed update

The convergence of the two ray paths results in the difference between the two solutions to decrease with depth. This is caused by the fact that while the sound speeds at the surface are in error, the ray parameter is correct as covered in section 3.5.5.3.1. Therefore as the depth increases to a point where the sound speed is no longer incorrect, the ray angle is also correct. Therefore a sound speed anomaly primarily at the surface will cause a smaller and smaller error as the depth is increased.

To illustrate this depth dependant error the percentage depth error versus the depth is plotted in Figure 45 for the outer beam as well as for nadir (0°). This illustrates how the errors in the shoaler waters have a higher percentage, approaching the 0.5 percent error in the very shallow areas. The graph also illustrates how the dominant error in this case is actually in the nadir beams where there are no refraction errors, due to the major surface sound speed anomaly that causes a direct propagation error
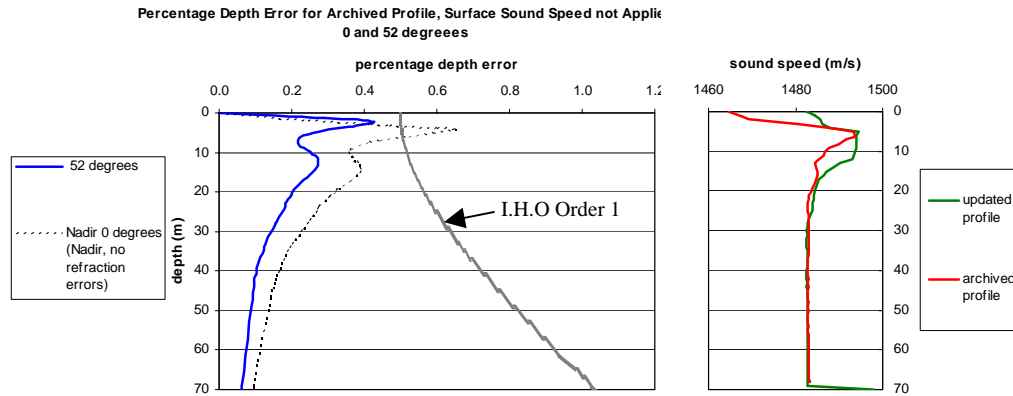
Figure 45. *Percentage depth error vs. depth for archived profile with sound speed not applied with I.H.O Order 1 maximum depth error for reference.*

. While the errors due to an incorrect surface sound speed are partially self-correcting, this is not the case if the transducer is rolled off from the vertical. Figure 46 illustrates the calculated ray angle vs. depth for roll angles of 5, 10 and 45 degrees.
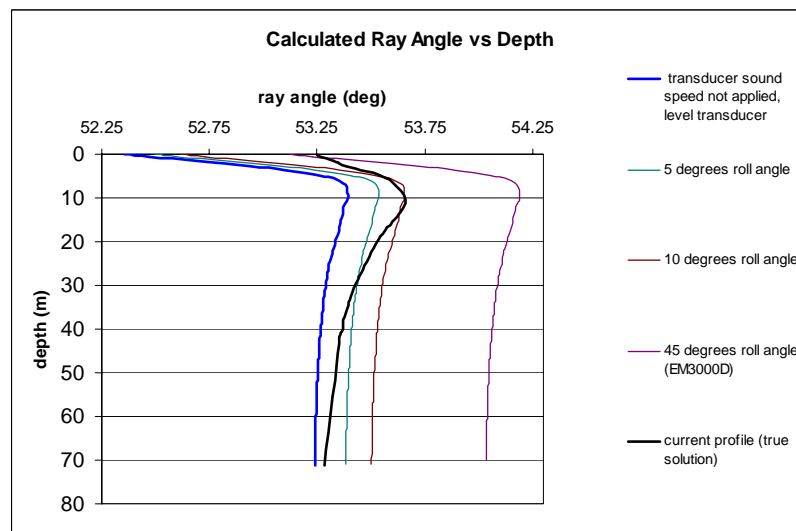
Figure 46. *Ray angle vs. depth for raytracing with archived profile and no surface sound speed with transducer rolled to 5, 10 and 45 degrees*

The roll angle of 45 degrees is significant in that it is a common angle for which a dual EM3000 transducer configuration is mounted as shown below.
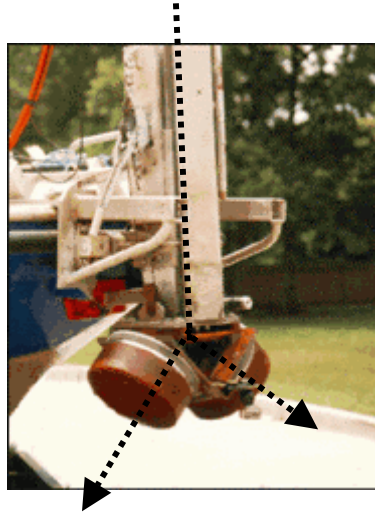
Figure 47. Installation of two Simrad EM3000 transducers in dual configuration.

It is clear that the use of a side mounted electronically steered array will result in significant errors if there is a surface sound speed mismatch. Figure 48 below illustrates the percentage error by depth for a tilted electronically steered array.

**Effect of Roll/Mount Angle on Percentage Depth Error
when using Archived Profile with Electronically Beam Steered Array
(52 degreees)**
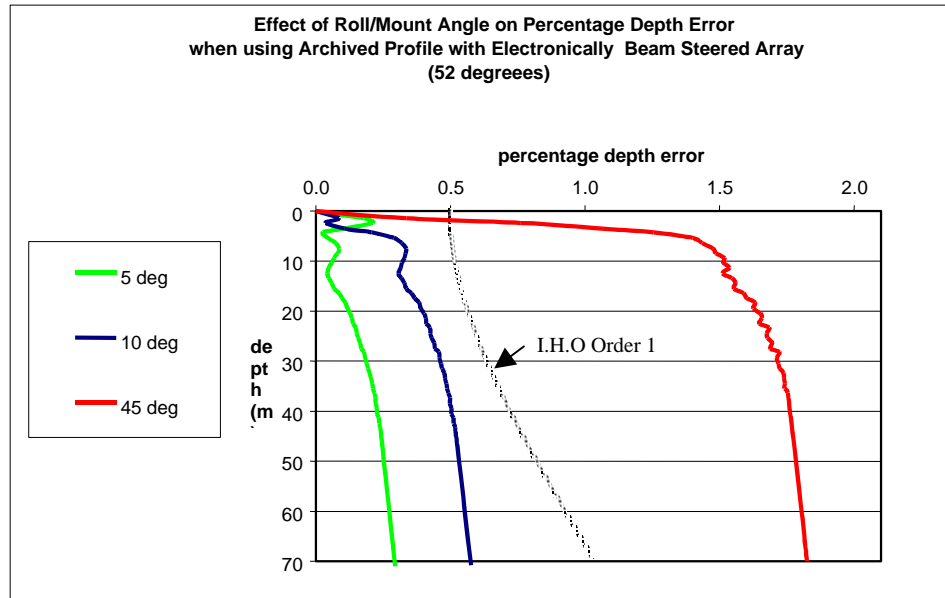
Figure 48. Example percentage depth errors due to using archived sound speed profile. The effect of applying an archived sound speed profile (with no update to the surface sound speed) is shown for a ray angle of 52 degrees with roll angles of 5, 10 and 45 degrees. I.H.O Order 1 error limits are shown for reference

Ray tracing using the archived profile and ignoring any changes in the water column (including sound speed at the transducer) resulted in profiles that were well within IHO accuracy values, even in the outer beams. Intuitively this would appear to be incorrect. However, for the special case of a flat transducer, the combination of the error at the transducer face and a cancelling effect of the erroneous sound speed surface layer have the effect of partially cancelling each other out [Dinn 1997]. In this case of a flat transducer, the result is that both ray traces will tend to converge to a parallel path once the ray paths reach a depth where the water column is the same. These offset parallel paths will still result in a depth and across track error, however, beyond the point where the two water columns have converged, these errors will be constant. As the depth

108

increases beyond this point, as the absolute value of the error is constant, it will become a much smaller percentage of the entire depth solution.

The cancellation of the errors at the transducer face can be accounted for by describing the two errors. The first error occurs at the transducer face. The wavelength of the acoustic signal is calculated by dividing the sound speed by the frequency of the transducer. Due to the use of the speed of sound from the archived profile rather than the true value at the transducer face, the assumed wavelength will be incorrect. As a result of using the incorrect wavelength, the calculated departure angle will be incorrect. This is quantified by: $\Delta\theta = \dfrac{\tan(\theta) * \Delta c * f}{\lambda}$, where θ is beam angle, c is speed of sound in water, Δc is the error in sound speed f is the frequency and $\Delta\theta$ is the resulting angular error. The use of an incorrect sound speed can also be considered in terms of the resulting error in wavelength determination. As wavelength is calculated by dividing sound speed by the frequency of the transducer, an error in sound speed will result in an incorrect wavelength as is schematically shown in Figure 49.

| Virtual array with homogeneous water column with known sound speed. (steering based on wavelength) | Virtual array pointing error from unknown decreased sound speed through homogenous water-column |
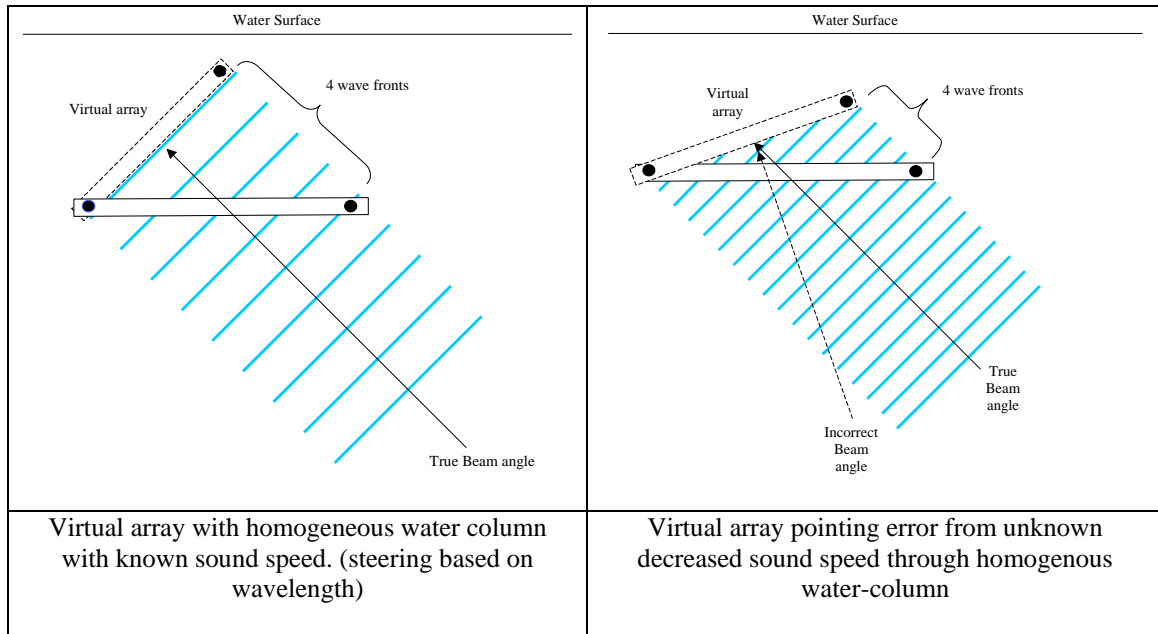
Figure 49. Effect of change in sound speed on beam pointing angle of electronically steered array

However, in reality the entire water column will not change sound speed and usually it is the surface that is most variable, with greater depths having more stable values. Therefore there is a second error which results from the first step in the raytrace that is induced by the layer of water with the incorrect (or unknown) sound speed change. Figure 50 illustrates the very simple case of a single surface layer with a decreased speed of sound where the first stage in the raytrace offsets the error in the departure angle. If the change in sound speed had occurred uniquely at the transducer face the resulting beam angles would be parallel.

Water Surface	Water Surface

| Virtual array with homogeneous water column with known sound speed. (steering based on wavelength) | Angular error cancellation in electronically steered level array with unknown change in sound speed at transducer resulting in actual raypath being quasi-parallel with expected raypath |
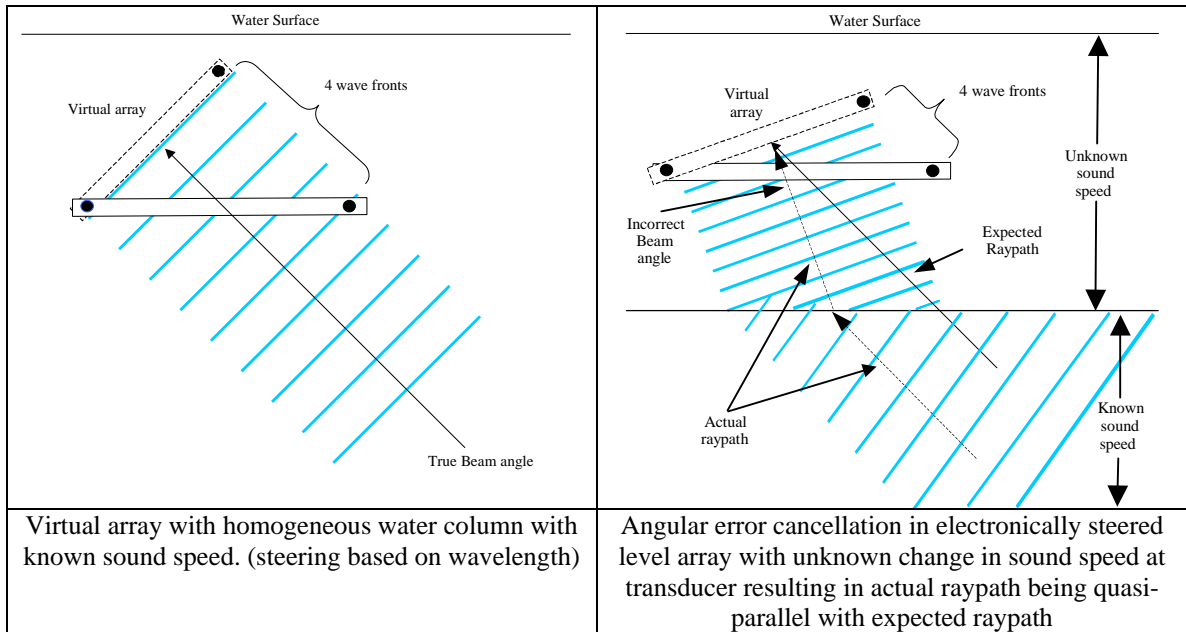
Figure 50. Errors with an unknown surface sound speed change with a electronically steered level array.

While the case illustrated in Figure 50 is unrealistically simple, it serves to illustrate how the incorrect departure angle is offset in the first step of the raytrace due to the refraction of the ray path caused by the change in sound speed at the surface.

3.5.5.3.2 Archived Profile raytracing with update to sound speed (Arcuate Array Equivalent)

3.5.5.3.2.1 Sound Speed updated in isolation

Figure 51 illustrates the effect of updating the sound speed at the transducer while using an archived profile. It is clear that this method results in a raytracing solution that diverges quickly from the updated profile and results in an error that will increase with depth.

Calculated Ray Angle vs Depth
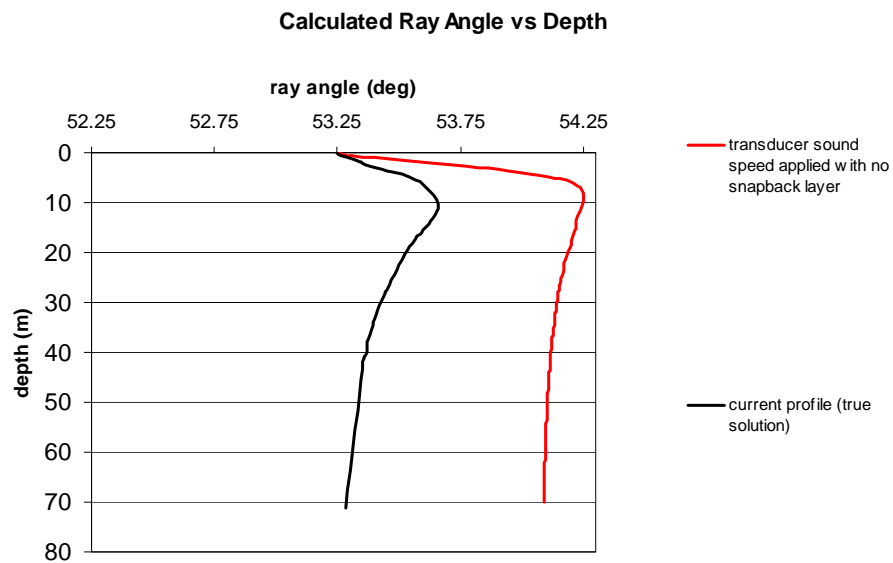
Figure 51. Raytrace with sound speed updated at transducer in isolation

Figure 52 illustrates once more the large error that is introduced when the sound speed at the transducer is changed in isolation. When the surface sound speed is applied

in this manner, the percentage depth error increases rapidly with depth, as would be consistent with a gross angular error.

Percentage Depth Error
sound speed applied in isolation

percentage depth error

Sound Speed Profiles
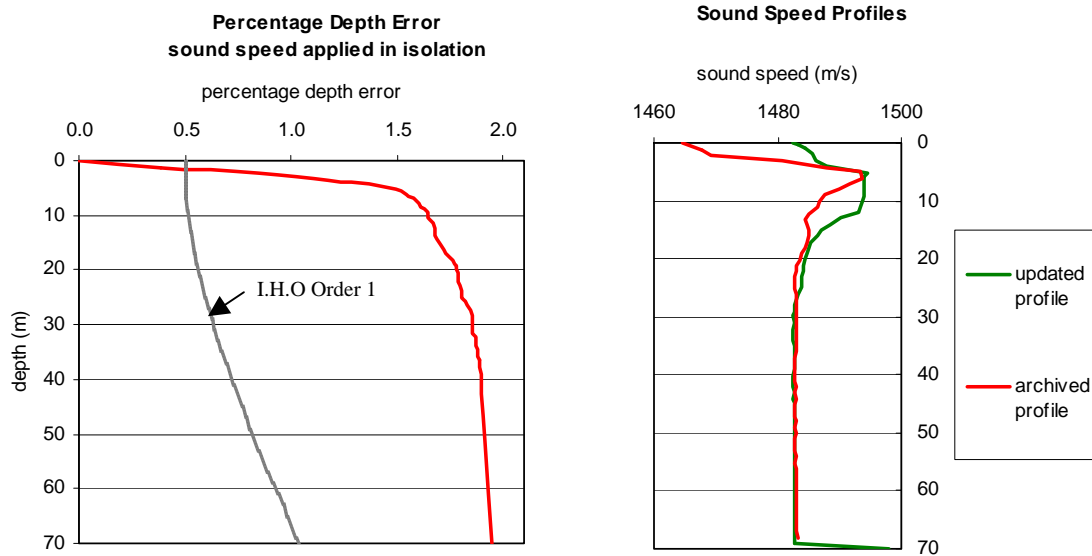
sound speed (m/s)

Figure 52. Percentage depth errors when sound speed is updated at the transducer in isolation with I.H.O Order 1 maximum depth error for reference

This condition of a corrected departure angle with an archived or incorrect profile is consistent with what would occur when using an arcuate array such as a barrel array that transits into a zone where the surface sound speed changes. Figure 53 illustrates the basic concept that a change in sound speed does not affect the departure angle of an arcuate array as it would with an electronically steered array.

Water Surface	Water Surface
Physically pointed array	Physically Pointed array
True Beam angle	True Beam angle
Arcuate array with homogeneous water column with known sound speed	Arcuate array with unknown decreased sound speed through homogeneous water column
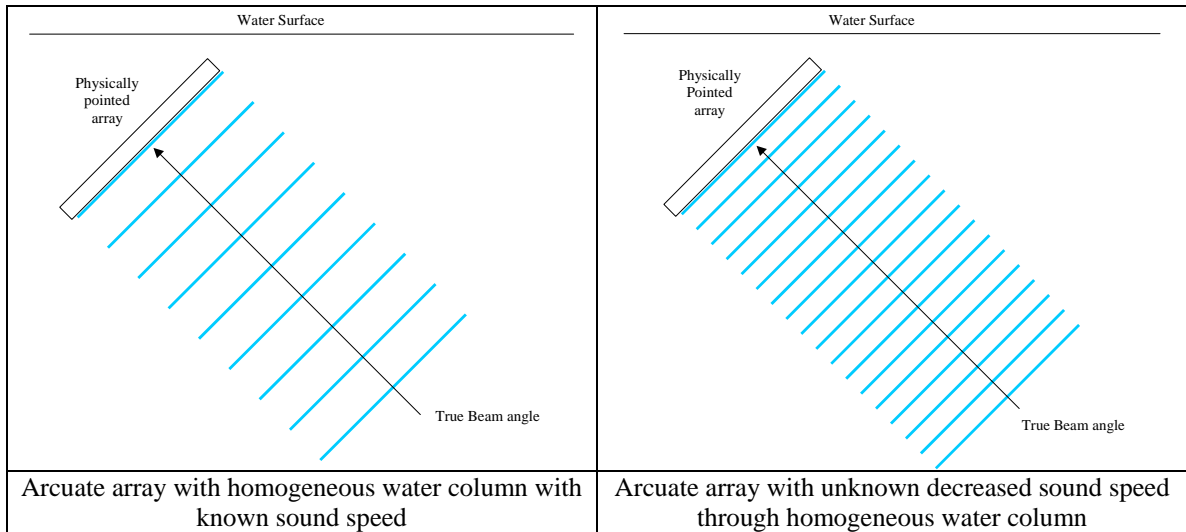
Figure 53. Invulnerability of departure angle of arcuate array to change in sound speed

While this might seem to be an advantage, it is not usually the case that the sound speed changes for the entire water column, but rather the surface layers tend to be the most variable. The following image illustrated the errors that result when a layer of surface sound speed changes with a system where the departure angle is correct. This situation is equivalent to the case of an arcuate array

| Change in surface sound speed (unknown to system) | Angular error in an arcuate array with unknown change in sound speed at transducer |
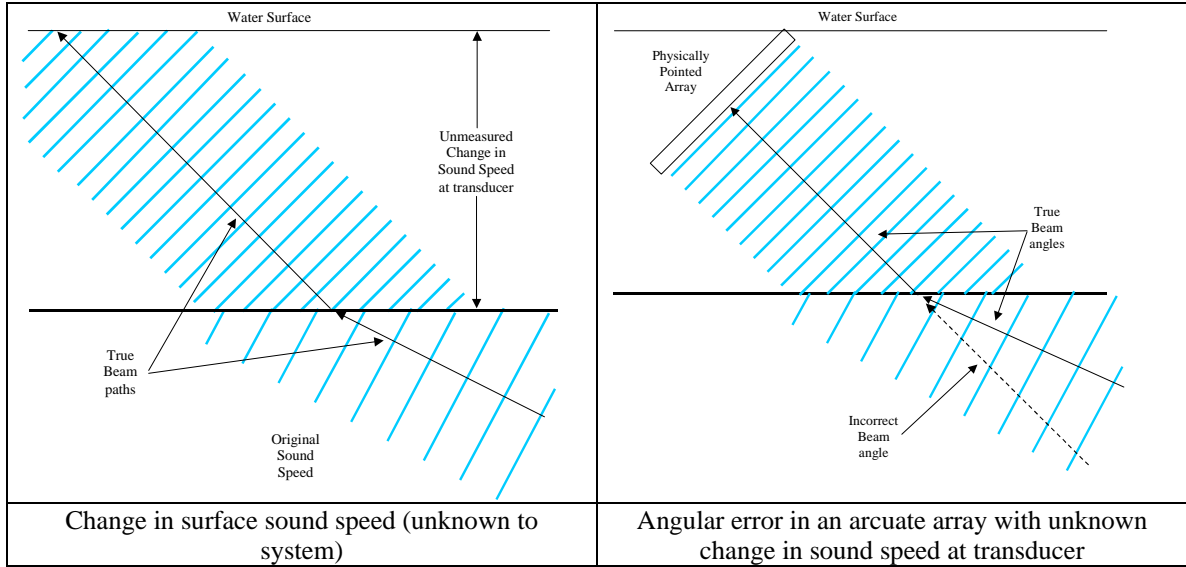
Figure 54. Angular caused by change in surface sound speed with arcuate array (correct departure angle)

As can be seen from Figure 54, having the correct departure angle with an unknown change in surface sound speed can be a disadvantage as a major angular error results. In order to mitigate this error it is necessary to have a recent surface sound speed value to compensate for the refractive effect in the first water layer.

3.5.5.3.2.2 Snapback layer (arcuate array)

In order to effectively use a surface sound speed in combination with an archived profile it is necessary to correct not only for the departure angle, but also for the error in the first step of the raytrace caused by the change in sound speed.

As was shown in section 3.5.5.3. using an archived profile with no update to the sound speed resulted in these errors "automatically" offsetting the departure angle error, however this effect is only valid when the electronically steered array is relatively level.

If the surface sound speed is available then it is preferable to correct for the departure angle and then correct for the refraction in the first step of the raytrace. This is done by using a "snapback" layer, which consists of an assumed layer of water at the transducer that has the same sound speed as the measured surface sound speed.

Calculated Ray Angle vs Depth
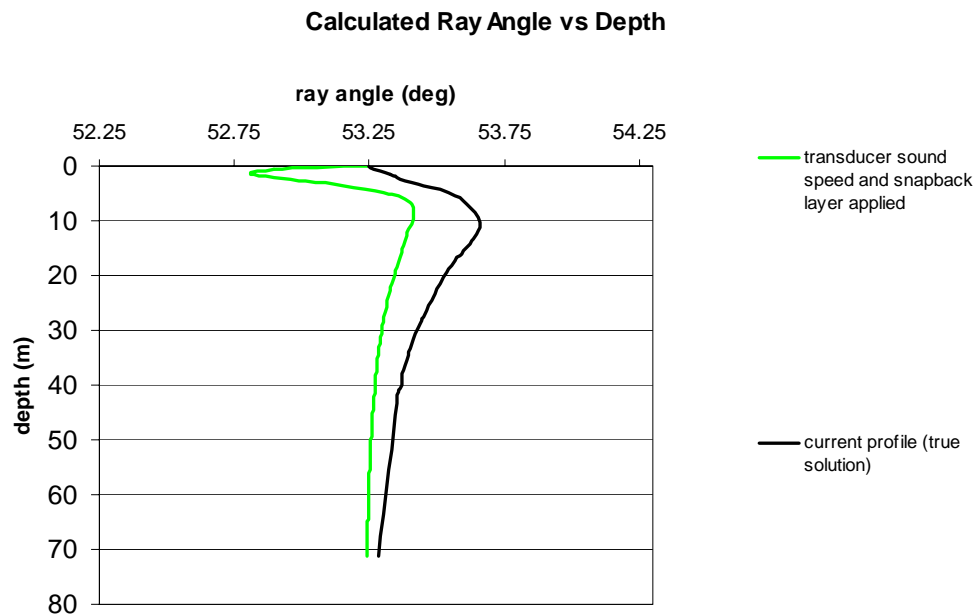
Figure 55. Raytrace using snapback layer with correct departure angle and snapback layer at surface

Figure 55 illustrates the ray path that results from using the correct departure angle (as is always the case in an arcuate array) and a surface "snapback" layer. While the calculated raytrace initially has an inherent error, the solution quickly converges to a

similar solution as the water column returns to where the sound speed is constant between archived and true profiles.

Percentage Depth Error
surface sound speed and snapback layer

percentage depth error

Sound Speed Profiles
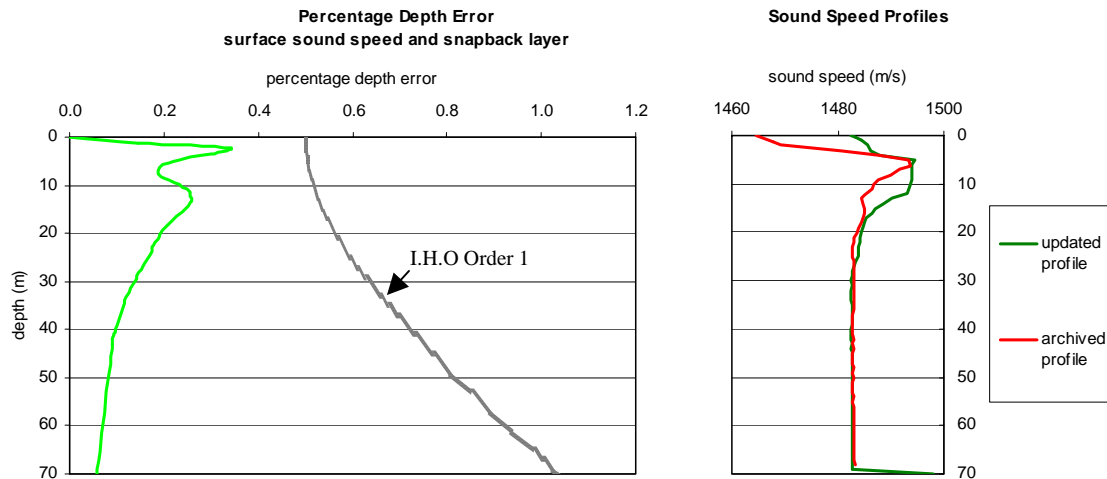
sound speed (m/s)

Figure 56. Percentage depth error using surface sound speed to correct departure angle and to correct for refraction through use of snapback layer

Ray tracing using the archived profile, an updated sound speed at the transducer and a small surface layer with same value as the sound speed at the transducer then results resulted in values that were within IHO specifications.

Figure 57 illustrates the effect of using a snapback layer when there is a correct departure angle. While the illustration is of an unrealistically simple water column, it illustrates the basic principle of the effect of the snapback layers in correcting the raytracing error and how, as the raypath enters known sound speeds, the raypath is restored, as the ray parameter is once again correct
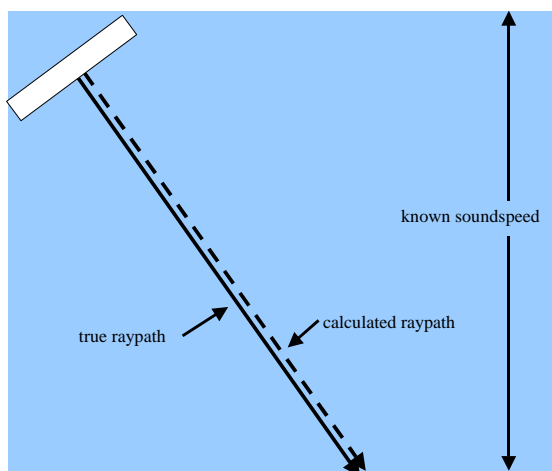
1. Homogeneous water column with known sound speed
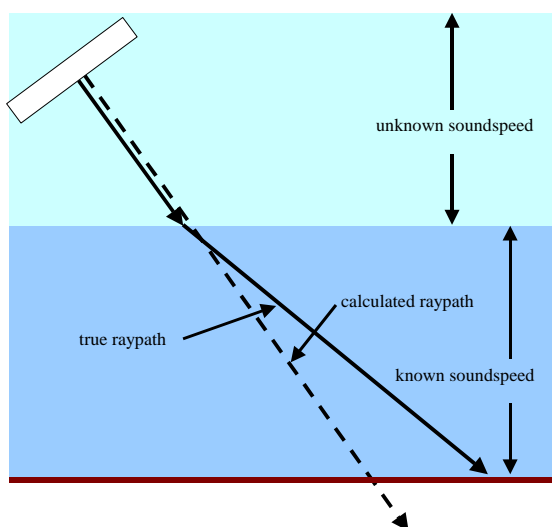
2. Introduction of surface freshwater layer produces large depth and position error that increases with depth
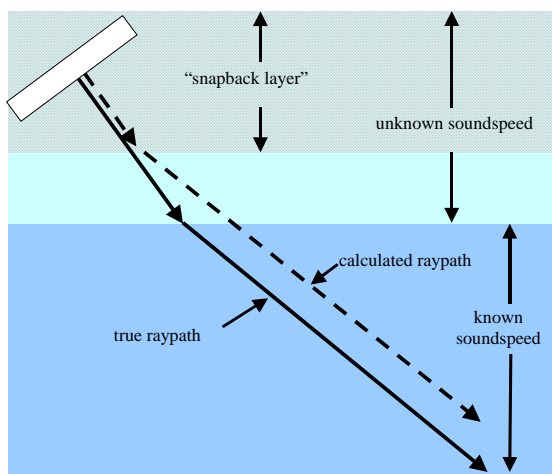
3. Using knowledge of surface sound speed, a snapback layer is introduced to arbitrary depth. The error between the arbitrary and true depth of the sound speed change introduces depth and position errors, however it is constant with increasing depth and therefore a decreasing percentage of the total depth.

Figure 57. The effect of using a snapback layer to correct for the error in the first step of the raytrace due to a change in the surface sound speed for an arcuate array

The use of such a layer becomes important for systems that use arcuate arrays. This is because there is no departure angle error associated with an incorrect sound speed at the transducer, the error cancelling effect seen with a level, electronically steered system is lost. This would affect barrel array systems such as the Simrad EM1002.

In the case of an electronically steered array, if a surface sound speed is used, resulting in the correct departure angle, then a snapback layer must be applied as with an arcuate array to correct for the ray bending error in the first part of the raytrace calculation.

3.5.6 Summary

The Fraser River Delta presents a unique challenge to oblique incidence echo sounding. Specifically the presence of a surface layer of water with an extremely variable sound speed means that it is critical to evaluate different methods of measuring and applying sound speed profiles and surface values.

The use of constantly updated profiles clearly presents the best option, with interpolating between the profiles representing the ultimate solution, there are times where other application, methods will be used.

In the case of an electronically steered array under minimum roll conditions, the use of an archived profile provides depths that are reasonable due to the fact the majority

of sound speed variability is in the upper layers of the water column. In the case of conditions where roll is a consideration the use of an archived profile with updated surface sound speed to correct for departure angle and initial refraction error provides acceptable results.

When using an arcuate array, or a permanently tilted electronic array, the use of an archived profile is not acceptable under the conditions present in the Fraser River Delta. In order to effectively use such a system it would be necessary to use a surface sound speed sensor to provide a value used in a snapback layer to correct for the initial refraction error.

CHAPTER 4 IMPACT ON C.H.S. MULTIBEAM SURVEY OPERATIONS

4.1 Introduction

The survey discussed in this report marks the first use by the Pacific Region of the Canadian Hydrographic Service of advanced sound profiling technology. This was also the first time that a survey in the extremely variable conditions that are present on the Fraser River Delta was examined in all its details. This presented a unique opportunity to evaluate and scrutinize the performance of the systems directly used and also enables the implied evaluation of alternate systems available to the Service.

4.2 MVP Profiling System Effectiveness

This was the first survey operation on the west coast of Canada to fully implement the MVP 30 near real time sound speed measurement system. The survey was an excellent test of the system as it took place in an estuarine environment with a very dynamic oceanography

4.2.1 Hydrography

It is clear from the results that the MVP 30 did an effective job in capturing the water column structure in a dynamic changing environment. The system enabled the survey to be conducted to within IHO specifications facilitating the detection of fine scale features for the use in geological studies. The system was not used at its maximum rate due to logistical and software limitations, however for the specific purpose of providing bathymetry to IHO specifications it was shown to be unnecessary to sample at this rate.

It was also shown that the use of archived profiles, without surface sound speed updates, in combination with a level electronically steered array resulted in satisfactory results. While this was a surprise, considering the conditions in the survey area, it highlights the flexibility of a level electronically steered array and provides the option of measuring the sound speeds at a lesser rate..

Logistically, the streaming of a line behind a survey vessels results in some danger to the equipment, increased workload, due to the standing of a stern watch, and reduced manoeuvrability, especially with respect to reversing. It is clear then, that when surveying specifically for hydrography, the MVP cycling rate must be balanced by other factors such as workload and risk management.

4.2.2 Oceanography

A significant disappointment of the survey was a lack of ability to correlate the sound speed data with other parameters such as tide and time of day. The MVP 30, as currently configured, has been shown to be ineffective in capturing the oceanographic parameters of the water column structure in a dynamic system such as the Fraser River Delta. This can be attributed to two factors. The most important factor is the lack of a temperature sensor to work in collaboration with the sound speed sensor. If a temperature sensor had been mounted along with the sound speed sensor, it would be possible to calculate the salinity using the relationship of salinity, temperature and sound speed. The second factor is that the frequency of the sound speed casts may not have been of adequate density to fully capture the changes.

While these statements are, by necessity, speculation, it is likely that it would be possible to model the oceanographic environment given a temperature sensor and a sufficient frequency of casts. This represents a unique opportunity to add significant value to a hydrographic survey by providing data that would be invaluable to physical oceanographers. This is particularly relevant in critical areas such as the Fraser Driver Delta [Crawford 2002]. There would be an increased risk of loss of the sensor and issues with manoeuvrability, but it is suggested that this would be more than offset by the collection of valuable oceanographic data.

4.3 Multibeam System Effectiveness

4.3.1 Electronically Steered Array (Simrad EM3000)

The Simrad EM3000 proved to be a very flexible system, able to effectively mitigate error in the depth and position solutions resulting from significant sound speed changes at, or near, the surface. This was due to the ability of the system to effectively cancel out the errors, under minimal roll conditions, that result from a beam pointing error as discussed in section 3.5.5.3.1. As this mitigation of errors caused by surface sound speed changes is reduced as the depth of the sound speed anomaly increases, it is also critical to that regular sound speed profiles are measured to maintain confidence in the accuracy of the data

The system is ideally suited to areas where there may be sudden, drastic changes to the surface sound speed that cannot be adequately sampled using current sound speed profiling systems. While it was shown that a surface sound speed sensor is not critical for this system, the additional information would clearly be useful for sound speed change monitoring. Particularly in combination with a surface temperature sensor, a sound speed sensor would also provide useful oceanographic information.

4.3.2 Simulated Physically Steered Array (Simrad EM1002)

By simulating the features of a physically steered array using raytracing calculations on EM3000 data, it was clearly demonstrated such an array could potentially result major errors if the surface sound speed is not continuously monitored and applied to the ray tracing solution. This is especially relevant in areas with significant freshwater influx such as the Georgia Strait or areas with significant up welling such as the West Coast of the Queen Charlotte Islands.

4.4 Summary

The selection of a multibeam survey system is generally dictated by the depth capability and the platform suitability to the area to be surveyed. However, once these primary constraints have been considered, the type of transducer array and the sound speed measurement system must be taken into account.

The type of oceanography encountered in a survey area will most drastically influence this selection. Ideally, an area with dynamically changing surface sound speeds would be surveyed with an electronically steered transducer array such as the Simrad EM3000. However, if the depths to be measured require the use of the Simrad EM1002

with its lower frequency and higher output power, it is critical that the system's requirement for a constant, accurate surface sound speed be considered.

The decision concerning optimal configurations must look at the entire surveying system, including the transducer design the sound speed measurement method, profile and surface and finally the goal of the survey whether hydrographic, oceanographic or both.

CHAPTER 5 CONCLUSION AND RECOMENDATIONS

The measurement of surface sound speed and profiles of sound speed are clearly a critical component of the multibeam survey. The measurement and application of this critical parameter must take into consideration a number of distinct but interrelated factors.

Considerations include the purpose of the survey, the required accuracies of the bathymetric data and the requirement for the determination of ancillary oceanographic parameters for non-hydrographic purposes.

The next consideration is the accuracy of the sound speed data used. The accuracy will be degraded by numerous sources such as sampling interval, whether traversing significant oceanographic interfaces and sensor accuracy and resolution. A critical consideration is the location of any sound speed anomalies within the water column, whether at the surface or deeper in the water column.

The method of beam steering employed must be considered as this produces different errors when exposed to a varying sound speed profile. The type of transducer used, whether it is a flat electronically steered array, or a curved physically steered array, dictates this beam steering. It is also necessary to consider the case of systems where a combination of these two methods is employed.

During the course of the writing of this report several recommendations came to light or were strongly reinforced. Of primary importance is the measurement and correct application of surface sound speed, particularly in the case of an arcuate array. It is also

recommended that survey data logging software be modified to enable the uninterrupted input of surface sound speed data enabling a survey to utilize the moving vessel profiler to its maximum potential. The addition of a relatively inexpensive temperature sensor collocated with the sound speed sensor would contribute to an enhanced data set with respect to the measurement of oceanographic parameters. And finally it is reinforced that when planning a survey, all parameters should be examined in order to select and properly utilise the correct tools to accomplish the goals of the survey.

This report has identified and isolated issues with respect to survey systems and the oceanographic conditions within which they function. This knowledge will help to make surveys in areas with challenging oceanography more effective and suited to the purpose for which the survey is conducted.

REFERENCES

Applanix Corporation, (2002). POS MV V3 Installation and Operation Guide. Richmond Hill, Ontario, Canada

Applied Microsystems Ltd. (2003). Sound Velocity – Sensors. http://www.appliedmicrosystems.com/sensors/sound-velocity-of-water.html

Barrie, J.V., Currie, R.G. and Kung, R. (2001) Surficial Sediment Distribution and Human Impact - Fraser Delta" http://www.pgc.emr.ca/marine/sed_dstbn.htm.

Brooke Ocean Technology Ltd., (2003). Moving Vessel Profiler – An Underway (Instride) Ocean Profiling System. http://www.brooke-ocean.com/mvp_main.html

Capell, W.J., (1999). Determination of Sound Velocity Profile Errors Using Multibeam Data. Proceedings of Oceans 99, Seattle, Washington, USA.

Carnvale, A., Bowen, P., Basileo, M., Sprenke, J.,(1983) Absolute Sound-Velocity Measurement in Distilled Water. J. Acoust. Soc. Am, 44 (5), 276 282.

Chen, C.T., and F. Millero (1977) Speed of Sound in Seawater at High Pressure. J. Acoust. Soc. Am, 62 (5), pp. 1129-1135

Colladon, J.D., Sturm, J.K. (1827) The Compression of Liquids (in French). Ann. Chim. Phys. Series 2(36), part IV, pp 236-237.

Crawford, W.R. (2002) Personal Communication, Research Scientist, Ocean Science and Produtivity, Department of Fisheries and Oceans, Sidney British Columbia, Canada, December.

Curtiss Technology (2002) Principles of Sonar Beamforming http://www.curtistech.co.uk/papers/beamform.pdf.

Del Grosso, V.A., Mader, C.W. (1972) Speed of Sound in Sea-Water Samples, J. Acoust. Soc. Am, 42 (3), 961-974.

de Lange Boom, B. R. (2003). Personal Communication, Tides and Current Analyst, Canadian Hydrographic Service, Sidney, Department of Fisheries and Oceans, British Columbia, Canada September.

De Moustier, C., (1998). Coastal Multibeam Hydrography Course Lecture Notes. University of New Brunswick, Fredericton, New Brunswick, Canada.

Dinn, D.F., (1995). The Effect of Sound Velocity Errors on Multibeam Sonar Depth Accuracy. Proceedings of the Oceans '95 Conference, Oct. 9 – 12, 1995, San Diego, California, USA.

Dushaw, B.D., Worcester, P.F., Cornuelle,B.D., Howe, B.M., (1993). On equations for the sped of sound in seawater, J. Acoust. Soc. Am. 93(1), pp 255-275.

Dyer, K.R. (1997) Estuaries A Physical Introduction. Wiley, Toronto.

Eaton, G, Dakin, D.T., (1996) Miniature Time of Flight Sound Velocimeter Offers Increased Accuracy over Sing-Around Technology and CTD Instrumentation. Proceedings of the Oceanology International '96 Conference, Brighton, U.K, March.

Environment Canada, British Columbia Ministry of Environment, (1992). State of the Environment for the Lower Fraser River Basin. SOE Report No. 92-1. Environment Canada, Ottawa, Canada.

Fujii K., Masui R. (1993) Accurate measurement of the sound velocity in pure water by combining a coherent phase-detection technique and a variable path-length interferometer. J. Acoust. Soc. Am, 93 (1), 276 282.

Geographic Data BC, (2003). British Columbia Standards, Specifications and Guidelines for Resource Surveys Using Global Positioning System (GPS) Technology. Ministry of the Environment, Government of British Columbia, Victoria, Canada.

GRASS Development Team, (2003). Official Grass GIS Homepage.
http://www.baylor.edu/~grass/

Greenspan, M, Tschiegg, C.E., (1957) Sing-Around Ultrasonic Velocimeter for Liquids.
The Review of Scientific Instruments, Vol 28(11), November.

Hampson, G.A., (1997). Implementing Multi-Dimensional Digital Hardware
Beamformers. PhD Thesis, Department of Digital Systems, Monash University,
Melbourne, Australia.

Hare, R. (2001). Error Budget Analysis for US Naval Oceanographic Office
(NAVOCEANO) Hydrographic Survey Systems. University of Southern Mississippi,
Hydrographic Science Research Centre.

Hart, B.S., Barrie, J.V. and Hamilton, T.S.(1998). Sedimentation rates and patterns on a
deep water delta (Fraser Delta, Canada): Integration of high-resolution seismic
stratigraphy, core lithofacies, and ^{137}Cs fallout stratigraphy. Journal of Sedimentary
Research, 68(4), 556-568.

Hogg, A. (2001) Experimental observations of shear instabilities in an exchange flow
http://www.cwr.uwa.edu.au/~hogg/inst/index.html.

Hughes Clarke J.E., (2003). Swathed Home Page http://flagg.omg.unb.ca/~jhc/swathed/

Hughes Clarke J.E., (1998). Coastal Multibeam Hydrography Course Lecture Notes.
University of New Brunswick, Fredericton, New Brunswick, Canada.

Hughes Clarke J.E., Godin , A. (1993). Investigation of the Roll and Heave Errors
Present in Frederick G. Creed –EM1000 Data When Using a TSS-335B Motion Sensor,
Contract Report No. FP7007-3-5731. Department of Fisheries and Oceans, Canada.

Hughes Clarke, J.E., Lamplugh, M. and Kammerer, E., (2000), Integration of Near-
Continuous Sound Speed Profile Information . Canadian Hydrographic conference 2000,
Proceedings CDROM, Victoria, BC, Canada.

International Hydrographic Organization, (1987), IHO Standards for Hydrographic Surveys. International Hydrographic Organization, Special Publication No. 44, 4th edition, 23pp.

Kammerer, E., (2000). A New Method for the Removal of Refraction Artifacts in Multibeam Echosounder Systems. PhD Thesis, Department of Geodesy and Geomatics Engineering, University of New Brunswick, Fredericton, New Brunswick.

Kongsberg Simrad AS, (1988). EM1002 Operational Principles. Horten, Norway.

Kongsberg Simrad AS, (2001). EM3000 Operational Principles. Horten, Norway.

L-3 Communications Seabeam Instruments, (2001). Multibeam Sonar Theory of Operation. L-3 Communications Seabeam Instruments.

Mackenzie K. V., (1981). Nine-term Equation for the Sound Speed in the Oceans, J. Acoust. Soc. Am. 70(3), pp 807-812.

McLaren, P. Ren, P. (1995). Sediment Transport and its Environmental Implications in the Lower Fraser River and Fraser River Delta. Environment Canada, Ottawa, Canada.

Medwin,H.,(1998). Fundamentals of Acoustical Oceanography. Academic Press, Toronto, Ontario, Canada.

Mosher, D.C., Christian, H.A., Hunter, J.A., and Luternauer, J.L. (2001) Onshore/Offshore geohazards in the Vancouver region of western Canada; field, modeling and mapping techniques and results http://www.pgc.emr.ca/marine/fraser.htm.

National Physical Laboratory, (2001). Technical Guides - Speed of Sound in Sea-Water. Her Majesty's Stationery Office, Teddington, Middlesex, UK.

Pickard, G.L., (1968) Descriptive Physical Oceanography. 1st Ed. Pergamon Press, Oxford.

Sverdrup, H.U. (1963) The Oceans Prentice-Hall Inc. N.J. U.S.A.

Thomson, R.E. (1981). Oceanography of the British Columbia Coast. Department of Fisheries and Oceans, Ottawa, Ontario, Canada.

Urick, R.J., (1983). Principles of Underwater Sound, Peninsula Publishing, Los Altos, California.

Williams, J. R., (1968). Fast Beam Forming Algorithm, J. Acoust. Soc. Am. 44(5), p. 1454.

Wilson, W. D., (1959). Speed of Sound in Distilled Water as a Function of Temperature and Pressure, J. Acoust. Soc. Am. 31(8), pp. 1067-1072.

Appendix I – Geographic Sound Speed Plots

– Diurnal Grouping

8:00 – 10:00

10:00 – 12:00

12:00 – 14:00

14:00 – 16:00

16:00 – 18:00

18:00 – 20:00
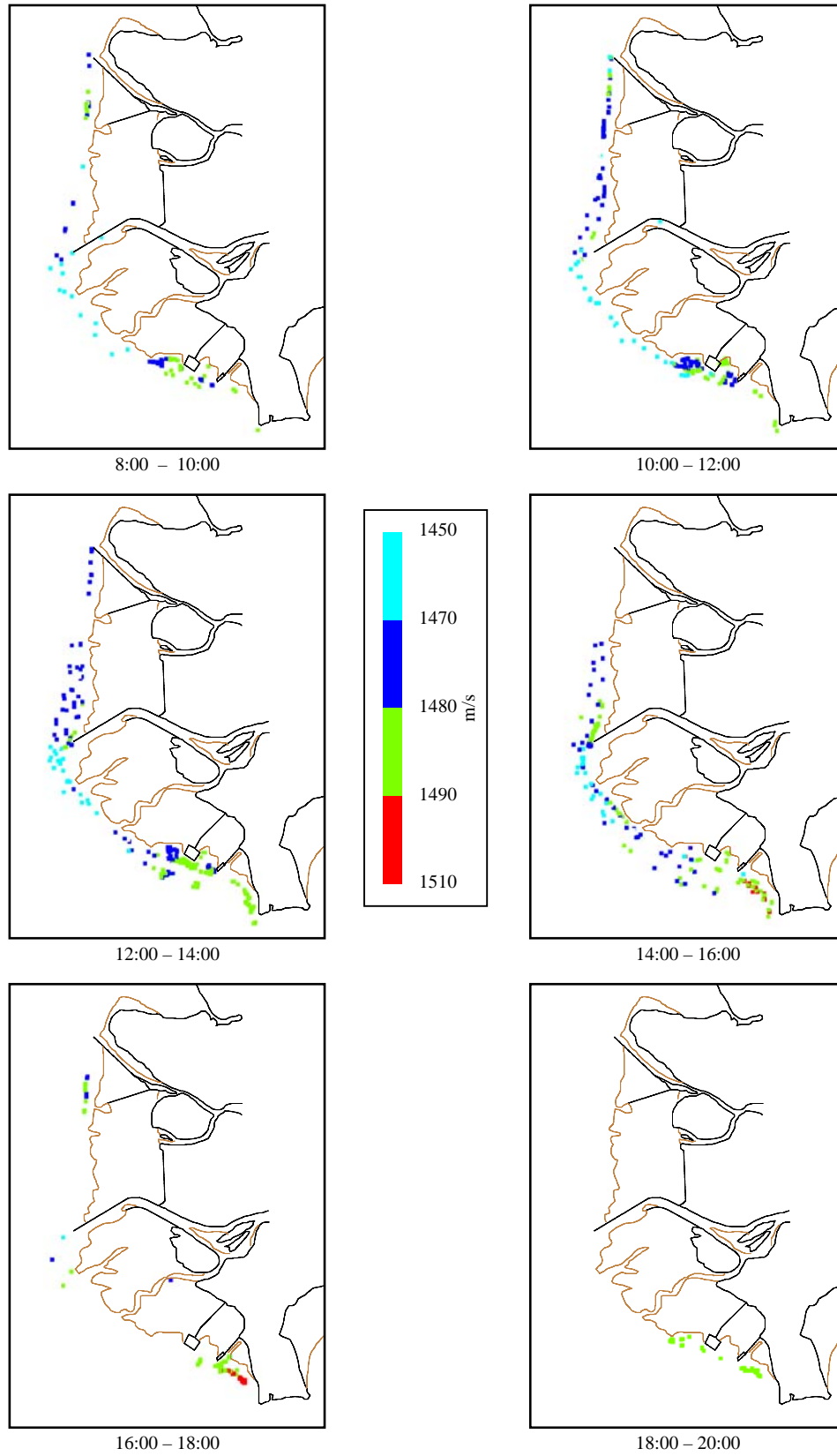
Figure 58. Sound speed of water surface relative to time of day (P.D.T. local time)

135

8:00 – 10:00

10:00 – 12:00

12:00 – 14:00

14:00 – 16:00

16:00 – 18:00

18:00 – 20:00
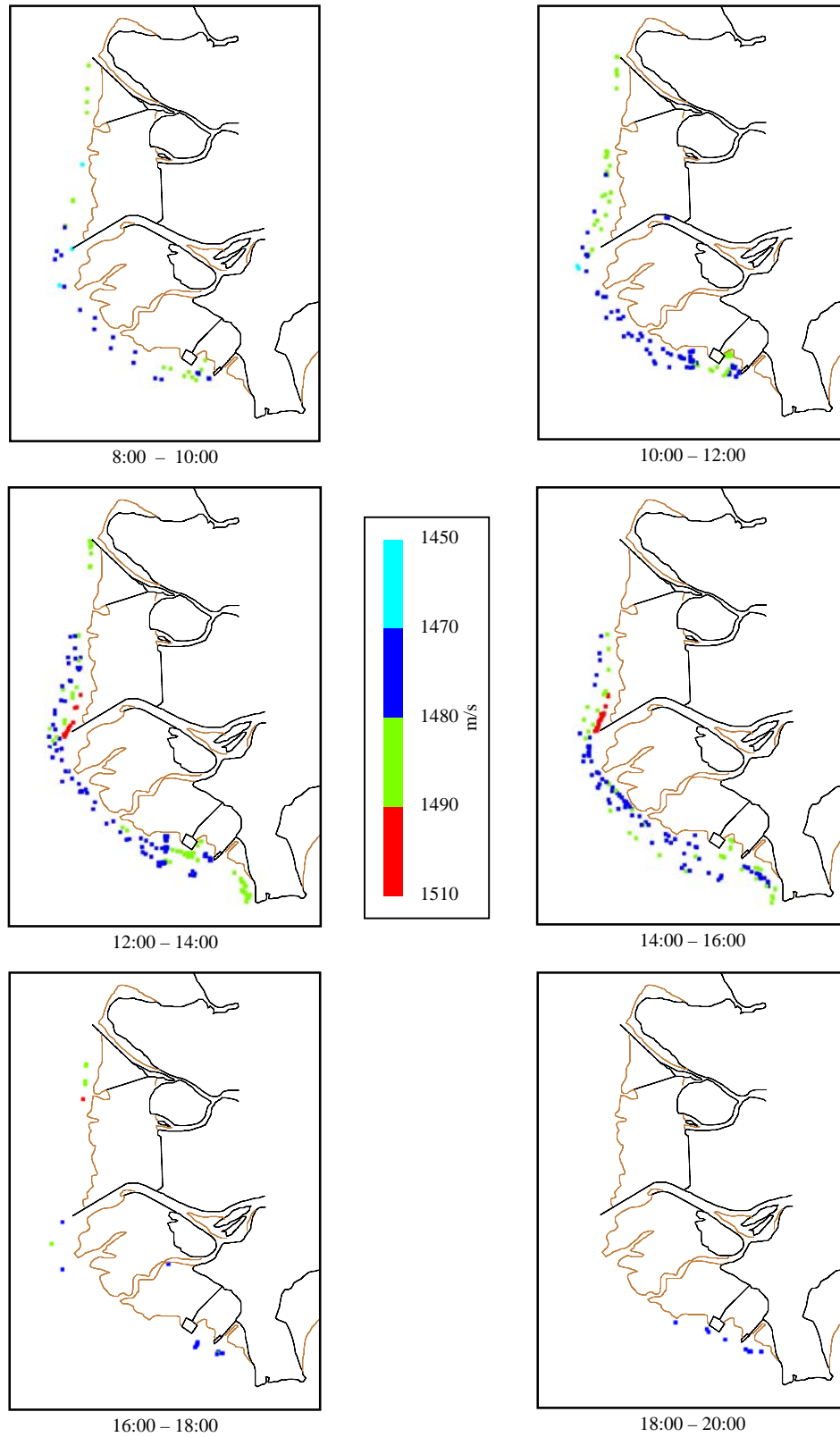
Figure 59. Sound speed of water at 5m depth relative to time of day (P.D.T.)
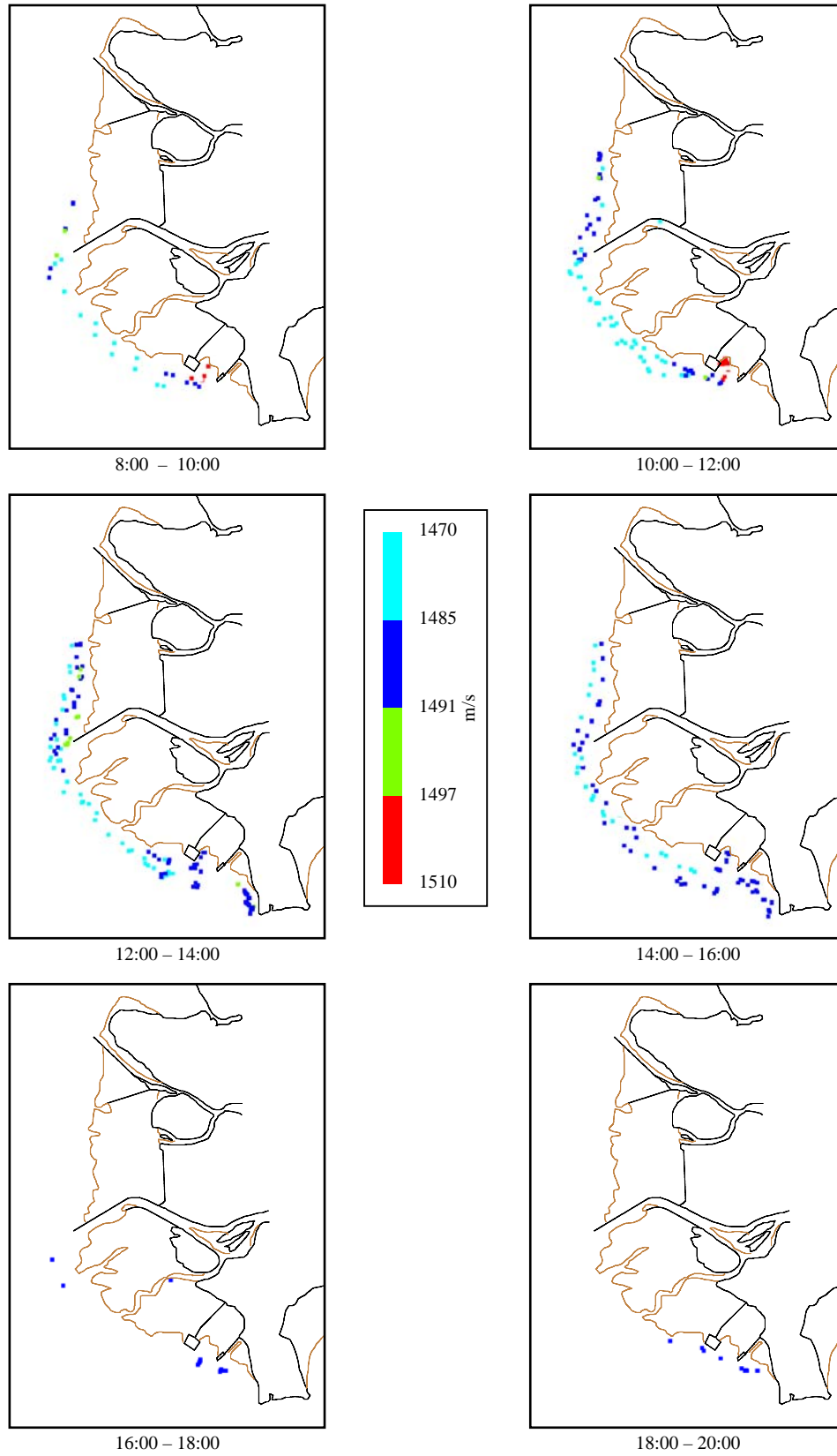
Figure 60. Sound speed of water at 10m depth relative to time of day (P.D.T.)

137
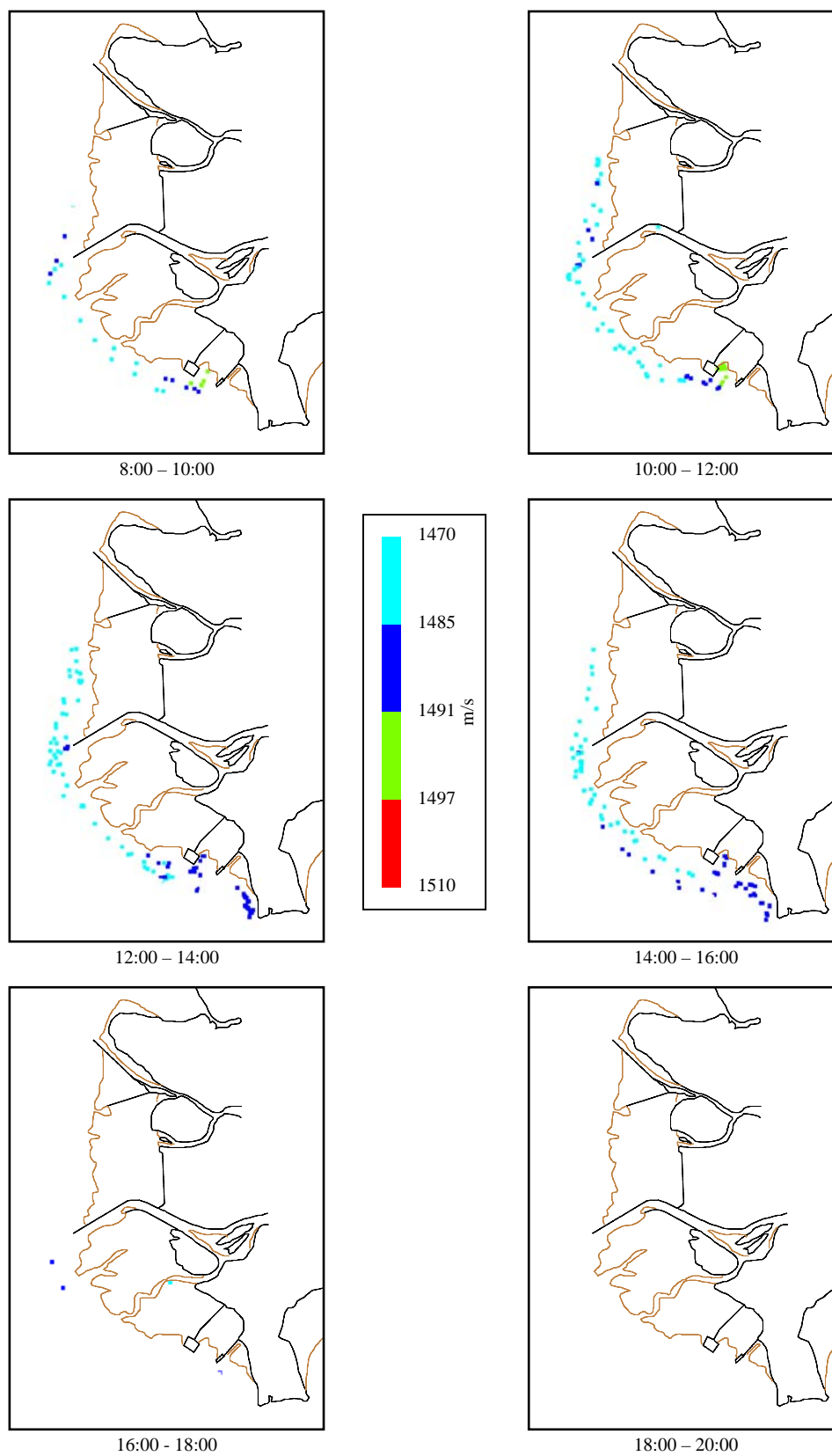
Figure 61. Sound speed of water at 15m depth relative to time of day (P.D.T.)
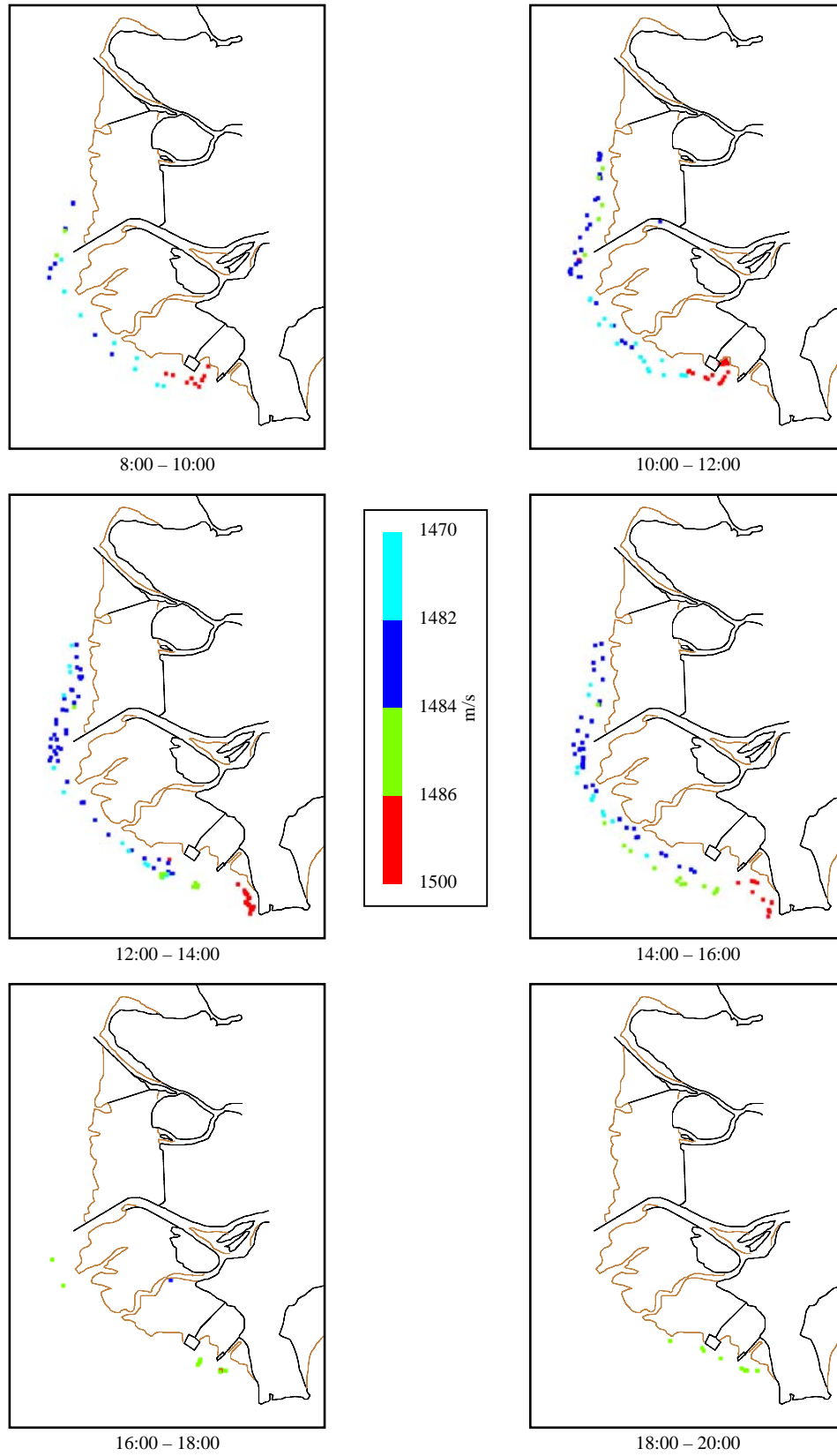
Figure 62. Sound speed of water at 20m depth relative to time of day (P.D.T.)
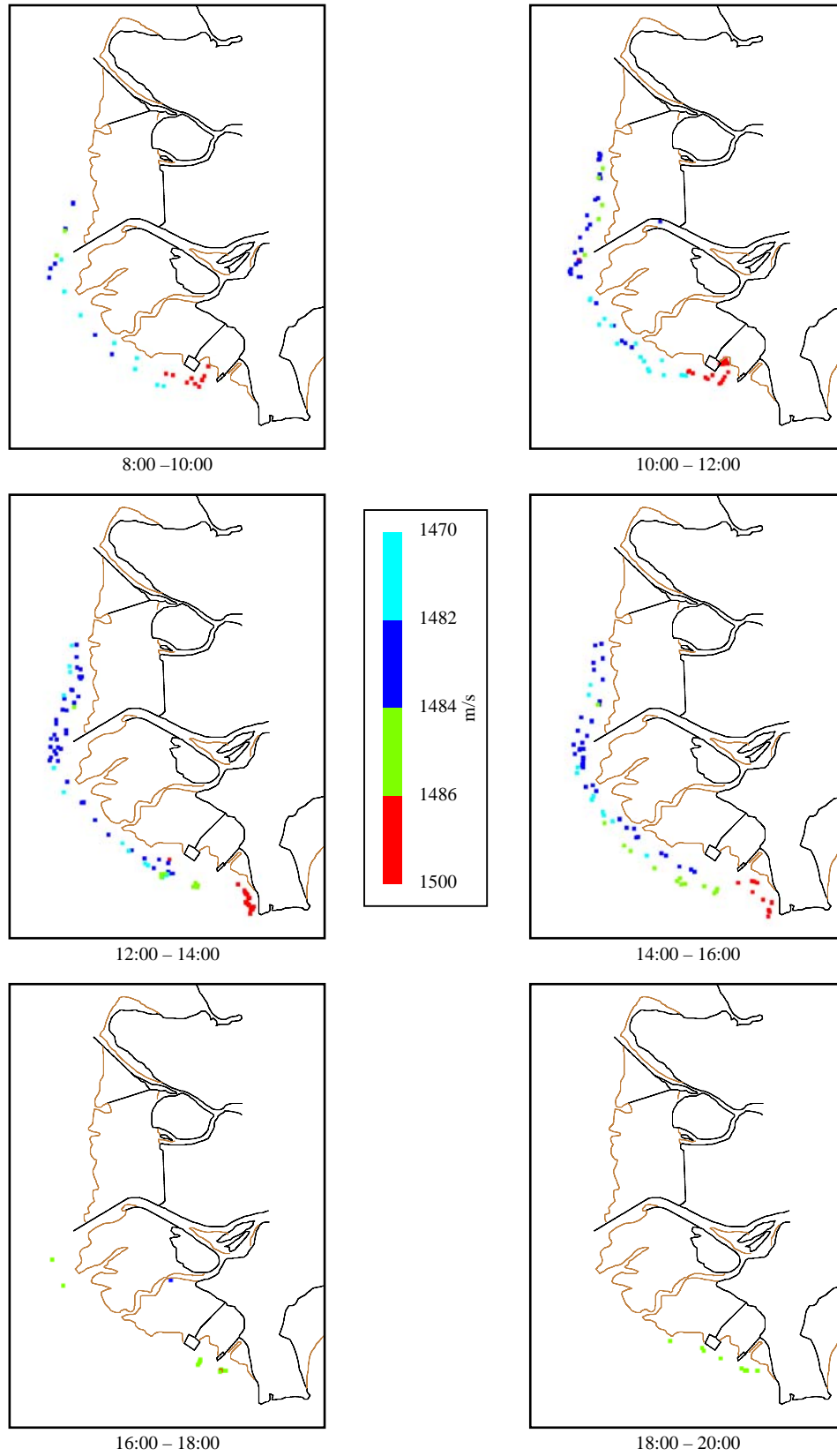
Figure 63. . Sound speed of water at 30m depth relative to time of day (P.D.T.)

140

Appendix II   – Geographic Sound Speed Plots

– Tidal Grouping
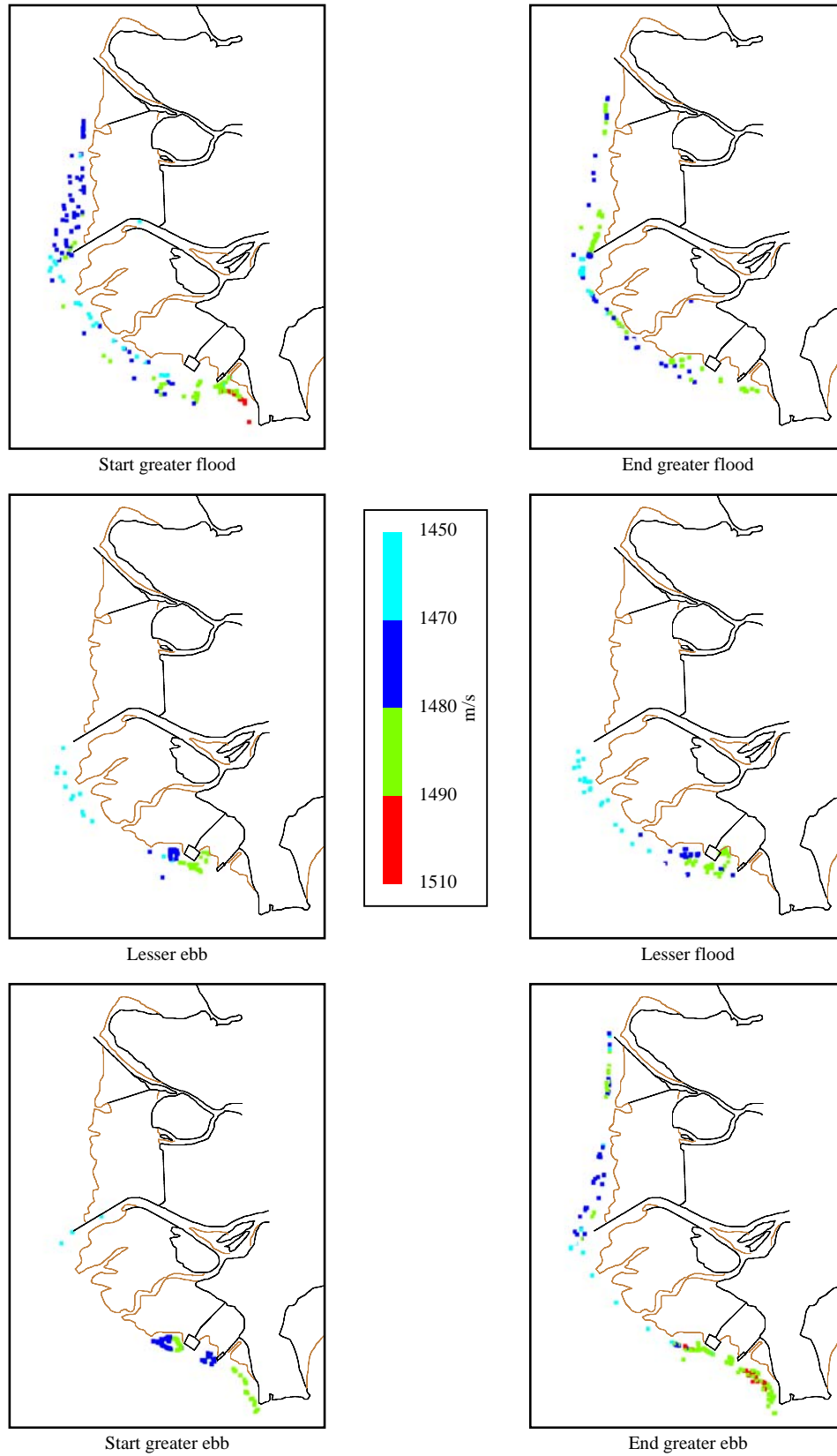
Figure 64. Sound speeds of water surface related to phase of tide
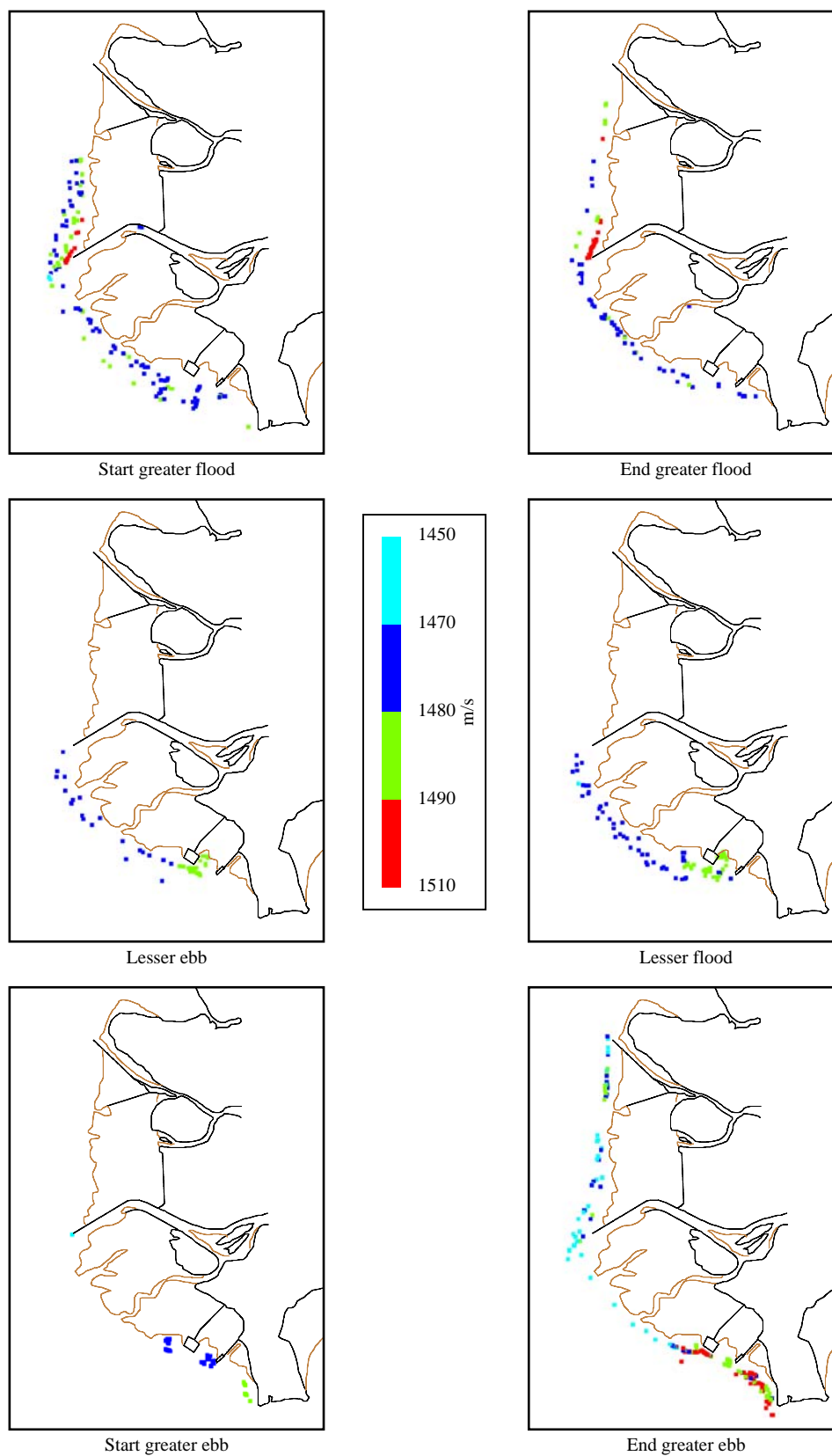
Figure 65. Sound speeds of water at 5m depth related to phase of tide

143

Start greater flood

End greater flood

Lesser ebb

Lesser flood

Start greater ebb

End greater ebb

1470

1485

1491 m/s

1497

1510
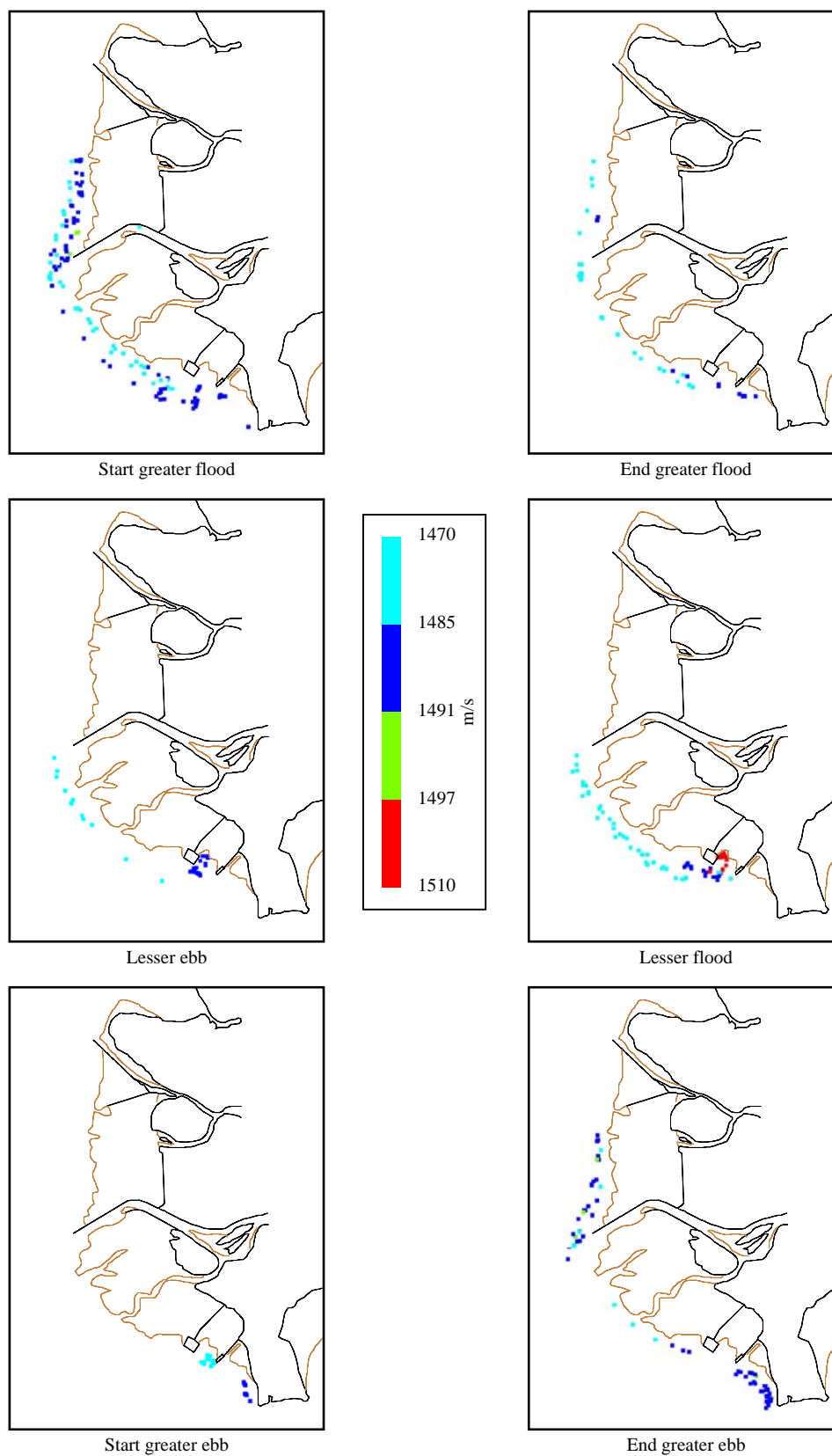
Figure 66. Sound speeds of water at 10 m depth related to phase of tide

144
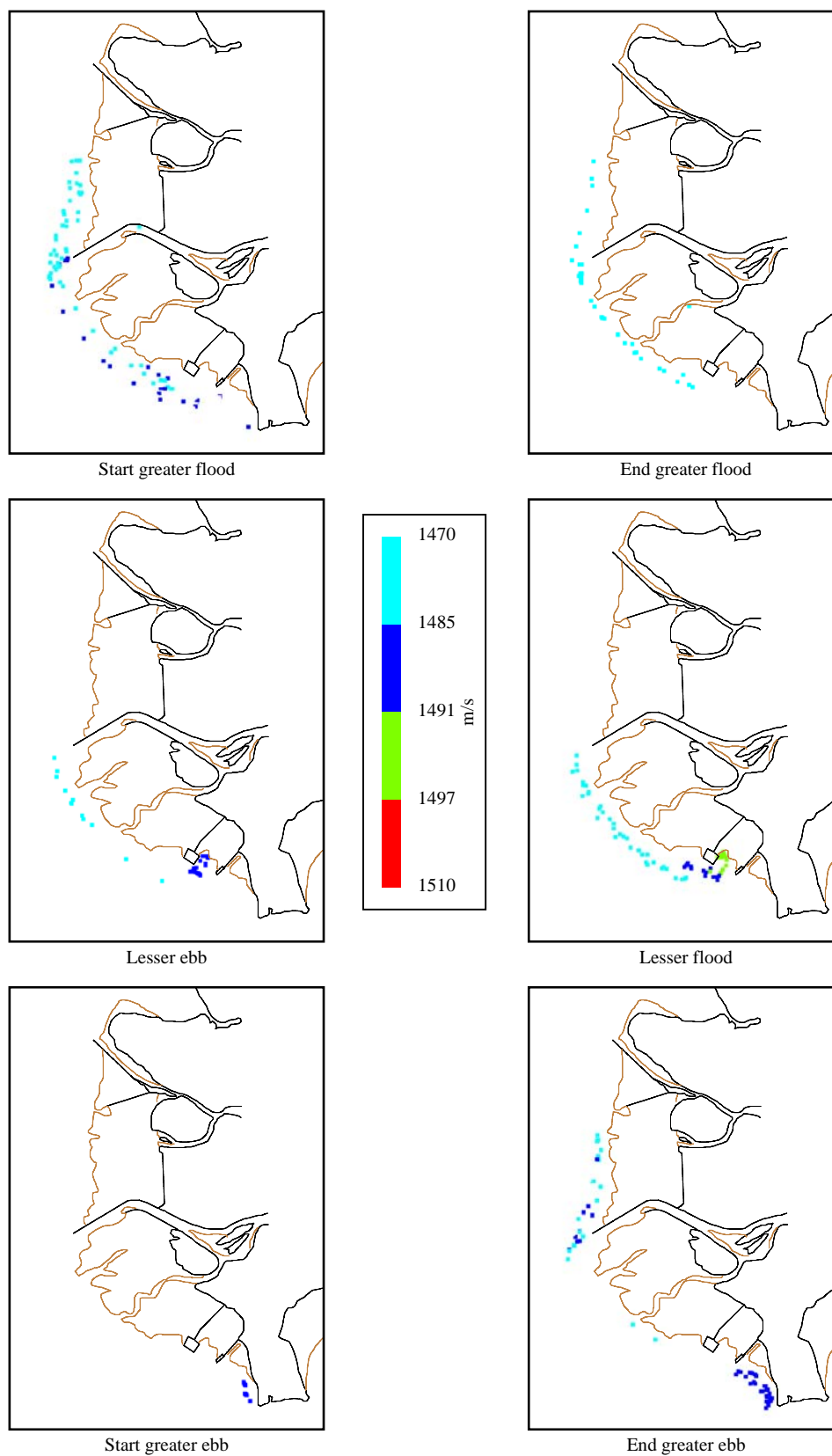
Figure 67. Sound speeds of water at 15 m depth related to phase of tide

145
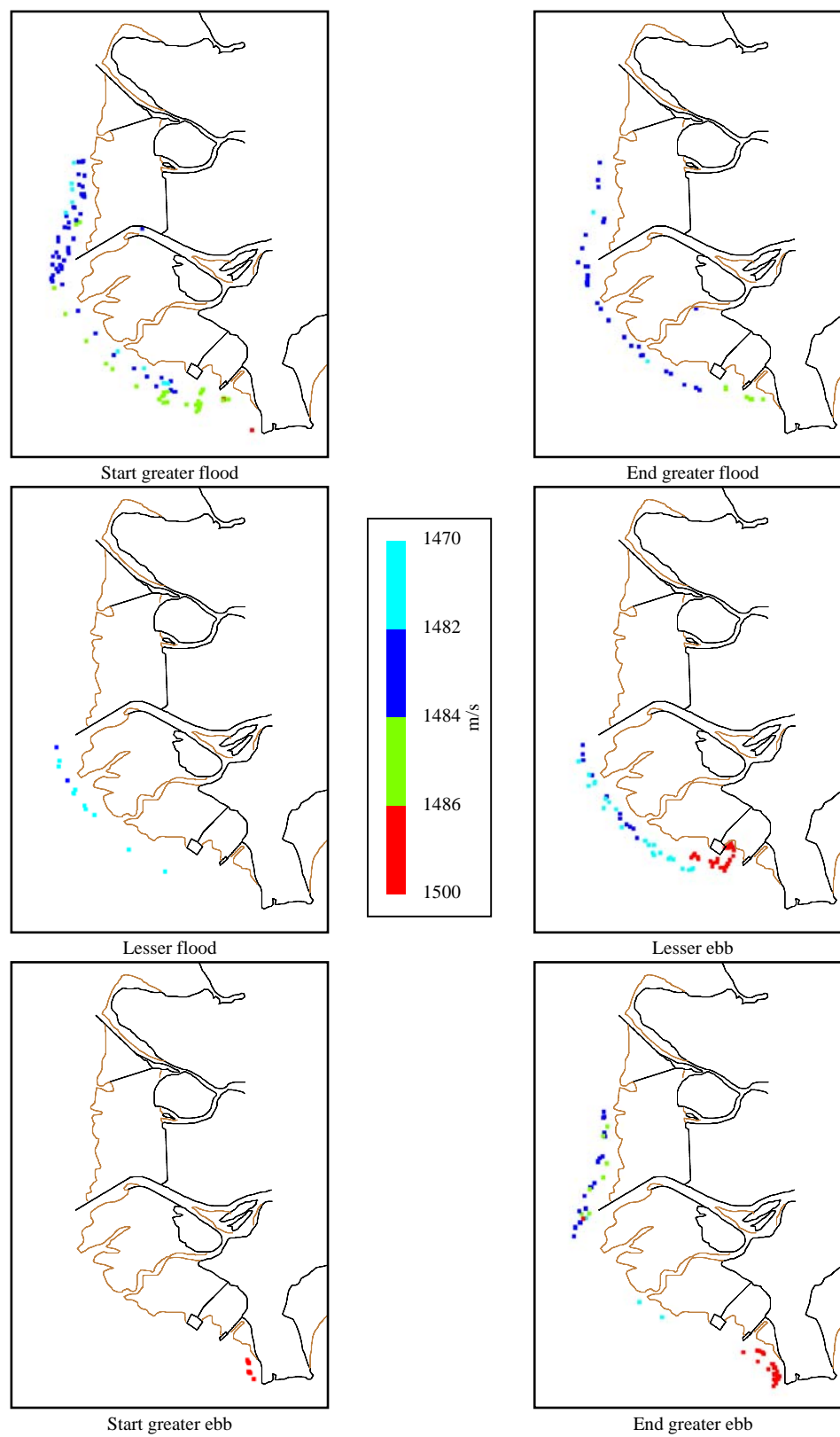
Figure 68. Sound speeds of water at 20 m depth related to phase of tide

146
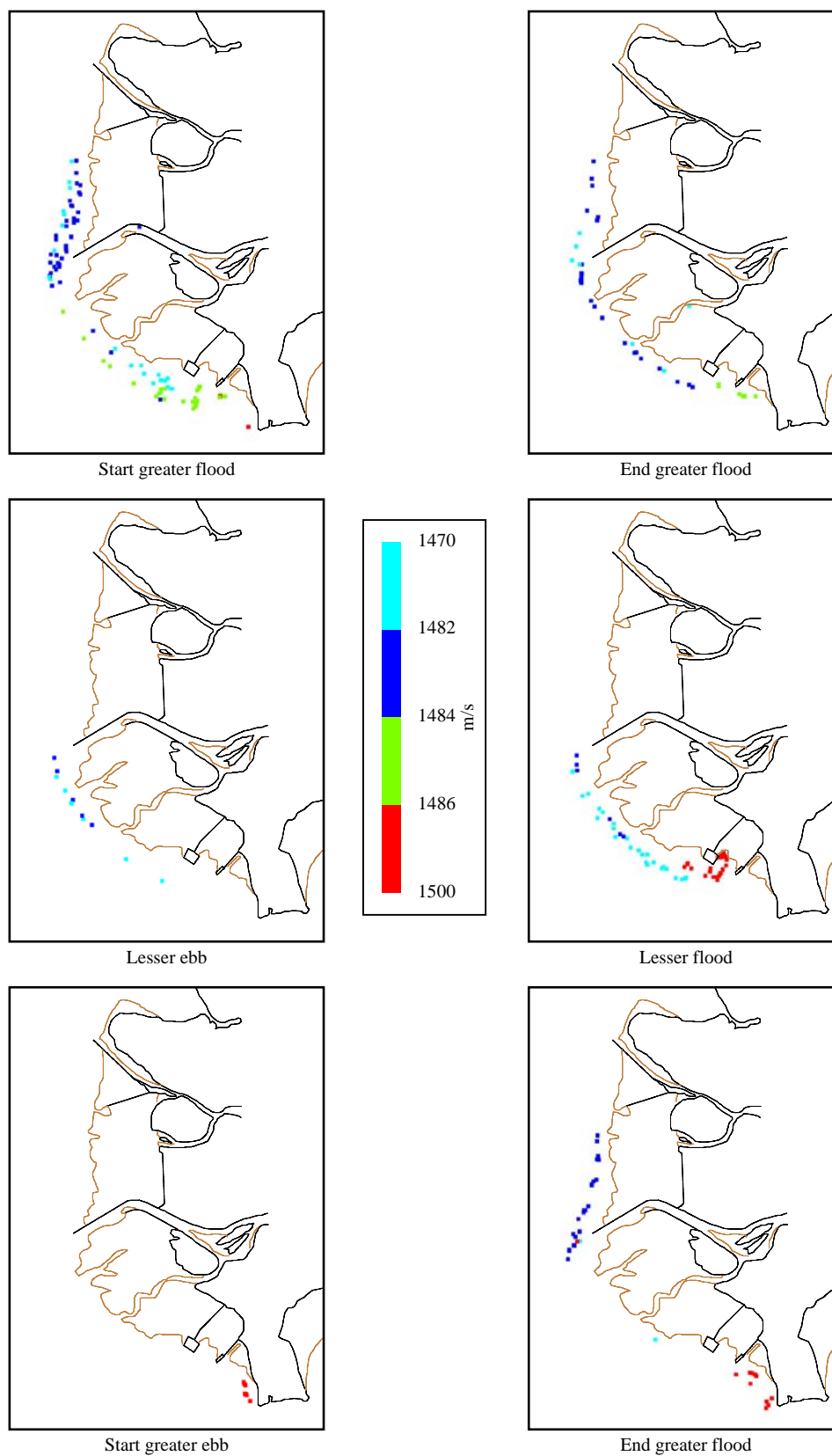
Figure 69. Sound speeds of water at 30 m depth related to phase of tide

Appendix III   - Source Code for raytrace.c

```
/***********************************************************/
/*********************   ray trace    *********************/
/***********************************************************/
void ray_calc ()
{
//locals
unsigned int tel_no=0;

unsigned int count =0;
unsigned int countb =0;
unsigned int countc =0;
unsigned int beam_count =0;

int  y=0;
double d =0;
double d1 =0;
double d2 =0;
double d3 =0;
double d4 =0;
double d5 =0;
double d6 =0;
double d7 =0;
double d8 =0;
double e = 0;


int z=1;
double azi=0;
double tim_max = 0;
double p =0;
double hor_range=0;
double error =0;
double depth = 0;
double tim_range=0;
double tot_time = 0;
double tot_range = 0;
double along = 0;
double thick = 0;
double time_diff =0;



/******************* read in svp profile *******************/
if (screwy == 0)
{
tel_no=1;

        for (count=1;y<tel_no; count++)
        {
                if (id_a[count] == prof_id_old)
                {
                y++;
                }

        }
```

```c
fseek ( fp , offset_a[count-1] + 1 , SEEK_SET );
fread (&dat_temp , length_a[count-1] , 1 , fp);


//printf("\n\n\tSVP profile (old) telegram # %d",tel_no);

printf("\n\n\tRay Tracing line %s \t",file_in);


memcpy (&temp_prof_tel_old.id, &dat_temp[0], 1);
/*printf ("\n\n\tID=%x \n",temp_prof_tel_old.id);*/
temp_prof_tel_old.model=mem2bytes(1);
/*printf ("\tmodel=%d \n",temp_prof_tel_old.model);*/
temp_prof_tel_old.date=mem4bytes(3);
date_con (temp_prof_tel_old.date);
/*printf("\tDate:%d/%02d/%02d (yyyy/mm/dd)\n",year,month,day);*/
temp_prof_tel_old.time=mem4bytes(7);
time_con (temp_prof_tel_old.time=mem4bytes(7));
/*printf("\tstart time:%02d:%02d:%02.3f\n",hours , mins , secs/1000);*/
temp_prof_tel_old.entries=mem2bytes(23);
/*printf ("\tNumber of entries =%d \n",temp_prof_tel_old.entries);*/
temp_prof_tel_old.res=mem2bytes(25);
/*printf ("\tDepth resolution =%d cm \n\n",temp_prof_tel_old.res);*/

beam_count=0;
countb=0;

for (count=0;count<temp_prof_tel_old.entries; count++)

{
        temp_prof_data_old.depth=mem2bytes(27+beam_count);
                d=temp_prof_data_old.depth*temp_prof_tel_old.res/100.0;
                svp_ray[0+countb]=d;

        temp_prof_data_old.speed=mem2bytes(29+beam_count);
                d=temp_prof_data_old.speed/10.0;
                svp_ray[1+countb]=d;

        beam_count=(beam_count + 4);
        countb++;
        countb++;
}
}


/******************** start manually input svp profile***************/

if (screwy == 1)
{
printf("\nRay Tracing line %s ",file_in);

printf("using archived profile  ");


 //12 48 17
```

```c
svp_ray [0] = 0.01  ;
svp_ray [2] = 1.17  ;
//……..
svp_ray [139] =1483.19 ;



}




getchar;
getchar;
y=0;
/***************** pick depth telegram*******************/
if (int_flag == 1)
{
        printf("\n\nThere are %d depth telegrams, pick number to calc ray trace: ",depth_no);
        scanf("%d",&tel_no);
        depth_no = tel_no;



if (int_flag==1) fp2 = fopen("raytrace.txt","w");


} else
{
tel_no = 1;
}

/*for (tel_no = 1; tel_no <= depth_no; tel_no++)*/

for (; tel_no <= depth_no; tel_no++)
{


        z=0;
        for (countc=1;z<tel_no; countc++)
        {
                if (id_a[countc] == depth_id)
                {
                z++;
                }

        }


/*printf(" %d\n",tel_no);*/
NEXT();

fseek ( fp , offset_a[countc-1] + 1 , SEEK_SET );
```
151

```c
fread (&dat_temp , length_a[countc-1] , 1 , fp);

/*printf("\n\n\tDepth telegram # %d",tel_no);*/

memcpy (&temp_depth.id, &dat_temp[0], 1);
/*printf ("\n\n\tID=%x \n",temp_depth.id);*/


temp_depth.model=mem2bytes(1);
/*printf ("\tmodel=%d \n",temp_depth.model);*/

temp_depth.date=mem4bytes(3);
date_con (temp_depth.date);
/*printf("\tDate:%d/%02d/%02d (yyyy/mm/dd)\n",year,month,day); */

temp_depth.time=mem4bytes(7);
time_con (temp_depth.time=mem4bytes(7));
/*printf("\tstart time:%02d:%02d:%02.5f\n",hours , mins , secs/1000);*/

temp_depth.ping_count=mem2bytes(11);
/*printf ("\tping count=%d \n",temp_depth.ping_count);*/

temp_depth.serial_no=mem2bytes(13);
/*printf ("\tserial #=%d \n",temp_depth.serial_no);*/

temp_depth.heading=mem2bytes(15);
        d=temp_depth.heading;
/*printf ("\theading=%.2f deg.\n",d/100);*/

temp_depth.surf_svp=mem2bytes(17);
        d=temp_depth.surf_svp;
/*printf ("\tsurface svp=%.1f m\/s \n",d/10);*/

temp_depth.trans_depth=mem2bytes(19);
/*printf ("\ttrans depth=%d cm\n",temp_depth.trans_depth);*/


memcpy (&temp_depth.max_beams, &dat_temp[21], 1);
/*printf ("\tmax beams=%d \n",temp_depth.max_beams);*/

memcpy (&temp_depth.valid_beams, &dat_temp[22], 1);
/*printf ("\tvalid beams=%d \n",temp_depth.valid_beams);*/

memcpy (&temp_depth.zres, &dat_temp[23], 1);
/*printf ("\tzres=%d cm\n",temp_depth.zres);*/

memcpy (&temp_depth.xyres, &dat_temp[24], 1);
/*printf ("\txyres=%d cm\n",temp_depth.xyres);*/

temp_depth.sample_rate=mem2bytes(25);
/*printf ("\tsample rate=%d \n",temp_depth.sample_rate);*/


//calculate time difference of entire ping
time_diff = temp_depth.time - temp_prof_tel_old.time;
```

```
/*getchar();
getchar();*/

if (int_flag == 1)
{
printf("------------------------------\n");
printf("|  \t|  \t|Calc.\t|  \t|\n");
printf("|Beam\t|Acc.\t|Acc.\t|Diff\t|along\t|along\t|depth\t|depth\t|Diff\t|\n");
printf("|no. \t|track\t|track\t|  \t|  \t|calc\t|  \t|calc\t|\n");
printf("|  \t|(m.) \t|  (m.)\t| (m.)\t|\n");
printf("------------------------------\n");
}




/*loop to print out individual beams */

beam_count=0;

for (count=0;count<temp_depth.valid_beams; count++)
        {

temp_beam.depth=mem2bytes(27+beam_count);

/*printf("countc =%d, beam_count %d = ",countc, beam_count);
getchar();*/


temp_beam.along=mem2bytes(31+beam_count);
        d=temp_beam.along;
temp_beam.beam_dep=mem2bytes(33+beam_count);
        d=temp_beam.beam_dep;
temp_beam.beam_az=mem2bytes(35+beam_count);
        azi=temp_beam.beam_az/100.0;

        if (azi > 180) azi= -(270.0-azi); else azi=90.0-azi;


temp_beam.range=mem2bytes(37+beam_count);
        d1=temp_beam.range;
        d2=temp_depth.sample_rate;
        tim_max=d1/d2/4;
memcpy (&temp_beam.quality, &dat_temp[39+beam_count], 1);
memcpy (&temp_beam.det_length, &dat_temp[40+beam_count], 1);
memcpy (&temp_beam.refl, &dat_temp[41+beam_count], 1);


        memcpy (&temp_beam.beam_no, &dat_temp[42+beam_count], 1);


        temp_beam.across=mem2bytes(29+beam_count);
        d1=temp_beam.across;
```
153

```
            d2=temp_depth.zres*100.0;
            d=d1/d2;
            /*printf ("|%.2f\t",temp_beam.across);*/

            d1=temp_depth.surf_svp/10.0;


            // get sound speed closes to transducer depth
            e = temp_depth.trans_depth/100.0;

            countb=0;

            while (svp_ray[0+countb] <= e ) countb = (countb + 2);

            // adjust depression angle for simrads beem steering
            if (beam_steer == 1)
                    {
                    //interpolate for ss at transducer
                    d5 = (svp_ray[1+countb] - svp_ray[-1+countb]);
                    d6 = (svp_ray[0+countb] - svp_ray[-2+countb]);
                    d7 = (svp_ray[0+countb] - temp_depth.trans_depth/100.0);

                    d8 = svp_ray[1+countb]-(d7*d5/d6);


                    //d2 = asin(sin((90-(temp_beam.beam_dep/100.0)) * pi/180.0) *(d8/d1));
                    d2 = asin(sin((90-(temp_beam.beam_dep/100.0)) * pi/180.0) *(d8/d1));

                    //d=(svp_ray[1+countb]);
                    d=d8;

                    } else
                            {
                            d2=((90-(temp_beam.beam_dep/100.0))* pi/180.0);

                            if (snap == 1)  d = temp_depth.surf_svp/10.0 +
(svp_ray_new[5+countb]*time_diff);else d=(svp_ray[1+countb]);
                            }

        p=sin(d2)/d;
        if (p == 0) p=0.00000001;

if (int_flag==1)
{
fprintf (fp2,"0 \t",tot_range);
fprintf (fp2,"0 \t");
fprintf (fp2,"%0.3f \t",d);
fprintf (fp2,"%0.3f \n",d2*180/pi);}

/*******complete ray trace constant speed gradient*/
// adjust for new svp profile


d=temp_depth.trans_depth/100.0;
```

```
thick = (svp_ray[0+countb]-d);


/*calc sound speed gradient (Gi)*/
//d2 = (svp_ray[3+countb]-d1)/thick;

if (snap == 1)  d3 = temp_depth.surf_svp/10.0 + (svp_ray_new[5+countb]*time_diff);else
d3=(svp_ray[1+countb]);

d2 = ((svp_ray[3+countb]+(svp_ray_new[5+countb]*time_diff))-d3)/thick;


/* must fix*/
if ( d2 == 0) d2 = 0.0000001;

tim_range = ((((asin(p*(d3+d2*thick)))-(asin(p*d3)))/
                         (p*d2*d2*thick))*
                         log(1.0+d2*thick/d3));


hor_range = (sqrt(1.0-pow((p*d3),2)) -
                         sqrt(1.0-pow((p*(d3+d2*thick)),2)))/
                         (p*d2);

/*printf ("first hor range = %.15f\n",hor_range);
printf ("first tim range = %.15f\n",tim_range);
getchar();*/

// add vlaues to total
depth = thick;
tot_range=hor_range;
tot_time=tim_range;




if (int_flag==1)
{fprintf (fp2,"%0.7f \t",tot_time);
fprintf (fp2,"%0.3f \t",tot_range);
fprintf (fp2,"%0.3f \t",depth);
fprintf (fp2,"%0.3f \n",svp_ray[1+countb]);}



do{
        /*******LAYER END - LAYER START*****/

        thick = (svp_ray[4+countb]-svp_ray[2+countb]);


// all rays need to be corrected for new profile
```

```c
        /*calc sound speed gradient*/

        d2 =      ((svp_ray[5+countb]+svp_ray_new[5+countb]*time_diff) -
                       (svp_ray[3+countb]+svp_ray_new[3+countb]*time_diff))/thick;

/*printf("diff =%.2f\n",(svp_ray[5+countb]-(svp_ray[5+countb]-svp_ray_new[5+countb]*time_diff)));*/

        d3 = svp_ray[3+countb]+(svp_ray_new[3+countb]*time_diff);
/*printf ("d2 = %.02f",d2);*/
/*getchar();
printf ("p = %.6f",p);*/

/*printf("total time = %0.10f\n\n",tot_time);*/
if (d2 != 0)
{

        tim_range = ((((asin(p*(d3+d2*thick)))-(asin(p*d3)))/
                       (p*d2*d2*thick))*
                       log(1.0+d2*thick/d3));

        hor_range = (sqrt(1.0-pow((p*d3),2)) -
                       sqrt(1.0-pow((p*(d3+d2*thick)),2)))/
                       (p*d2);
} else

{
        //  corrected for new profile
        d4 = svp_ray[5+countb] + (svp_ray_new[5+countb]*time_diff);

        d=sqrt(1-((d4*p)*(d4*p)));

        hor_range = (d4*p*thick)/d;

        tim_range = thick/(d4*d);

}
        /*printf ("time range = %.10f\n",tim_range);*/

        /*printf ("hor range = %.10f\n",hor_range);*/


        depth = depth + thick;
/*        printf ("depth = %.10f\n",depth);*/

        tot_time = tot_time + tim_range;

        /*printf("total time = %0.10f\n\n",tot_time);*/

        tot_range = tot_range + hor_range;

        /*printf("total range = %0.10f\n",tot_range);*/

/*printf ("coutb =%d",countb);*/
```

```c
        if (int_flag==1){
                fprintf (fp2,"%0.7f \t",tot_time);
                fprintf (fp2,"%0.3f \t",tot_range);
fprintf (fp2,"%0.3f \t",depth);
fprintf (fp2,"%0.3f\n",svp_ray[3+countb]+(svp_ray_new[3+countb]*time_diff));}




countb ++;
countb ++;
}while (tot_time < tim_max);

tot_range= tot_range - hor_range;
depth = depth - thick;
tot_time = tot_time - tim_range;
d3 = svp_ray[1+countb]+(svp_ray_new[1+countb]*time_diff);
d=sqrt(1-((d3*p)*(d3*p)));

do{
        /*iteration for last bit, sound speed kept constant */

        /*gradient = d2 = m/s per m*/
        thick = 0.01;

        /**** new speed of sound is original spped of sound multiplied by 100th the gradient??*/
        /*d3 = d3 + d2/100 ;*/
        /*d3 = svp_ray[1+countb];*/

        hor_range = (d3*p*thick)/d;

        tim_range = thick/(d3*d);

        depth = depth + thick;

        tot_time = tot_time + tim_range;
        /*printf("total time = %0.10f\n\n",tot_time);*/

        tot_range = tot_range + hor_range;
        /*printf("total range = %0.10f\n",tot_range);*/



        if (int_flag==1){
                fprintf (fp2,"%0.7f \t",tot_time);
                fprintf (fp2,"%0.3f \t",tot_range);
fprintf (fp2,"%0.3f \t",depth);
fprintf (fp2,"%0.3f \n",svp_ray[3+countb]+(svp_ray_new[3+countb]*time_diff));}




}while (tot_time <= tim_max);
/*depth = depth -0.01;*/
```

```
if (int_flag==1)fclose (fp2);
/*******end of  ray trace constant speed gradient */

/**** account for alongtrack*****/


along = sin(azi*pi/180.0) * tot_range;



tot_range = sqrt(pow(tot_range,2) - pow(along,2));



/*******printout*****/

/*beam no*/
if (int_flag == 1) printf ("| %d\t",temp_beam.beam_no);

d1=temp_beam.across;
d2=temp_depth.zres*100;
d=d1/d2;
/*simrad accross*/
if (int_flag == 1)printf ("|%.2f\t",d);



if (temp_beam.beam_az/100.0 > 180 && temp_beam.beam_az/100.0 < 360) tot_range = -tot_range;

/*calc across*/
if (int_flag == 1)printf("| %.1f\t",tot_range);
d=fabs(d)-fabs(tot_range);
/*range error*/
if (int_flag == 1)printf("| %.2f\t",d);

d1=temp_beam.along;
d2=temp_depth.zres*100.0;
d=d1/d2;
/*simrad along*/
if (int_flag == 1) printf("| %.2f\t",d);

/* calc along*/
if (int_flag == 1)printf("| %.2f\t",along);

/* simrad depth*/
d=temp_beam.depth;
if (int_flag == 1)printf ("\|%.2f\t",d/(temp_depth.zres*100.0));

/* calc depth */
if (int_flag == 1)printf("| %.2f\t",depth);

/* depth error*/
d = (d/(temp_depth.zres*100.0)-depth);
if (int_flag == 1)printf("| %.2f\n",d);
```

```c
/******************overwrite data in file******************/
{
/**** always plus 1***/

/*** depth ****/
y = (depth*100.0);
y = short_swap (y);

fseek ( fp , offset_a[countc-1] + (28+beam_count) , SEEK_SET );
fwrite (&y,sizeof(short),1,fp);


/***** across ****/
y=0;
y = (tot_range*100.0);
y = short_swap (y);

fseek ( fp , offset_a[countc-1] + (30+beam_count) , SEEK_SET );
fwrite (&y,sizeof(short),1,fp);


/**** along *****/
y=0;
y = (along*100.0);
y = short_swap (y);

fseek ( fp , offset_a[countc-1] + (32+beam_count) , SEEK_SET );
fwrite (&y,sizeof(short),1,fp);
fflush(stdout);

}
/******************end of overwriting data in file******************/

beam_count = (beam_count + 16);

} /*end of beam for loop*/

/*memcpy (&temp_depth.mult, &dat_temp[43 + beam_count -16], 1);
d=error/temp_depth.valid_beams;
/*printf ("\t\t\t\tmean error = %.2f\n",d);*/
/*printf("-------------------------------\n");
printf ("\tTransducer offset multiplier =%d\n\n\n\n",temp_depth.mult);*/




}
/* last bracket !!!!!!!!*/

}
```

Appendix IV   – National Physical Laboratory

Underwater Acoustics

Technical Guides

– Speed of Sound in Sea-Water

Mackenzie

$c(D,S,T) =$ $1448.96 + 4.591T - 5.304 \times 10^{-2}T^2 + 2.374 \times 10^{-4}T^3 + 1.340 (S-35) + 1.630 \times 10^{-2}D + 1.675 \times 10^{-7}D^2 - 1.025 \times 10^{-2}T(S-35) - 7.139 \times 10^{-13} TD^3$

T = temperature in degrees Celsius
S = salinity in parts per thousand
D = depth in metres

Range of validity: temperature 2 to 30 °C, salinity 25 to 40 parts per thousand and depth 0 to 8000 m

The above equation for the speed of sound in sea-water as a function of temperature, salinity and depth is given by Mackenzie (1981).

Coppens

$c(D,S,t) =$ $c(0,S,t) + (16.23 + 0.253t)D + (0.213-0.1t)D^2 + [0.016 + 0.0002(S-35)](S-35)tD$

$c(0,S,t) =$ $1449.05 + 45.7t - 5.21t^2 + 0.23t^3 + (1.333 - 0.126t + 0.009t^2)(S-35)$

t = T/10 where T = temperature in degrees Celsius
S = salinity in parts per thousand
D = depth in metres

Range of validity: temperature 0 to 35 °C, salinity 0 to 45 parts per thousand and depth 0 to 4000 m

The above equation for the speed of sound in sea-water as a function of temperature, salinity and depth is given by Coppens (1981).

UNESCO Equation: Chen and Millero

The international standard algorithm, often known as the UNESCO algorithm, is due to Chen and Millero (1977), and has a more complicated form than the simple equations above, but uses pressure as a variable rather than depth. For the original UNESCO paper see Fofonoff and Millard (1983). Wong and Zhu (1995) recalculated the coefficients in this algorithm following the adoption of the International Temperature Scale of 1990 and their form of the UNESCO equation is:

$$c(S,T,P) = Cw(T,P) + A(T,P)S + B(T,P)S^{3/2} + D(T,P)S^2$$

$$
\begin{aligned}
Cw(T,P) = &\ (C_{00} + C_{01}T + C_{02}T^2 + C_{03}T^3 + C_{04}T^4 + C_{05}T^5) + \\
&\ (C_{10} + C_{11}T + C_{12}T^2 + C_{13}T^3 + C_{14}T^4)P + \\
&\ (C_{20} + C_{21}T + C_{22}T^2 + C_{23}T^3 + C_{24}T^4)P^2 + \\
&\ (C_{30} + C_{31}T + C_{32}T^2)P^3
\end{aligned}
$$

$$
\begin{aligned}
A(T,P) = &\ (A_{00} + A_{01}T + A_{02}T^2 + A_{03}T^3 + A_{04}T^4) + \\
&\ (A_{10} + A_{11}T + A_{12}T^2 + A_{13}T^3 + A_{14}T^4)P + \\
&\ (A_{20} + A_{21}T + A_{22}T^2 + A_{23}T^3)P^2 + \\
&\ (A_{30} + A_{31}T + A_{32}T^2)P^3
\end{aligned}
$$

$$B(T,P) = B_{00} + B_{01}T + (B_{10} + B_{11}T)P$$

$$D(T,P) = D_{00} + D_{10}P$$

T = temperature in degrees Celsius
S = salinity in Practical Salinity Units (parts per thousand)
P = pressure in bar

Range of validity: temperature 0 to 40 °C, salinity 0 to 40 parts per thousand, pressure 0 to 1000 bar (Wong and Zhu, 1995).

Table of Coefficients

Coefficients	Numerical values	Coefficients	Numerical values
C_{00}	1402.388	A_{02}	7.166E-5
C_{01}	5.03830	A_{03}	2.008E-6
C_{02}	-5.81090E-2	A_{04}	-3.21E-8
C_{03}	3.3432E-4	A_{10}	9.4742E-5
C_{04}	-1.47797E-6	A_{11}	-1.2583E-5
C_{05}	3.1419E-9	A_{12}	-6.4928E-8
C_{10}	0.153563	A_{13}	1.0515E-8
C_{11}	6.8999E-4	A_{14}	-2.0142E-10
C_{12}	-8.1829E-6	A_{20}	-3.9064E-7
C_{13}	1.3632E-7	A_{21}	9.1061E-9
C_{14}	-6.1260E-10	A_{22}	-1.6009E-10
C_{20}	3.1260E-5	A_{23}	7.994E-12

Coefficients	Numerical values	Coefficients	Numerical values
C_{21}	-1.7111E-6	A_{30}	1.100E-10
C_{22}	2.5986E-8	A_{31}	6.651E-12
C_{23}	-2.5353E-10	A_{32}	-3.391E-13
C_{24}	1.0415E-12	B_{00}	-1.922E-2
C_{30}	-9.7729E-9	B_{01}	-4.42E-5
C_{31}	3.8513E-10	B_{10}	7.3637E-5
C_{32}	-2.3654E-12	B_{11}	1.7950E-7
A_{00}	1.389	D_{00}	1.727E-3
A_{01}	-1.262E-2	D_{10}	-7.9836E-6

Del Grosso's equation

An alternative equation to the UNESCO algorithm, which has a more restricted range of validity, but which is preferred by some authors, is the Del Grosso equation (1974). Wong and Zhu (1995) also reformulated this equation for the new 1990 International Temperature Scale and their version is:

$c(S,T,P) = $ $\quad C_{000} + \Delta C_T + \Delta C_S + \Delta C_P + \Delta C_{STP}$

$$\Delta C_T(T) = C_{T1}T + C_{T2}T^2 + C_{T3}T^3$$
$$\Delta C_S(S) = C_{S1}S + C_{S2}S^2$$
$$\Delta C_P(P) = C_{P1}P + C_{P2}P^2 + C_{P3}P^3$$
$$\Delta C_{STP}(S,T,P) = C_{TP}TP + C_{T3P}T^3P + C_{TP2}TP^2 + C_{T2P2}T^2P^2 + C_{TP3}TP^3 +$$
$$C_{ST}ST + C_{ST2}ST^2 + C_{STP}STP + C_{S2TP}S^2TP + C_{S2P2}S^2P^2$$

T = temperature in degrees Celsius
S = salinity in Practical Salinity Units
P = pressure in kg/cm^2

Range of validity: temperature 0 to 30 °C, salinity 30 to 40 parts per thousand, pressure 0 to 1000 kg/cm^2, where 100 kPa=1.019716 kg/cm^2. Wong and Zhu (1995)

Table of Coefficients

Coefficients	Numerical values
C_{000}	1402.392
C_{T1}	0.5012285E1
C_{T2}	-0.551184E-1
C_{T3}	0.221649E-3
C_{S1}	0.1329530E1
C_{S2}	0.1288598E-3
C_{P1}	0.1560592
C_{P2}	0.2449993E-4
C_{P3}	-0.8833959E-8
C_{ST}	-0.1275936E-1
C_{TP}	0.6353509E-2
C_{T2P2}	0.2656174E-7
C_{TP2}	-0.1593895E-5
C_{TP3}	0.5222483E-9
C_{T3P}	-0.4383615E-6
C_{S2P2}	-0.1616745E-8
C_{ST2}	0.9688441E-4
C_{S2TP}	0.4857614E-5
C_{STP}	-0.3406824E-3

Both the UNESCO equation and Del Grosso's equation use pressure rather than depth as a variable. Useful guidance and suitable equations for converting pressure into depth and depth into pressure can be found in Leroy and Parthiot (1998) . The key equations here are:

Conversion of pressure into depth

$$Z_S(P, \Phi) = \frac{9.72659 \times 10^2 P - 2.512 \times 10^{-1} P^2 + 2.279 \times 10^{-4} P^3 - 1.82 \times 10^{-7} P^4}{g(\Phi) + 1.092 \times 10^{-4} P}$$

Where $g(\Phi)$, the international formula for gravity, is given by:

$$g(\Phi) = 9.780318 (1 + 5.2788 \times 10^{-3} \sin^2\Phi + 2.36 \times 10^{-5} \sin^4\Phi)$$

Z = depth in metres
P = pressure in MPa
Φ = latitude

The above equation is true for the oceanographers' standard ocean, defined as an ideal medium with a temperature of 0 °C and salinity of 35 parts per thousand.

Leroy and Parthiot (1998) give a table of corrections which are needed when the standard formula is applied to specific oceans and seas. The above equation and interactive version do not apply any corrections.

Conversion of depth into pressure

$h(Z\Phi)$ $h(Z,45) \times k(Z,\Phi)$

$h(Z,45) =$ $1.00818 \times 10^{-2} Z + 2.465 \times 10^{-8} Z^2 - 1.25 \times 10^{-13} Z^3 + 2.8 \times 10^{-19} Z^4$

$k(Z,\Phi)$ $(g(\Phi) - 2 \times 10^{-5} Z)/(9.80612 - 2 \times 10^{-5} Z)$

$g(\Phi) =$ $9.7803(1 + 5.3 \times 10^{-3} \sin^2\Phi)$

Z = depth in metres
h = pressure in MPa
Φ = latitude

The above equation is true for the oceanographers' standard ocean, defined as an ideal medium with a temperature of 0 °C and salinity of 35 parts per thousand.

Leroy and Parthiot (1998) give a table of corrections which are needed when the standard formula is applied to specific oceans and seas. The above equation and interactive version do not apply any corrections.

Uncertainties

Although the UNESCO algorithm is the international standard algorithm, there is much debate in the scientific literature about the accuracy and range of applicability of this equation and of Del Grosso's equation. Some researchers prefer Del Grosso's equation, especially for calculations within its own domain of validity. It is important to recognise that the equations presented here are derived from fitting to experimental data from several different experiments and each has an associated uncertainty in its prediction of sound speed. The choice of equation may depend on the accuracy and precision which is acceptable for the particular application in which it is being employed. For further discussion on this topic please refer to Dushaw et al (1993), Meinen and Watts (1997), Millero and Xu Li (1994), Speisberger and Metzger (1991a, 1991b) and Speisberger (1993).

The Hydrographic Society (Pike and Beiboer, 1993) has a good summary of the main algorithms for sound speed in the ocean. This sets out more detailed advice and information than can be provided on this web-site, including information of the domains of validity of the main equations and on depth to pressure conversions.

Any comments or suggestions about further speed of sound equations?

Please contact:

Dr Trevor Esward   OR   **Justin Ablitt**
Tel: +44 (0)20 8943 6695   Tel: +44 (0)20 8943 6695
Fax: +44 (0)20 8943 6217   Fax: +44 (0)20 8943 6217
E-mail: trevor.esward@npl.co.uk   E-mail: justin.ablitt@npl.co.uk

References

1. C-T. Chen and F.J. Millero, Speed of sound in seawater at high pressures (1977) J. Acoust. Soc. Am. 62(5) pp 1129-1135

2. A.B. Coppens, Simple equations for the speed of sound in Neptunian waters (1981) J. Acoust. Soc. Am. 69(3), pp 862-863

3. V.A. Del Grosso, New equation for the speed of sound in natural waters (with comparisons to other equations) (1974) J. Acoust. Soc. Am 56(4) pp 1084-1091

4. B.D. Dushaw, P.F. Worcester, B.D. Cornuelle and B.M. Howe, On equations for the speed of sound in sea water (1993) J. Acoust. Soc. Am. 93(1) pp 255-275

5. N.P. Fofonoff and R.C. Millard Jr. Algorithms for computation of fundamental properties of seawater (1983), UNESCO technical papers in marine science. No. 44, Division of Marine Sciences. UNESCO, Place de Fontenoy, 75700 Paris.

6. C. C. Leroy and F Parthiot, Depth-pressure relationship in the oceans and seas (1998) J. Acoust. Soc. Am. 103(3) pp 1346-1352

7. K.V. Mackenzie, Nine-term equation for the sound speed in the oceans (1981) J. Acoust. Soc. Am. 70(3), pp 807-812

8. C.S. Meinen and D.R. Watts, Further evidence that the sound-speed algorithm of Del Grosso is more accurate than that of Chen and Millero (1997) J. Acoust. Soc. Am. 102(4) pp 2058-2062

9. F.J. Millero and Xu Li, Comments on "On equations for the speed of sound in seawater" (1994), J. Acoust. Soc. Am. 95(5), pp 2757-2759

10. J.M. Pike and F.L. Beiboer, A comparison between algorithms for the speed of sound in seawater (1993) The Hydrographic Society, Special Publication no. 34

11. J.L. Speisberger and K. Metzger, New estimates of sound speed in water (1991a) J. Acoust. Soc. Am. 89(4) pp 1697-1700

12. J.L. Speisberger and K. Metzger, A new algorithm for sound speed in seawater (1991b) J. Acoust. Soc. Am. 89(6) pp 2677-2687

13. J.L. Speisberger, Is Del Grosso's sound-speed algorithm correct ? (1993) J. Acoust. Soc. Am. 93(4) pp 2235-2237

14. G.S.K. Wong and S Zhu, Speed of sound in seawater as a function of salinity, temperature and pressure (1995) J. Acoust. Soc. Am. 97(3) pp 1732-1736

VITA

Name: Douglas Stuart Cartwright

Date/Place of Birth   18, July, 1964

Address: 9860 West Saanich Road
                    Sidney, B.C.

Secondary School: Dr. E.P. Scarlett High School
                    Calgary, Alberta
                    1980-1982

College/Program Southern Alberta Institute of Technology
                    Calgary, Alberta
                    Diploma, Survey and Mapping
                    1979-1981